LOCALISATION AND QUANTIFICATION OF CHEMICAL FUNCTIONAL GROUPS ON PULP FIBRES

Dissertation presented for the degree of
Doctor of Philosophy (Polymer Science)
at the University of Stellenbosch

by

Abdalah Klash

Supervisor: Dr. M. Meincken
Co-supervisor: Prof. R. D. Sanderson

Department of Chemistry and Polymer Science,
University of Stellenbosch
South Africa

December 2010

DECLARATION

By submitting this dissertation electronically, I declare that the entirety of the work contained therein is my own, original work, that I am the owner of the copyright thereof (unless to the extent explicitly otherwise stated) and that I have not previously in its entirety or in part submitted it for obtaining any qualification.

Signature: ..... Date: .....

Abstract

The distribution of different free chemical functional groups on wood and pulp fibres was determined by means of atomic force microscopy (AFM) with chemically modified tips. Because these functional groups show a higher affinity to similar groups on the substrate surface during scanning, AFM images were recorded using an additional digital pulsed-force mode (DPFM) controller. This allowed the distribution of the chemical components to be imaged and to a degree, also to be quantified. The investigated tip coatings showed different sensitivities towards the major chemical components present in wood fibres. These components were determined on spin-coated films as well as wood fibres. It was possible to make a clear distinction between cellulose and lignin in both cases. This technique could therefore be used to differentiate between cellulose and lignin present on pulp fibre surfaces and to confirm the successful removal of lignin by pulping.

The chemical composition of wood fibres and fibre surfaces of several acacia and eucalyptus species, and hybrids originating from various growth sites in South Africa, are compared. The objective was to determine the differences in chemical surface composition due to genetics or site. The motivation for this was to eventually facilitate a tailor-made supply of wood for pulping which results in an optimal blend of fibres that can be pulped together with similar yields. This, however, first requires a sound knowledge of the fibre properties. The surface functionality on the single fibre level is a key property because it determines how good inter-fibre bonding will be when paper is formed, which in turn depends to a large degree on the amount of free hydroxyl groups that are available and therefore on the cellulose content on the fibre surface.

The cellulose and lignin contents on the fibre surface were determined with chemical force microscopy (CFM), a variation of AFM. CFM involves the use of chemically modified tip using selected functional groups. Since, the general bulk composition of the fibre and the surface composition differ, both parameters were determined. Significant differences in the cellulose and lignin content on fibre surfaces were found, with regard to genotype and site,

respectively. In some, but not all, cases the surface composition of wood fibres followed the bulk composition and differences were generally more pronounced. Differences due to genotype were significant, especially with regards to the surface lignin content - but variation due to site was also distinctly recognisable.

This variation in surface functionality could be the reason why some pulpwood blends result in a lower pulp yield and different quality.

Opsomming

Die verspreiding van verskillende vrye chemiese funksionele groepe op hout en pulpvesels is bepaal deur middel van atoomkragmikroskopie (AFM), met chemies-gemodifiseerde punte (tips). Omdat hierdie funksionele groepe 'n hoër verwantskap tot soortgelyke groepe op die substraat se oppervlak gedurende skandering toon, kan AFM-beelde wat met 'n addisionele digitalepulskragmodusbeheerstel bepaal word dit moontlik maak om die verspreiding van die chemiese komponente uit te beeld en tot op ‘n sekere vlak te kwantifiseer. Die ondersoekte punt-oppervlakmiddels het verskillende sensitiwiteite teenoor die hoof chemiese komponente in die houtvesels en spin-bestrykte films getoon. 'n Duidelike onderskeid kon in beide gevalle tussen sellulose en lignien gemaak word. Hierdie tegniek kon dus gebruik word om te onderskei tussen sellulose en lignien wat op die pulpveseloppervlak teenwoordig was en om die suksesvolle verwydering van lignien gedurende die pulpproses (pulping) te bevestig.

In hierdie studie is die chemiese samestelling van houtvesels en die veseloppervlaktes van verskeie akasia en eucalyptus spesies, asook dié van gekruisde spesies wat van verskeie werfliggings in Suid-Afrika afkomstig is, vergelyk. Die doel was om te toets vir verskille in chemiese oppervlaksamestellings, wat veroorsaak kan word deur genetika of werf verskille, met die uiteindelike mikpunt om ‘n spesiaal-gemaakte voorraad van hout vir pulping te fasiliteer, wat kan lei tot 'n optimale mengsel van vesels wat saam gepulp kan word met soortgelyke opbrengs. Dit vereis natuurlik 'n goeie kennis van die veseleienskappe. Die oppervlakfunksionering van enkel vesels is ‘n kritiese eienskap omdat dit bepaal hoe goed interveselverbindings sal wees wanneer papier gevorm word. Dit hang tot ‘n groot mate af van die hoeveelheid vry hydroksielgroepe wat beskikbaar is en dus ook van die sellulose inhoud op die veseloppervlak.

Die sellulose- en lignieninhoud op die veseloppervlak is bepaal met chemiese kragmikroskopie – 'n variasie van atoomkragmikroskopie. Omdat die algemene grootmaat samestelling van die vesel en die oppervlaksamestelling

mag verskil, is altwee parameters bepaal. Beduidende verskille in die sellulose- en lignieninhoud, met betrekking tot genotipe en werfligging, op veseloppervlaktes is gevind. In sommige, maar nie alle, gevalle het die oppervlaksamestelling van houtvesels ooreengestem met die grootmaatsamestelling, en verskille was oor die algemeen meer beduidend. Verskille as gevolg van genotipe was beduidend, veral met betrekking tot die oppervlak lignieninhoud, maar variasie as gevolg van werfligging was ook duidelik herkenbaar.

Hierdie variasie in oppervlakfunksionering kan die rede wees hoekom sommige pulp–hout mengsels lei tot 'n laer pulpopbrengs en verskille in kwaliteit.

Acknowledgements

First and foremost, I would like to express my most sincere thanks to my advisor and supervisor, Dr. M. Meincken, for her continuous guidance and support throughout this work. I am also sincerely grateful to Prof. R. D. Sanderson, my co-supervisor, for his invaluable advice, guidance and assistance, which led to the completion of this project. It was an honour to know and to work with them.

Furthermore, I am thankful to all the members of Department of Chemistry and Polymer Science for their cooperation.

I also acknowledge the financial support received from the International Centre for Macromolecular Chemistry and Technology in Libya.

Finally, I would like to dedicate this thesis to my family for their continuous love and encouragement, and to my friends for their help and support.

Dedication

To my parents

To my wife and daughter

To all my family members

To everyone, who believed in me and supported me

Table of contents

List of Figures

List of Tables

List of Abbreviations

A	Acacia
AFM	Atomic force microscopy
ATR-FTIR	Attenuated total reflectance Fourier transform infrared spectroscopy
BA	Basal area
BP	Bio-pulping
BSE	Back-scattered electron microscopy
CFM	Chemical force microscopy
DBH	Diameter at breast height
DP	Degree of polymerization
DPFM	Digital pulsed-force mode
E	Eucalyptus
EDX	Energy dispersive x-ray
FE-SEM	Field emission scanning electron microscopy
HWE	Hot water extraction
IRE	Internal reflection element
MAI	Mean annual increment
MAP	Mean annual precipitation
MAT	Mean annual temperature
ML	Middle lamella
P	Primary wall
S1	Secondary wall outer layer
S2	Middle layer

S3	Inner layer
SAM	Self-assembling monolayers
SEM	Scanning electron microscopy
STM	Scanning tunnelling microscope
TEM	Transmission electron microscopy
ToF-SIMS	Time-of-flight secondary ion mass spectrometry
XPS	X-ray photoelectron spectroscopy

1 Introduction and Objectives

1.1 Introduction

Wood fibres are the main source of pulp and paper, and the strength of the final product depends largely on the degree of bonding between individual fibres. This bonding is facilitated by van der Waals forces and hydrogen bonds between hydrophilic groups on the fibre surfaces [1]. A better understanding of the surface chemistry of the wood fibres and the distribution of these polar groups could help to further improve paper quality.

The most important source of pulp fibres is wood, which is a natural composite consisting of cellulose, hemicelluloses, lignin and extractives. The inter-fibre bonding depends largely on the number of free hydroxyl groups provided by the cellulose. In order to utilise wood fibres effectively, the cellulose and hemicelluloses need to be isolated from the other wood components, which affect strength properties negatively [2, 3]. This isolation process involves extraction and pulping [4].

Extractives can be removed with hot water, which removes tannins and inorganic salts, or with organic solvents such as hexane, acetone, or diethyl ether, which remove terpenes, fats, wax, and phenols [5]. Despite the fact that extractives typically only constitute a small part of the total wood composition, they have a major effect on wood properties such as odour, colour, decay properties, density, flammability, hygroscopicity, permeability, and mechanical and chemical processability [6]. It is therefore vital for further processing to reduce the extractive content as much as possible.

Inter-fibre bonding in paper is negatively affected by the presence of hydrophobic lignin on fibre surfaces, which obstructs the formation of hydrogen bonds between fibres. The removal of lignin during pulping exposes

the cellulose and hemicelluloses, and their hydrophilic hydroxyl groups, on the fibre surface [6].

In various previous studies attempts have been made to find a correlation between the chemical bulk composition of wood fibres and their surface properties, which were determined by X-ray photoelectron spectroscopy (XPS) [7, 8], scanning electron microscopy (SEM) [9] and atomic force microscopy (AFM). AFM has been used to investigate the surface morphology of wood, pulp and paper fibres by various groups [10-12]. Koljonen et al. [13] used AFM in tapping mode to reveal the morphological structure of various mechanical pulps, and attempted to relate it to the chemical composition of the pulp. These experiments were however performed with unmodified, commercial AFM tips either made from Si_3N_4 or SiO_2. Fardim et al. [14] examined the structure of extractives in wood fibres with AFM and related results to the chemical composition, determined by X-ray photoelectron spectroscopy (XPS) and time-of-flight secondary ion mass spectrometry (ToF-SIMS). Fromm et al. [15] determined the lignin distribution in cell walls of spruce and beech wood by high-voltage transmission electron microscopy (TEM) in sections stained with potassium permanganate as well as by field emission scanning electron microscopy (FE-SEM) combined with a back-scattered electron detector on mercurised specimens. The latter is a new technique based on the mercurisation of lignin and the concomitant visualization of mercury by back-scattered electron microscopy (BSE).

South Africa is the largest African pulp and paper producer: it produces approximately 1.9 million tons of wood pulp; 1.2 million tons of newsprint, printing and writing paper; and more than 1 million tons of other paper products per year [16]. South Africa has a relatively rich source of raw materials from its plantation forests in the Kwazulu-Natal and Mpumalanga regions. The warm climate of these areas leads to a faster tree growth than in most paper and pulp producing countries north of the equator [16].

South Africa’s major pulpwood source is Eucalyptus and several eucalyptus genotypes are commercially grown, depending on the site characteristics. The

growth regions for pulpwood production encompass different climate zones, ranging from warm, subtropical areas near the east coast, to cooler sites on the escarpment with elevations above 1000 meters. Species choice is usually based on climatic risk factors (e.g. snow, frost, or drought risk), mean annual temperature (MAT), mean annual precipitation (MAP), soil characteristics, as well as wood and pulping characteristics.

On subtropical sites near the coast (MAT>19 ℃), *E. grandis x urophylla* and *E. grandis x camaldulensis* are the most widely planted genotypes. These hybrids have a superior disease resistance compared to pure species, such as *E. grandis,* which can also be grown in this zone. In addition, *E. grandis x urophylla* has excellent pulping properties and is thus the preferred genotype in the subtropical area.

In the warm, temperate climates (KwaZulu-Natal Midlands and Mpumalanga escarpment with MAT 16-19 ℃), *E. grandis, E. dunnii*, *E. saligna* and *E. smithii* are commonly planted. *E. grandis* has a fast growth rate but may be prone to drought risk on sites with low levels of available soil water, and it is sensitive to snow damage and to frost when young. *E. smithii* has highly desirable pulp properties but is more susceptible to *Phytophthora* root rot on soils with poor drainage.

On cold temperate sites with a MAT of 15-16 ℃, *E. dunnii, E. grandis x nitens, E. saligna* and *E. smithii* can still be grown since they are moderately hardy to frost. However, on sites with a MAT below 15 ℃, species tolerant of snow - such as *E. nitens* - or frost and drought - such as *E. macarthurii* - are often preferred, despite having slightly less desirable pulping properties, especially in the latter case. Other species with desirable wood properties that show promise for cold temperate sites are *E. benthamii* and *E. badjensis* [17].

The pulp and paper quality of these species depends strongly on fibre properties, such as fibre length, diameter and chemical composition. The fibre dimensions determine how well the inter-fibre contact will be when paper is formed, and the chemical composition, i.e. the availability of free hydroxyl

groups to form hydrogen bonds, determines how well these fibres will bind together, which in turn affects the paper quality. The importance of fibre properties - in addition to other tree improvement efforts - for any further use, such as pulping, has been highlighted by Lundqvist [18].

That wood quality, and more specifically fibre properties, depends strongly on the environment has been demonstrated by many studies. For example, Gindl et al. [19] show that the lignin content in the secondary cell wall correlates positively with temperature in terminal latewood tracheids. Leal et al. [20] report tree growth variability within five different conifer species in the Austrian Alps depending on species and altitude. Kaakinen et al. [21] studied the effects of growth differences due to geographic location and nitrogen fertilisation on the chemical composition of Norway spruce (*Picea abies* (L.) Karst.) at two sites in Finland. They found that nitrogen fertilisation caused only small changes in the chemical composition, while the differences due to different sites were significantly larger.

The wood and fibre quality of Eucalyptus has been addressed in various studies. Clarke et al. [22] studied a variety of wood characteristics, including the average density, fibre length and chemical composition, of nine Eucalyptus species in three provences, from established trial sites in South Africa. They found significant differences in density, fibre length and chemical composition between the species and between sites. They also reported on differences in pulp quality, mainly in the yield and kappa number. Naidoo et al. [23] found a negative correlation between moisture availability and wood density and vessel ratio in *Eucalyptus grandis* in the warm temperate region of South Africa. Miranda and Pereira [24] studied the differences in wood density, fibre morphology, chemical composition and pulp yield in four provenances of *Eucalyptus globulus* at three different sites in Portugal. Their findings suggest no significant effect of provence and site on the wood density. However, provence and site caused significant variation in fibre length, cell wall thickness and lumen diameter. With regards to the chemical composition, only the extractives content showed any significant provenance and site effects.

Based on these fibre properties this study explores further ways of investigating the fibres quality. This is to be done by using chemical force microscopy (CFM) to characterise the chemical surface composition of pulpwood fibres and compare the findings to the chemical bulk composition, which might differ considerably. Nevertheless, it is typically the bulk chemical composition that is determined to describe pulpwood fibres.

The surface properties of fibres are especially important for further processing, such as pulping, as they determine, for example, the degree of inter-fibre bonding. The formation of hydrogen bonds between pulp fibres depends on available hydrophilic hydroxyl (–OH) groups and small inter-fibre distances. The removal of the hydrophobic lignin from the fibre surface during pulping exposes cellulose and hemicelluloses containing –OH groups. Furthermore, any lignin still present in pulp fibres results in an increased fibre stiffness, which inhibits good inter-fibre bonding. The fibres become more flexible when lignin is removed and simultaneously the amount of free hydroxyl groups on the fibre surface is increased, which promotes the formation of hydrogen bonds between the fibres. These bonds are responsible for the mechanical strength of the final paper product [25]. For example, the tensile strength of a paper sheet depends mostly on the number of hydrogen bonds per unit volume available between the fibre surfaces.

In this study I investigated the feasibility of digital pulsed force mode AFM (DPFM-AFM) to identify and localise functional groups on pulpwood fibres**.** In a previous study by Meincken [26] it was shown that DPFM-AFM can be used with unmodified silicon tips, to detect polar areas on the surface of wood fibres. This is because the SiO_2 layer forming on the tip is more sensitive towards polar groups on the sample surface.

1.2 Objectives

The first objective was to investigate the feasibility of different tip coatings in order to determine their respective sensitivities towards the different chemical

components in wood fibres, namely cellulose and lignin, in order to localise, identify and possibly quantify them.

The second objective was to track changes in the chemical surface composition of various pulp fibres after different treatments, such as extraction or pulping.

The third objective was to reveal possible differences in chemical composition of the fibre surfaces with regards to growth site and genotype. The investigated species comprised different Eucalyptus species grown at various sites in South Africa. These sites varied in terms of the availability of water, or MAP and MAT. All of which can be expected to have an influence on the chemical composition of wood fibres. A difference in surface functionality can be expected to affect the pulp quality and explain variations therein.

The final objective was to test the adhesion properties between different wood fibres and starch–a component that is used in the pulp and paper industry as filler and sizing agent.

1.3 Layout of the thesis

A brief background to the major chemical wood components is given in Chapter 2. The principles and operation modes of the analytical equipment used in this project are described in Chapter 3. In Chapter 4 sample preparation and the experimental setups are described. Results and discussions are presented in Chapter 5. It includes results obtained using the following techniques: Scanning electron microscopy-energy dispersive X-ray (SEM-EDX), Fourier transform infrared spectroscopy (FTIR) and Chemical force microscopy (CFM) on various model compounds and pulp fibres. An effort was also made to make correlations between the results.

1.4 References

[1] G. Koch, *Raw material for pulp*, in *Handbook of Pulp*, H. Sixta, Editor. 2006, Wiley-VCH: Weinheim. p. 21-68.

[2] T. Lindstroem, C. Soeremark, and L. Westman, *The colloidal behaviour of kraft lignin.* Colloid and Polymer Science, 1977, **258**: p. 168-173.

[3] X. Zhang, R. P. Beatson, Y. J. Cai, and J. N. Saddler, *Accumulation of specific dissolved colloidal substances during white water recycling affecting paper properties.* Journal of Pulp and Paper Science, 1999. **25**: p. 206-210.

[4] J. Schurz, *A bright future for cellulose.* Progress in Polymer Science, 1999. **24** p. 481-483.

[5] R. Alen, *Structure and chemical composition of wood*, in *Forest Products Chemistry*, P. Stenius, Editor. 2000, Helsinki, Finland: Fapet Oy. p. 12-54.

[6] H. H. Nimz, U. Schmitt, E. Schwab, O. Wittmann, and F. Wolf, *Wood*. Ullmann's Encyclopedia of Industrial Chemistry 2002, Weinheim: Wiley-VCH Verlag, p.1-54.

[7] W. T. Tze, G. Bernhardt, D. J. Gardner, and A. W. Christiansen, *X-ray photoelectron spectroscopy of wood treated with hydroxymethylated resorcinol.* International Journal of Adhesion and Adhesives, 2006. **26**: p. 550-554.

[8] F. P. Liu and T. G. Rials, *Relationship of wood surface energy to surface composition.* Langmuir, 1998. **14**: p. 536-541.

[9] P. Fardim and N. Duran, *Modification of fibre surfaces during pulping and refining as analysed by SEM, XPS and ToF-SIMS.* Colloids and Surfaces A, 2003. **223**: p. 263-276.

[10] G. Piantanida, M. Bicchieri, and C. Coluzza, *Atomic force microscopy characterization of the ageing of pure cellulose paper.* Polymer, 2005. **46**: p. 12313-12321.

[11] T. C. Pesacreta, L. C. Carlson, and B. A. Triplett, *Atomic force microscopy of cotton fiber cell wall surfaces in air and water: quantitative and qualitative aspects.* Planta, 1997. **202**: p. 435-442.

[12] K. Koljonen, M. Osterberg, M. Kleen, A. Fuhrmann, and P. Stenius, *Precipitation of lignin and extractives on kraft pulp: effect on surface chemistry, surface morphology and paper strength.* Cellulose, 2004. **11**: p. 209-224.

[13] K. Koljonen, M. Österberg, L. S. Johansson, and P. Stenius, *Surface chemistry and morphology of different mechanical pulps determined by ESCA and AFM.* Colloids and Surfaces A, 2003. **228** p. 143-158.

[14] P. Fardim, J. Gustafsson, S. Schoultz, J. Peltonen, and B. Holmbom, *Extractives on fiber surfaces investigated by XPS, ToF-SIMS and AFM.* Colloids and Surfaces A, 2005. **255**: p. 91-103.

[15] J. Fromm, B. Rockel, S. Lautner, E. Windeisen, and G. Wanner, *Lignin distribution in wood cell walls determined by TEM and backscattered SEM techniques.* Journal of Structural Biology, 2003. **143**: p. 77-84.

[16] Mbendi Information Services (2009), http://www.mbendi.com [accessed 8/04 2009].

[17] C. W. Smith, R. N. Pallett, R. P. Kunz, R. A. Gardner, and M. Du Plessis, *A strategic forestry site classification for the summer rainfall region of southern Africa based on climate, geology and soils.* ICFR Bulletin Series 03/05, Pietermaritzburg, South Africa, 2005.

[18] S. O. Lundqvist, *Efficient wood and fiber characterization - a key factor in research and operation.* Annals of Forest Science, 2002. **59**: p. 491-501.

[19] W. Gindl, M. Grabner, and R. Wimmer, *The influence of temperature on latewood lignin content in treeline Norway spruce compared with maximum density and ring width.* Trees, 2000. **14**: p. 409-414.

[20] S. Leal, T. M. Melvin, M. Grabner, R. Wimmer, and K. R. Briffa, *Tree-ring growth variability in the Austrian alps: the influence of site, altitude, tree species and climate.* Boreas, 2007. **36**: p. 427-440.

[21] S. Kaakinen, P. Saranpaa, and E. Vapaavuori, *Effects of growth differences due to geographic location and N-fertilisation on wood chemistry of Norway spruce.* Trees, 2007. **21**: p. 131-139.

[22] C. R. Clarke, D. C. Garbutt, and J. Pearce, *Growth and wood properties of provences and trees of nine eucalypt species.* Appita, 1997. **50**: p. 121-130.

[23] S. Naidoo, A. Zboňák, and F. Ahmed, *The effect of moisture availability on wood density and vessel characteristics of Eucalyptus grandis in the warm temperate region of South Africa.* IUFRO symposium “Wood Structure and Properties", 2006.

[24] I. Miranda and H. Pereira, *Variation of pulpwood quality with provences and site in Eucalyptus globulus.* Annals of Forest Science, 2002. **59** p. 283-291.

[25] N. Maximova, M. Österberg, K. Koljonen, and P. Stenius, *Lignin adsorption on cellulose fibre surfaces: effect on surface chemistry, surface morphology and paper strength.* Cellulose, 2001. **8**: p. 113-125.

[26] M. Meincken, *Atomic force microscopy used to determine the surface roughness and surface polarity of different cell types of hardwoods commonly used for pulping* South African Journal of Science, 2007. **103**: p. 4-6.

2 Wood Fibres

2.1 Chemical composition of wood

The chemical components of wood can be divided into four major components: cellulose, hemicelluloses, lignin and extractives. Generally, the first three components have high molecular weights and contribute to the mass, while the extractives are of small molecular size, and only present in small quantities. Based on weight percentage, cellulose and hemicelluloses contents are higher in hardwoods compared to softwoods, while softwoods have higher lignin content [1-7].

Table 1: Average chemical composition of softwoods and hardwoods [1]

Chemical component	Weight, % of dry material	
	Softwoods	Hardwoods
Cellulose	42	45
Hemicelluloses	27	30
Lignin	28	20
Extractives	3	5

2.2 Cell wall structure

The basic model of the wood cell wall structure is well described and understood. In nature, the layers of the cell wall structure are illustrated using the wood model shown in Figure 1.

The middle lamella (ML) separates the individual cells. The first layer of the cell wall is the primary wall (P). The primary wall can be divided into an outer and an inner surface, and the arrangement of cellulose microfibrils changes

from the inner to the outer surface. The lignin content in P is relatively high and decreases towards the inner cell wall [2, 8]. The relative thickness of the primary cell wall is about 5% of the entire cell wall. The secondary wall consists of three layers: the outer layer (S1) with a thickness of about 10%; the middle layer (S2), which is the thickest layer, contributing about 75% to the cell wall; and the inner layer (S3), with a thickness of about 10%. In the S1 layer the microfibrils are oriented in a cross-helical structure and have a large micro-fibril angle. The middle layer of the secondary wall (S2) has a relatively consistent orientation of microfibrils with a smaller angle, whereas the microfibrils in the S3 layer are oriented similarly to the S1 layer [9].

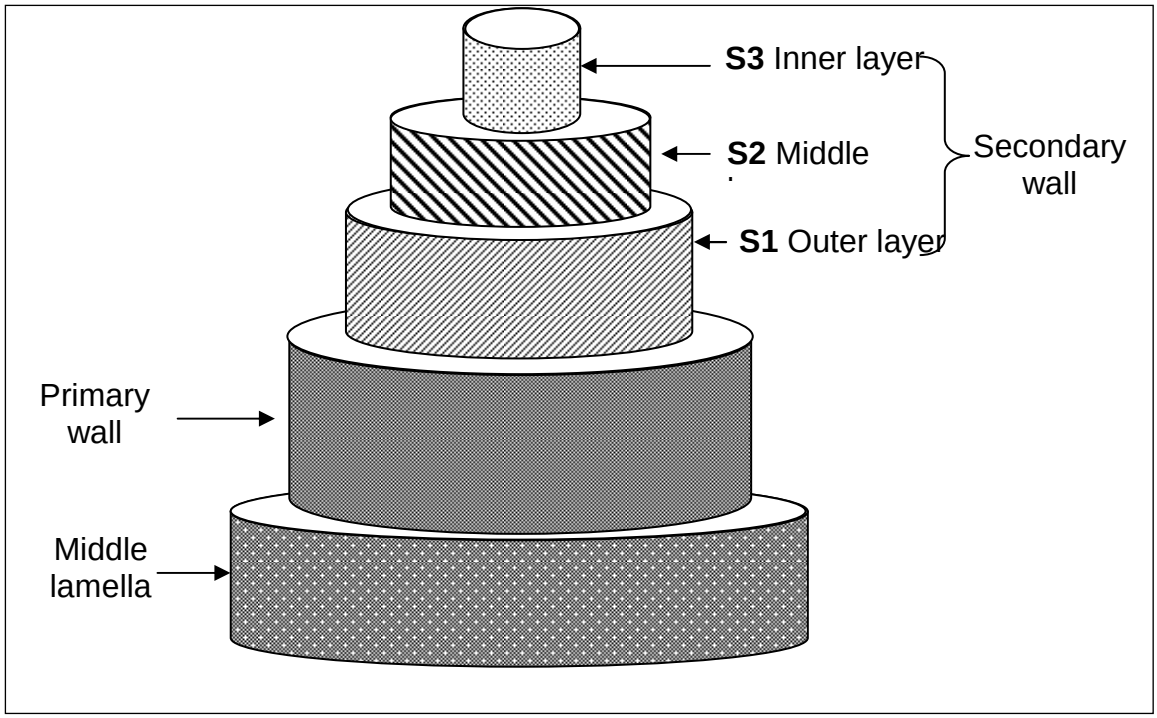

Figure 1: *Schematic illustration of the cell wall of wood cells, which generally applies to cells in both softwoods and hardwoods [9].*

2.2.1 Cellulose

Cellulose is one of the most abundant natural polymers. It is renewable, biodegradable, and can be chemically modified to obtain a range of useful products. It is a major building block of plant cells, but can also be produced enzymatically from bacterial cellulose. The most important source of cellulose

is wood, which is a natural composite of cellulose, hemicelluloses, lignin and extractives. Although cellulose and wood are abundant in nature, there are disadvantages, e.g., its expensive production (isolation), its hygroscopicity and its slow regeneration [10, 11]. Annually about 130×10^6 t of pulp are used for paper production worldwide [9]. The use of cellulose for paper manufacturing requires its isolation from the other wood components. This isolation process is called pulping.

The cellulose content of wood varies between species in the range of 40-50 % and some ligno-cellulosic materials contain more cellulose than wood. Cellulose is a linear polymer chain, which is formed by joining the anhydroglucose units into glucan chains. These anhydroglucose units are bound together by β-(1,4)-glycosidic linkages. Due to this linkage, cellobiose is established as the repeat unit for cellulose chains (Figure 2) [12].

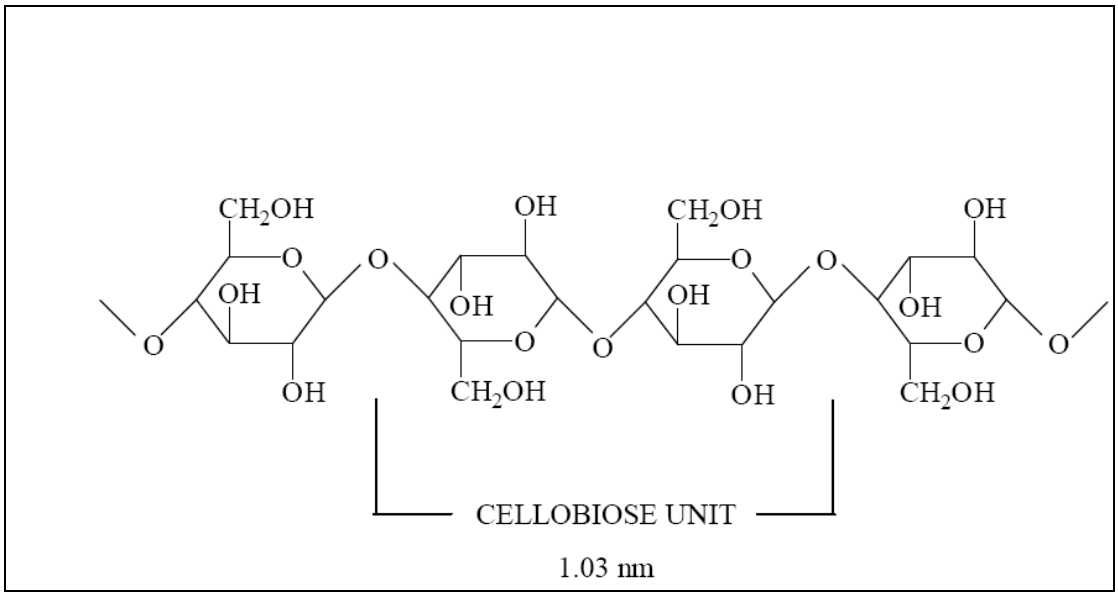

Figure 2: *Schematic illustration of a cellulose chain [12].*

The degree of polymerization (DP) of native cellulose is between 10 000 and 14 000. In industrial pulping however, cellulose is degraded to DP values of 1000–3000.

When a cellulose molecule is fully extended it takes the form of a flat ribbon with the hydroxyl groups protruding laterally. These can form both inter- and intra-molecular hydrogen bonds. These two features of the molecular structure of cellulose are responsible for its supramolecular structure and this, in turn, determines most of its chemical and physical properties [13, 14].

By forming intra- and inter-molecular hydrogen bonds between –OH groups within the same cellulose chain and the surrounding cellulose chains, the chains tend to arrange in parallel and form a crystalline supermolecular structure. Bundles of linear cellulose chains in the longitudinal direction form microfibrils, which form the skeleton of the cell wall.

The properties and functions of cellulose are mainly determined by the aggregation of the molecules into crystalline, structural fibrils. Cellulose fibrils are highly insoluble and inelastic. The native cellulose made by higher order plants is classified as cellulose I and consists of the microfibrils that contain parallel extended glucan chains. Cellulose II is formed when native cellulose is dissolved and precipitated or treated with a concentrated alkaline swelling agent and washed with water (mercerization). Cellulose II forms adjacent antiparallel glucan chains that are more thermodynamically stable [15] than cellulose I.

In order to use cellulose as a raw material for paper production, pulping processes are necessary to isolate the cellulose. The pulping processes involve of a number of purification steps, including the removal of lignin and extractives, bleaching, degradation and removal of the low molecular weight cellulose. In dissolving pulp, for example, the remaining cellulose fraction is higher than 90%, and for some applications even higher than 95%. Currently great efforts are being made to devise pulping processes that are less harmful to the environment but still yield a high cellulose content [9, 16, 17].

2.2.2 Lignin

Lignin is a three-dimensional, highly complex, cross-linked polymer that forms a large molecular structure. It provides mechanical strength to plant cells and acts as a natural adhesive between the other cell components. In order to separate fibres, lignin must be removed or weakened, which is the main aim of pulping. Lignin is dark in nature, especially after reacting with alkali, and pulp therefore needs to be bleached [3, 18].

Lignins are amorphous, mainly aromatic polymers made up of phenylpropane units (C9), which are linked together by at least ten different C–C and C–O bonds. The building blocks of lignin biosynthesis are p-coumaryl alcohol (4-{(E)-3-hydroxyprop-1-enyl}phenol), coniferyl alcohol (4-(3-hydroxy-1-propenyl)-2-methoxyphenol), and sinapyl alcohol (4-hydroxy-3,5-dimethoxycinnamyl alcohol). The monomeric building units of lignin are shown in Figure 3.

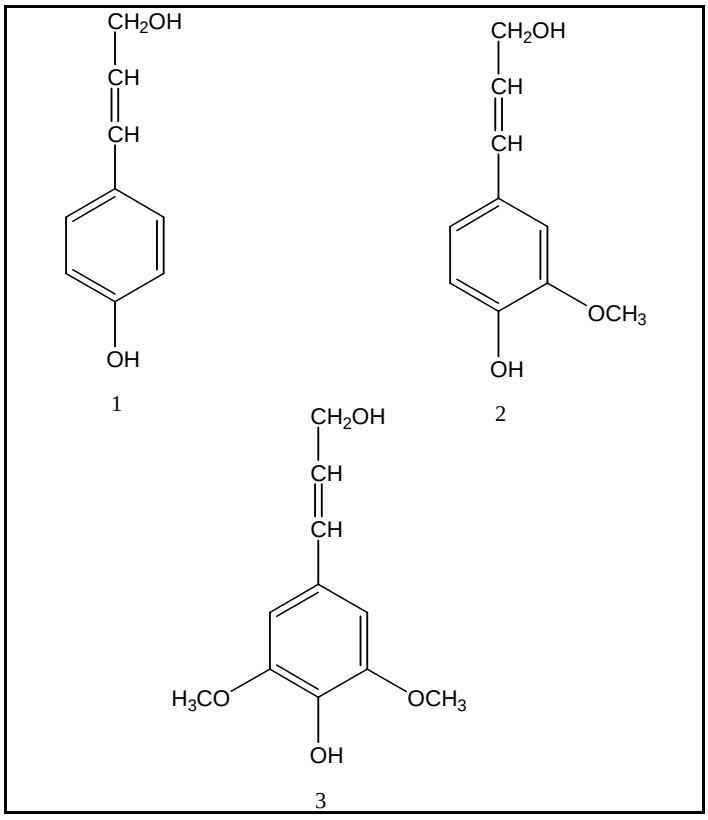

Figure 3: *The monomeric building units of lignin p-coumaryl alcohol (1), coniferyl alcohol (2), and sinapyl alcohol (3).*

p-Coumaryl alcohol is a minor precursor of both softwood and hardwood lignins, while coniferyl alcohol is the predominate precursor of softwood lignin, and coniferyl alcohol and sinapyl alcohol are both precursors of hardwood lignin [15, 19]. The lignin content of hardwoods is usually in the range 18–25%, whereas the lignin content of softwoods varies between 25 and 35%. Softwood lignin has a methoxyl content of 15–16% and hardwood of about 21%. Lignin does not have a single repeating unit like cellulose does, but instead consists of a complex arrangement of substituted phenolic units.

The irregular structure of lignin arises from its biosynthesis, in which a nonenzymatic, random recombination of phenoxyl radicals of coniferyl, sinapinyl, and *p*-coumaryl alcohols occurs. The dimeric and oligomeric intermediates, obtained in vitro in the dehydrogenative polymerisation, of coniferyl alcohol form the basis of the constitutional scheme of spruce lignin (Figure 4) proposed by Freudenberg [16, 20-23].

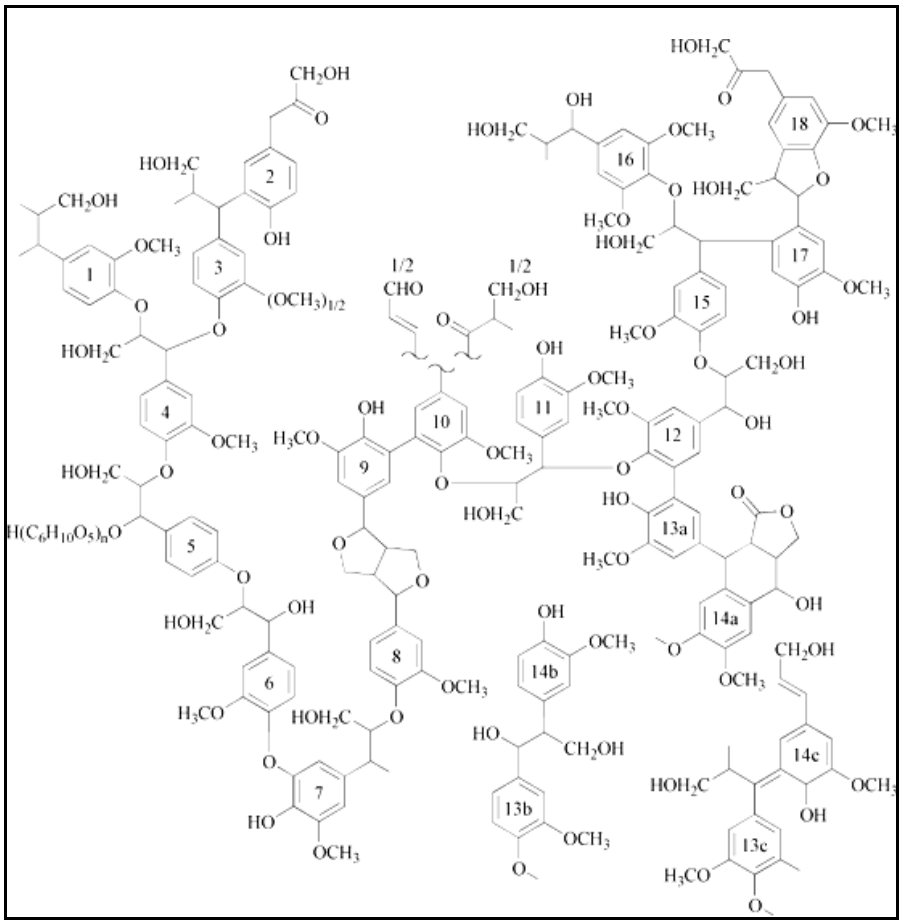

Figure 4: *Constitution of spruce lignin [20].*

Lignins are removed from wood by pulping under partial degradation and isomerisation. Lignin can be selectively removed from wood under laboratory conditions by using chlorine, chlorine dioxide, or peracetic acid [16, 24].

Lignin can be isolated from wood in several ways. Klason lignin is obtained after hydrolysing the polysaccharides with ≅ 70% sulphuric acid. It is highly condensed and does not truly represent the lignin in its native state in the wood. The polysaccharides can be isolated using enzymes to give an enzyme lignin that is much closer to a native lignin than Klason lignin. Milled wood lignin or Björkman lignin can be isolated by using a vibratory ball mill on wood, and then extracting with suitable organic solvents [9, 18]. For these experiments a technical lignin with low sulphur content, namely lignin alkali, was used. The molecular weight of lignin depends on the method of extraction. Klason lignin, since it is highly condensed, has molecular weights as low as 260 and as high as 50 million. Björkman lignin has a molecular weight of approximately 11,000.

Lignins are associated with the hemicelluloses, forming lignin–carbohydrate complexes that are resistant to hydrolysis, even under pulping conditions. There is no evidence that lignin is associated with cellulose [25]. Lignin is distributed throughout the cell wall, with the highest concentration in the middle lamella and primary cell wall. Because of the difference in the volume of the middle lamella to secondary cell wall, about 70% of the lignin is located in the primary cell wall.

2.2.3 Extractives

Extractives can be regarded as non-structural wood constituents, mostly composed of extracellular and low-molecular-weight compounds [12, 26]. Extractives consist of fats, fatty acids, fatty alcohols, phenols, terpenes, steroids, resin acids, rosin, waxes, many other minor organic compounds and inorganic materials [25, 27, 28]. They exist as monomers, dimers and polymers. Usually the extractive content in wood is less than 10% in the wood of trees from temperate zones, but in some tropical and sub-tropical wood

species the amounts can be much larger [1, 16, 29, 30]. Extractives can also be grouped according to the solvent used to extract them, as is shown in Figure 5.

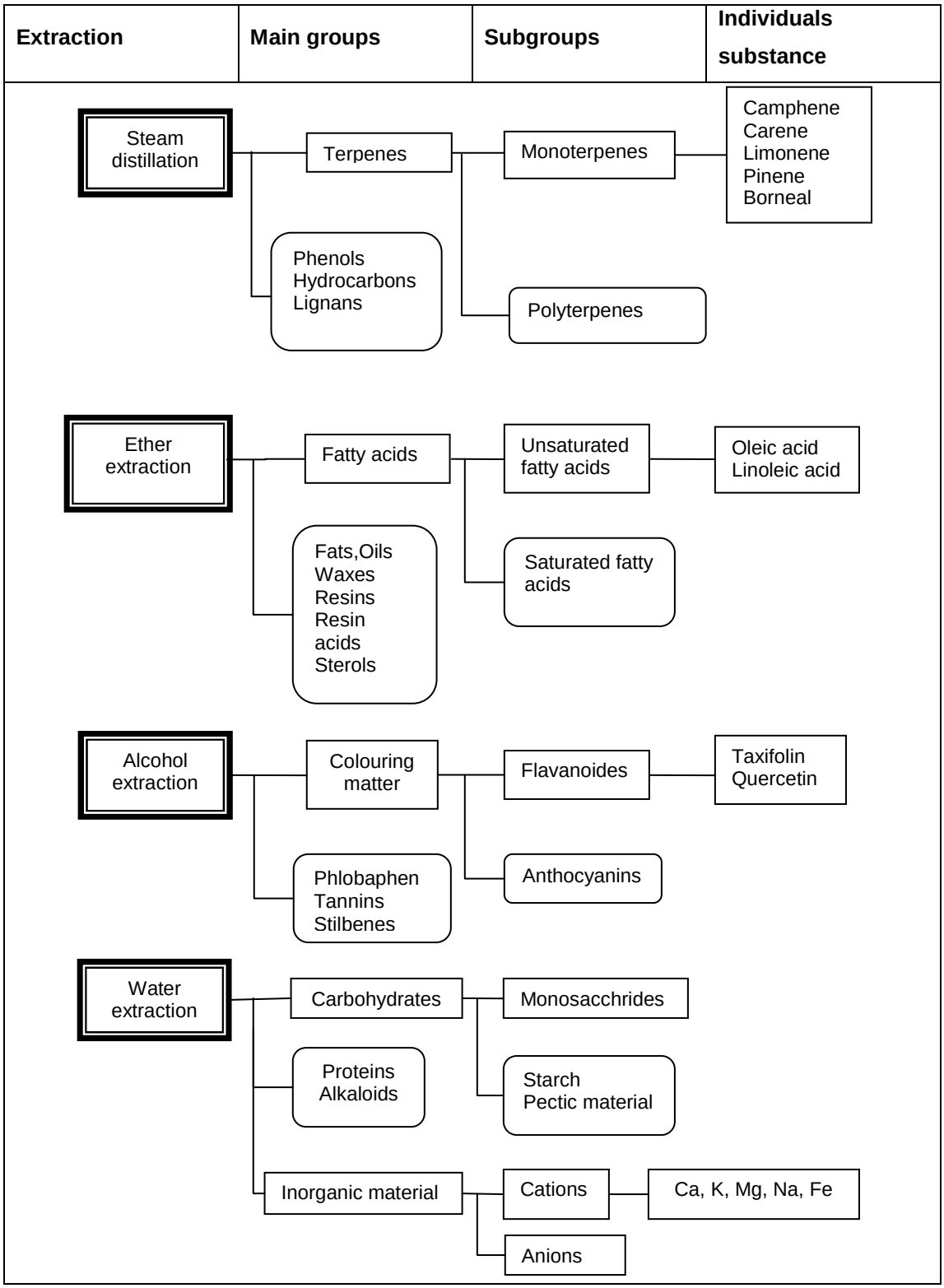

Figure 5: *Classification of the extractives with examples according to analysis groups [29].*

Some extractives commonly found in *Eucalyptus* and *Acacia* species are listed in Tables 2 and 3.

Table 2: Extractives identified in E. grandis and E. dunnii [31]

Lipophilic extractives
Fatty acids Sterols and Sterol esters Steroid ketones and hydrocarbons Mono-, di- and tri-glycerides
Essential oils
Terpenes and Terpenoids

Table 3: Extractives identified in Acacia mearnsii [15]

Nitrogenous compounds	Pipecolic acid; 4-hydroxypipecolic acid; trans-(-)-4-hydroxypipecolic acid
Carbohydrates	Fructose; Glucose; Sucrose; Pinitol
Polyphenols (flavonoids and tannins)	(-)-Fisetinitol; (+)-Fustin; (-)-Butin; Butein ; Fisetin Dimeric and trimeric polymeric Leuco-fisetinidin; (+) Mollisacacidin; (+)-2,3-trans-3,4-cis-Mollisacidin; (+)-2,3-cis-3,4-cis-Mollisacacidin; Myricitrin Quercitrin; (-)-Robinetinidol

2.3 References

[1] D. Fengel and G. Wegener, *Wood Chemistry Ultrastructure Reactions*. 1984, Berlin: Walter de Gruyter. p.10-40.

[2] B. Christopher J, *Essentials of Pulping and Papermaking*. 1993, London: Academic Press. p.1-50.

[3] L. S Johansson, J. M. Campbell, K. Koljonen and P. Stenius, *Evaluation of surface lignin on cellulose fibers with XPS.* Applied Surface Science, 1999. **144-145**: p. 92-95.

[4] Patterson, *The chemical composition of wood*, in *The Chemistry of Solid Wood.* R.M. Rowel, Editor. 1984, American Chemical Society. p. 20-35.

[5] A. Ferraz, J. Baeza, J. Rodriguez and J. Freer, *Estimating the chemical composition of biodegraded pine and eucalyptus wood by DRIFT spectroscopy and multivariate analysis.* Bioresource Technology, 2000. **74**: p. 201-212.

[6] F. P. Liu and T. G. Rials, *Relationship of wood surface energy to surface composition.* Langmuir, 1998. **14**: p. 536-541.

[7] K. Koljonen, M. Osterberg, M. Kleen, A. Fuhrmann and P. Stenius, *Precipitation of lignin and extractives on kraft pulp: effect on surface chemistry, surface morphology and paper strength.* Cellulose, 2004. **11**: p. 209-224.

[8] W. E. Hillis, *Heartwood and Tree Exudates.* 1987, Berlin: Springer-Verlag. 15-26.

[9] G. Koch, *Raw Material for Pulp*, in *Handbook of Pulp*, H. Sixta, Editor. 2006, Weinheim: Wiley. p. 21-68.

[10] J. Schurz, *A bright future for cellulose.* Prog. Polym. Sci., 1999. **24:** p. 481-483.

[11] D. F. Caulfield, J. D. Passaretti, and S. F. Sobczynski, *The structures of cellulose.* Materials Research Society, 1990. **197**: p. 89-98.

[12] R. Alen, *Structure and chemical composition of wood*, in *Forest Products Chemistry*, P. Stenius, Editor. 2000, Helsinki, Finland: Fapet Oy. p. 12-54.

[13] D. Klemm, B. Heublein, H. P. Fink, and A. Bohn, *Cellulose: fascinating biopolymer and sustainable raw material.* Angewandte Chemie International Edition, 2005. **44**: p. 3358-3393.

[14] H. T. Sahin and M. B. Arslan, *A study on physical and chemical properties of cellulose paper immersed in various solvent mixtures.* International Journal of Molecular Sciences, 2008. **9**: p. 78-88.

[15] H. H. Nimz, U. Schmitt, E. Schwab, O. Wittmann, and F. Wolf, *Wood*. Ullmann's Encyclopedia of Industrial Chemistry 2002, Weinheim: Wiley-VCH Verlag.1-54.

[16] J. C. F. Walker, *Primary Wood Processing: Principles and Practice*. 2006, Dordrecht, Netherlands: Springer. 23-67.

[17] M. Kacurakova and R. H. Wilsonb, *Developments in mid-infrared FT-IR spectroscopy of selected carbohydrates.* Carbohydrate Polymers, 2001. **44**: p. 291-303.

[18]. K. V. Sarkanen and C. H. Ludwig, *Lignins, occurrence, formation, structure and reaction*. 1971: Johe Wiley & Sons. 1-94.

[19] W. Gindl, M. Grabner, and R. Wimmer, *The influence of temperature on latewood lignin content in treeline Norway spruce compared with maximum density and ring width.* Trees, 2000. **14**: p. 409-414.

[20] A. Sakakibara, *Chemistry of lignin*, in *Wood and Cellulosic Chemistry*, N.S. Hon and N. Shirashi, Editors. 1991, Marcel Dekker: New York. p. 113-175.

[21] A. Gutierrez, P. Bocchini, G. C. Galletti, and A. T. Martinez, *Analysis of lignin-polysaccharide complexes formed during grass lignin degradation by cultures of pleurotus species.* Applied and Environmental Microbiology, 1996. **62**: p. 1928-1934.

[22] S. Y. Lin and C. W. Dence, *Carbon-13 nuclear magnetic resonance spectrometry* in *Methods in Lignin Chemistry*, C.W. Dence and S.Y. Lin, Editors. 1992, Springer-Verlag: Berlin Heideberg. p. 250-273.

[23] T. Lindstroem, C. Soeremark, and L. Westman, *The colloidal behaviour of kraft lignin.* Colloid and Polymer Science, 1977. **258**: p. 168-173.

[24] T222om-88, *Acid-insoluble lignin in wood and pulp.* TAPPI, 1988

[25] R. M. Rowell, *Handbook of Wood Chemistry and Wood Composites*. 2005, CRC Press: New York. 36-74.

[26] B. B. Sitholé, *Pulp and paper matrices analysis: introduction*, in *Encyclopedia of Analytical Chemistry*, R.A. Meyers, Editor. 2006, John Wiley & Sons. p. 8337-8360

[27] M. Nuopponena, S. Willför, A. S. Jääskeläinen, A. Sundberg, and T. Vuorinen, *A UV resonance Raman (UVRR) spectroscopic study on the extractable compounds in Scots pine (Pinus sylvestris) wood, Part II. Hydrophilic compounds.* Spectrochimica Acta Part B, 2004. **60**: p. 2963-2968.

[28] M. Nuopponena, S. Willför, A. S. Jääskeläinen, A. Sundberg, and T. Vuorinen, *A UV resonance Raman (UVRR) spectroscopic study on the extractable compounds of Scots pine (Pinus sylvestris) wood Part I: Lipophilic compounds.* Spectrochimica Acta Part A, 2004. **60**: p. 2953-2961.

[29] D. Fengel and M. Przyklenk, *Comparative extract determination for replacing benzene with cyclohexane*. Holz Roh-Werks. Vol. 41. 1983. 193-194.

[30] P. Fardim, J. Gustafsson, S. Schoultz, J. Peltonen, and B. Holmbom, *Extractives on fiber surfaces investigated by XPS, ToF-SIMS and AFM.* Colloids and Surfaces A, 2005. **255**: p. 91-103.

[31] J. Rencoret, A. Gutierrez, and J. C. del Rıo, *Lipid and lignin composition of woods from different eucalypt species.* Holzforschung, 2007. **61**: p. 165-174

3 Experimental Techniques

3.1 Atomic force microscopy (AFM)

Atomic force microscopy (AFM) is one of the most powerful techniques for surface analysis. It is a member of the family of scanning probe microscopes and can be used to study a wide variety of material surfaces, including coatings, ceramics, composites, glasses, synthetic and biological membranes, metals, polymers, and semiconductors. AFM is an information rich technique, which provides images of the surface topography and morphology on a nanometre scale [1-3]. It can also be used to study properties, such as hardness, adhesion, abrasion, friction and many other physical properties. The atomic force microscope was developed by Binnig et al. in 1986 [2] after the scanning tunnelling microscope (STM), which works well for conductive surfaces only [4-6]. AFM can generate images of a native sample surface in ambient conditions as well as under a liquid layer for non-conductive materials [1]. Schematic illustration of the atomic force microscope is shown Figure 6.

3.1.1 AFM operation

In order to obtain a topography image on a molecular level, very small interaction forces between the tip and the sample at very small distances are measured. These forces, mostly van der Waals forces, are typically in the nano-Newton range, and provide information on the material properties, such as stiffness and adhesion, in addition to the topography of the surface [4, 5].

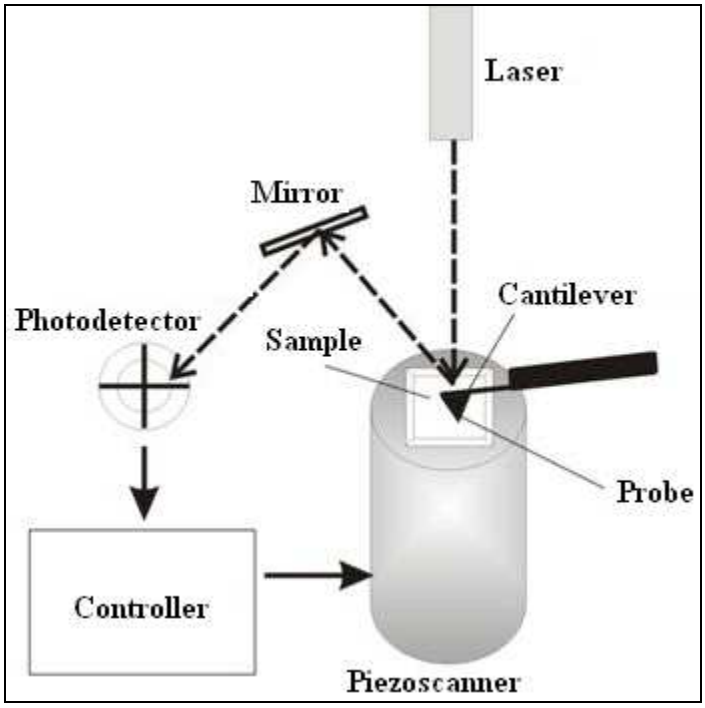

Figure 6: *Schematic illustration of the atomic force microscope, showing the probe, cantilever, photodetector, scanner, computer control and sample.*

To obtain an AFM image, a fine tip is raster scanned across a surface with a feedback control that enables the determination of inter-atomic forces acting between the tip and the sample surface. A topographical image is acquired by keeping this force at a constant value. The tips are mainly manufactured from silicon nitride (Si_3N_4) or silicon (Si), and mounted on the end of a soft, flexible cantilever. A laser beam is focused onto the back of this cantilever and reflected by a mirror into a segmented photodetector. As the tip traces the surface of the sample, moving up and down, it follows the surface features, depending on the attractive or repulsive forces, the voltage measured in the photodetector varies. Since the AFM is based on the determination of forces between the tip and sample, measuring these forces is the key to imaging the sample surface [6]. If, for example, the probe comes closer to the surface, the cantilever is bent away because of the repulsive force acting between the electrons of the surface atoms and the probe. This movement can be detected by the photodetector.

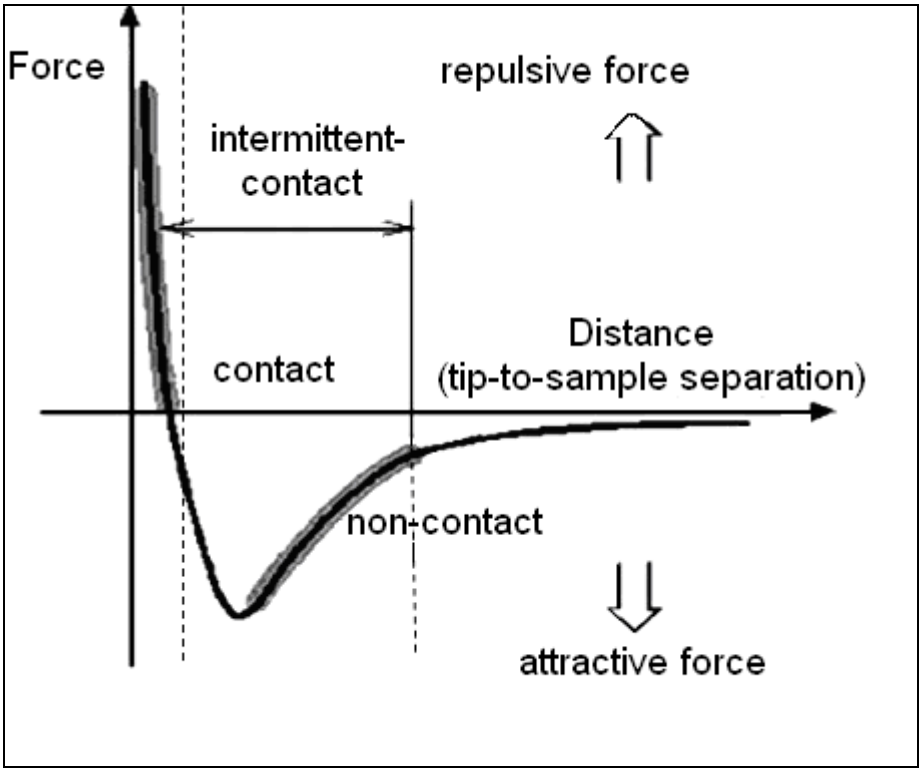

Figure 7: *Schematic illustration of the interatomic forces acting between tip/sample atoms for contact, non-contact and tapping mode imaging.*

3.1.2 Contact mode

In contact mode [4, 7], as the name suggests, the tip follows the sample in direct contact with the surface. The repulsive force acting between the tip and the sample is in the order of 10^{-9} Newton. Since this force is weak, no damage to the surface is observed.

An image is acquired by scanning the tip across the sample surface. The cantilever is deflected by repulsive forces acting between the atoms of the tip and the sample, depending on topographical changes. This cantilever deflection is measured and compared to a given set point by the control electronics. If this value is not equal to 0, the feedback system applies a voltage to the z-piezo until the set point deflection is obtained again. This voltage can be converted directly into height information in nanometers. The main problem of contact mode is the substantial frictional force as the tip

scans across the sample. These frictional forces might cause damage to soft sample surfaces or rearrange loose surface structures.

The AFM can also be operated in the static 'force-versus-distance' (*F–d*) mode, whereby the approaching/retracting tip senses interactions at the interface. The AFM probe is first lowered into contact with the sample, then slightly indented into the surface, and finally lifted off the sample surface. The cantilever deflection is measured as a function of the distance between the sample and the probe, resulting in a deflection versus distance curve. Knowing the spring constant, the cantilever deflection can be converted into a force value, which results in a force–distance curve [8]. The deflection can be converted into a force value by applying Hooke's law for small displacements:

$$F = - kx$$

where k is the spring constant and x is the displacement of the cantilever [4]. These curves can be used to study surface properties, such as the stiffness or surface polarity of a sample [9].

3.1.3 Non-contact and tapping mode

In the non-contact mode the AFM is typically operating in the attractive force range to avoid any damage to soft samples that might occur in contact mode [7, 10-12]. Attractive forces are mainly van der Waals and capillary forces. The tip is oscillated at its resonance frequency above the sample surface. A change in topography results in a change in amplitude or resonance frequency of the oscillating cantilever, which is detected by the feedback system. Again the control system applies a voltage to the z-piezo to obtain the set-point amplitude. This voltage is then converted into a topography image. Due to the larger distance between the tip and the cantilever, the resolution of non-contact images is less than for contact images.

Tapping mode provides high-resolution topographic images and overcomes the problems associated with frictional forces or the lower resolution obtained in non-contact mode. In this mode the tip is oscillated close to the surface and

intermittently contacts the sample once in each oscillation cycle, and inelastic sample deformation is therefore avoided. The cantilever is oscillated with amplitude of about 20 nm. As the oscillating tip approaches the surface the cantilever amplitude is damped and the resonance frequency shifted to lower values. This decrease in oscillation amplitude is used to image topographical surface features. The main advantages of tapping mode are for, example, that it prevents the tip from sticking to the sample surface and hence surface modifications are avoided. The adhesive forces are reduced because of the tip oscillation. There are no shear forces acting on the sample surface. Tapping mode is therefore suitable for most routine sample measurements [4].

3.1.4 Digital pulsed force mode

In the digital pulsed force mode (DPFM) [13, 14] the AFM is operated in contact mode, while a sinusoidal modulation is applied to its z-piezo. The modulation frequency is typically between 1 and 10 kHz, which is well below the resonance frequency (fr) of the cantilever (a force modulation cantilever with a nominal resonance frequency of ≈ 70 kHz). In this way force–distance curves are measured at every scan point, by continuously bringing the tip into contact with the surface and subsequently retracting it. Thus, topography and physical surface properties, such as stiffness or adhesion, can be measured simultaneously, and with the same spatial resolution. They are represented by images displaying either the topography, stiffness or the adhesive force.

As can be seen in Figure 8a, a complete force–distance cycle is carried out at every oscillation cycle. Figure 8b shows the resulting force signal as a function of time.

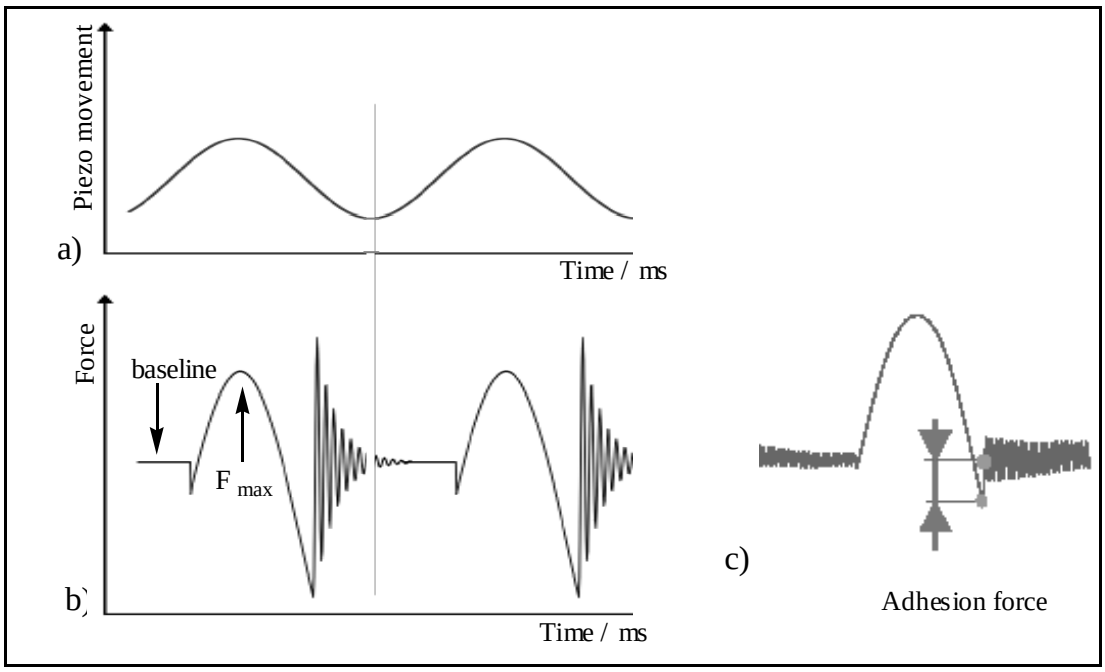

Figure 8: *a) Modulation of the z-piezo, b) force signal versus time and c) adhesion force measured for each cycle.*

At the beginning of each cycle the freely oscillating tip is above the sample surface, approaching the surface. The tip snaps into contact due to the attractive force acting between tip and sample surface. As the tip is pushed further to the sample the repulsive force reaches a maximum. Then the z-piezo withdraws and the repulsive force decreases until the tip oscillates freely again. This requires some additional force, because of the adhesive interaction between tip and surface. Once the tip has detached, the subsequent free oscillation of the probe is damped towards the baseline. After this, the cycle starts again. Because of the high amplitude, the tip jumps in and out of contact with the sample, performing a force–distance curve measurement within each cycle. The adhesion force is defined as the highest attractive force occurring while the tip jumps out of contact, as shown in Figure 8c. The stiffness signal is derived from the slope of the approaching part of the force–distance curve, and the topography image is generated from the maximum force signal, as in contact mode.

In order to quantify the adhesion measured in an adhesion image, the image can be displayed as a histogram, as shown in Figure 9. It shows the distribution of adhesive force values determined across the image and allows

the determination of an average adhesive force value and its standard deviation, which is shown as error bars in our data presentation.

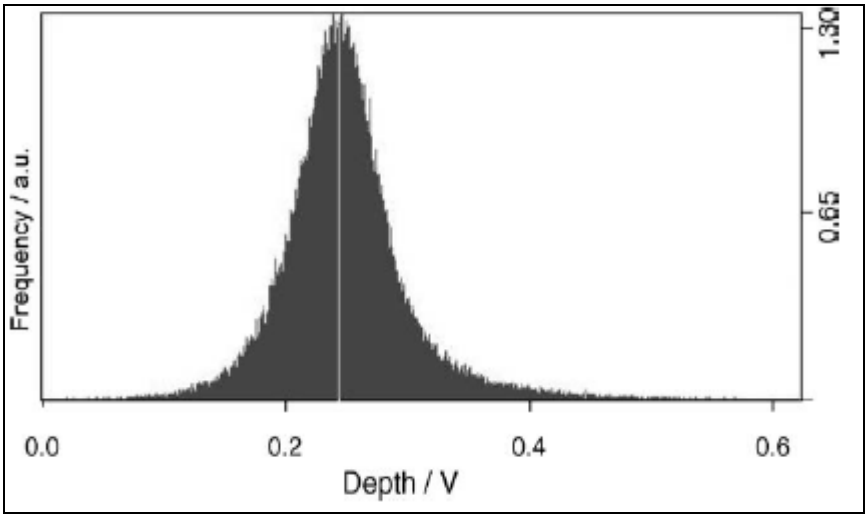

Figure 9: *Histogram of the values obtained from an adhesion image.*

The quantitative value of the adhesive force F_{adh} is given by

$$\mathbf{F_{adh} = V_{adh}kS}$$

where V_{adh} is the average voltage value determined from the adhesion image, k is the spring constant of the cantilever and S is the sensitivity of the photodiode. The spring constant k of the force modulation cantilever was 2.8 N/m [15] and the sensitivity S was determined to be 500 nm/V.

3.1.5 Resolution and noise artefacts

There are many factors that affect the image resolution and generate artefacts in AFM microscopy. These include the probe geometry and noise from the surroundings.

Probe geometry

Images acquired with an atomic force microscope represent both the probe geometry and the shape of the sample surface [16-28]. If the probe is smaller than the features of interest, the outline of these structures will be accurate

and size artefacts will be at a minimum. Blunt tips or probes with a large opening angle will cause steps to appear sloped and peaks to appear round. To obtain molecular resolution a very sharp probe with a high aspect ratio is necessary and the instrument should be operated at low forces of about 10^{-10} N [19], in order to minimize the contact area. Probes with high aspect ratio, are preferred for rough surfaces. In some cases, however, it is still possible to get accurate information from the image even if the probe diameter is slightly larger than the object being imaged [20].

Thermal noise

One of the most significant sources of noise in an AFM image is thermal noise [22-23]. Drift in the images can occur because of thermal drift in the piezoelectric scanners and because the cantilever is susceptible to external temperature changes. Drift will cause lines that should appear straight to have a curvature. To minimize the effect of the thermal drift on geometrical parameters of the image, it is necessary to carry out the imaging after thermal equilibrium has been reached between the sample and microscope stage, i.e. leave the instrument on for a few hours before imaging and then conduct the measurements with a high scanning speed [24].

Mechanical noise

Environmental vibrations produced by people moving in the building, elevators, street traffic or a person's voice are noticeable in the image [25]. This can cause the probe in the microscope to vibrate and produce artefacts in the image. Typically, these appear as localized oscillations in the image. These artefacts can be reduced using an air table that keeps the AFM level at all times and isolates it from surrounding mechanical oscillations.

Electronic noise

Image artefacts can become visible in AFM scans because of faulty or inadequate electronic components and bad isolation of components. This form of noise is as unavoidably present as the Brownian motion of the observed object and of the probe that is interacting with the objects at room temperature. Electronic artefacts most often appear as oscillations or

repeating patterns in an image. Periodic patterns can be removed by Fourier transformation, and filtering of the image, resulting in a clearer image [25].

3.2 Chemical force microscopy

Chemical force microscopy (CFM) is an AFM based technique in which a chemically modified AFM tip is used to scan the sample surface and to examine and map the distribution of chemically distinct functional groups [26-39]. Depending on the exposed functional groups and the interaction force the adhesion between the tip and sample changes. CFM maps the distribution of functional groups on the sample surface with a high resolution due to the small tip sample contact area. This resolution can be in the nanometer range.

CFM has been established as a method to probe various adhesive and repulsive interaction forces at surfaces [26, 33, 37, 40], including van der Waals forces, hydrogen bonding and electrostatic charge interactions. A chemical contrast can be obtained via adhesive forces [31] as well as frictional forces [37], using functionalised tips. The chemical contrast obtained due to adhesive forces is based on the difference in attractive intermolecular interactions, while frictional forces reflect the difference in repulsive interactions [33].

CFM allows both the imaging of surfaces with chemical specificity and the quantitative measurement of site specific interactions between the tip and sample, theoretically with a nanometer-scale resolution. For example, quantitative measurements of the Hamaker constant for tip/sample systems in various solvents have been made [34].

Although early work concentrates on the interaction between unmodified silicon nitride tips and sample surfaces [13, 41], more recent work concentrates on chemically modified tips terminated with various end groups, such as alkylsilanes [42], alkylthiols [31], DNA and proteins [22, 35, 36, 43]. The outermost functional groups on the modified tip surfaces have proven to

be dominant in the chemical interaction between the tip and sample surface. An example of this is the determination of adhesive forces measured via force-distance curves between chemically modified tips and sample surfaces containing SAMs with various terminal groups [32].

CFM has also been used to study the pull-off force (adhesion forces) on cellulose model surfaces and bleached softwood kraft pulp fibers in aqueous media [28]. It was found that for –COOH terminated tips, the adhesion forces were dependent on the pH, whereas for $–CH_3$ and –OH terminated tips the adhesion was not strongly affected by the pH.

3.2.1 Chemical functionalisation of AFM tips

To determine the adhesion between a functionalised AFM tip and a sample surface the tips are typically modified via self-assembling monolayers (SAM) consisting of organosilanes, or created from thiols on gold coated tips [46].

Despite the fact that the modification of AFM tips for chemical force measurements is relatively simple, it should be noted that details regarding the packing density of the SAMs deposited on the tip are not yet fully understood. Due to this lack of detail, careful consideration is required when quantifying the adhesive forces and molecular interactions, as the measured adhesion is correlated to the density of functional groups on the tip.

Most commercially available tips are made from silicon (Si) or silicon nitride (Si_3N_4), with a radius of 30 – 50 nm [43]. Typical AFM tips have a pyramidal geometry with an aspect ratio of about 1:2. Most commercially available tips, however, have a poorly controlled chemical surface composition, which can result in various problems. For example, the surface of the silicon based tip has a large number of silanol groups, which results in a surface that can be readily modified by the adsorption of contaminants, leading to a varying surface composition of the tip.

Obtaining control over the surface composition of the tip is therefore important and necessary to improve the general reliability of the technique. These

following sections focus on approaches used for the modification of commercially available Si or Si_3N_4 tips.

3.2.2 Alkanethiols

Chemical modification of the surface of an AFM tip is usually achieved by using functionalised alkyl thiols, which immediately form SAMs on gold surfaces [36, 45]. The thiol molecules chemisorb readily from solution onto gold via –S–H terminal groups, forming a densely packed, ordered monolayer film due to inter-chain van der Waals interactions. The tail group points away from the surface and defines the chemical characteristics of the newly generated film.

A range of functionalised alkyl thiols are commercially available, including those with methyl, amine, carboxylic acid, hydroxyl and phenyl groups [46]. The modification procedure of the tip using alkyl thiols is illustrated in Figure 10. The procedure involves the vapour deposition of a thin chromium adhesive layer (≅5 nm) onto a tip followed by deposition of a thicker gold layer (50 –100 nm). The gold-coated tip is then immersed in a dilute (0.1 – 1.0 mM) thiol solution, which results in a covalently bound monolayer that is the thiolate analogue of the thiol precursor.

These modified tips are chemically stable and mechanically robust. Indeed, an investigation of the lubrication and wear properties of such tips has clearly demonstrated a lower susceptibility to wear than uncoated Si/Si_3N_4 tips. Furthermore, thiols with a variety of terminal functionalities are commercially available or readily synthesised. Because they are easy to prepare and offer a wide range of flexibility with respect to functionalisation, thiols are extensively used for tip modification.

A possible disadvantage of this type of modification however is that the radius of the tip could increase significantly because of the metallisation process and this increase may lead to a reduction in lateral resolution. Careful control of the deposition rate is therefore important. During metallisation, one must also

avoid heating the cantilever because the differences in the thermal expansion coefficients of gold and Si/Si_3N_4 may cause irreversible bending of the cantilever.

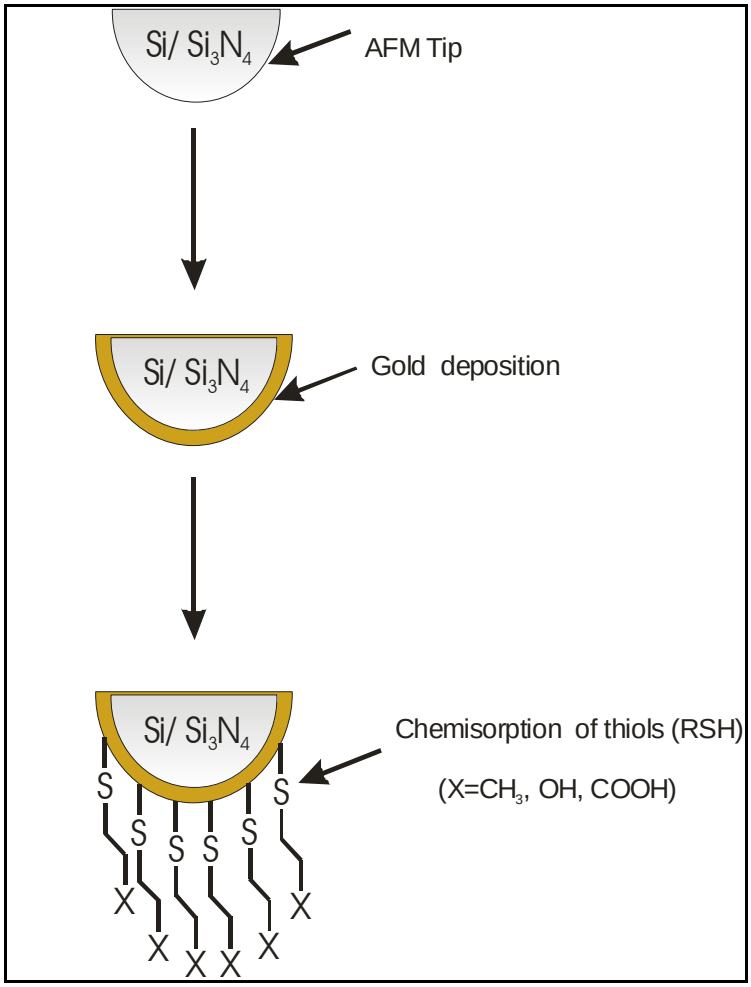

Figure 10: *Schematic of tip modification using thiol based monolayers chemisorbed on gold. The R in RSH represents an alkyl chain with terminal group X (CH_3, COOH, CH_2OH, NH_2, etc.).*

3.2.3 Organosilanes

The tips can also be modified with organosilane ($R_nSi(Y)_{4-n}$) adlayers e.g., alkyltrichlorosilane (n = 1,Y = Cl) or alkyltrialkoxysilane (n = 1,Y = OR), which directly connect to the surface silanol groups of a Si or Si_3N_4 tip [49]. The process is illustrated in Figure 11. It is often preceded by a tip-cleaning step using ozone plasma. This modification method changes the surface chemistry

of a tip without the need for prior metallisation. The formation of organosilane films begins with the hydrolysis of the silane precursor. Subsequent condensation reactions between the precursor and surface silanol result in the formation of a two-dimensional lateral network comprising Si–O–Si bonds. After drying or curing, the silane film is covalently attached to the tip with a concomitant loss of water.

Although, the first attempts to use chemically modified tips in AFM were based on the silane system, organosilanes are not used as widely for tip modification as thiols are. This could be as a result of a combination of problems with the silanisation process, including the sensitivity of chlorosilanes to moisture as well as the difficulty in controlling the polymerisation process and film thickness.

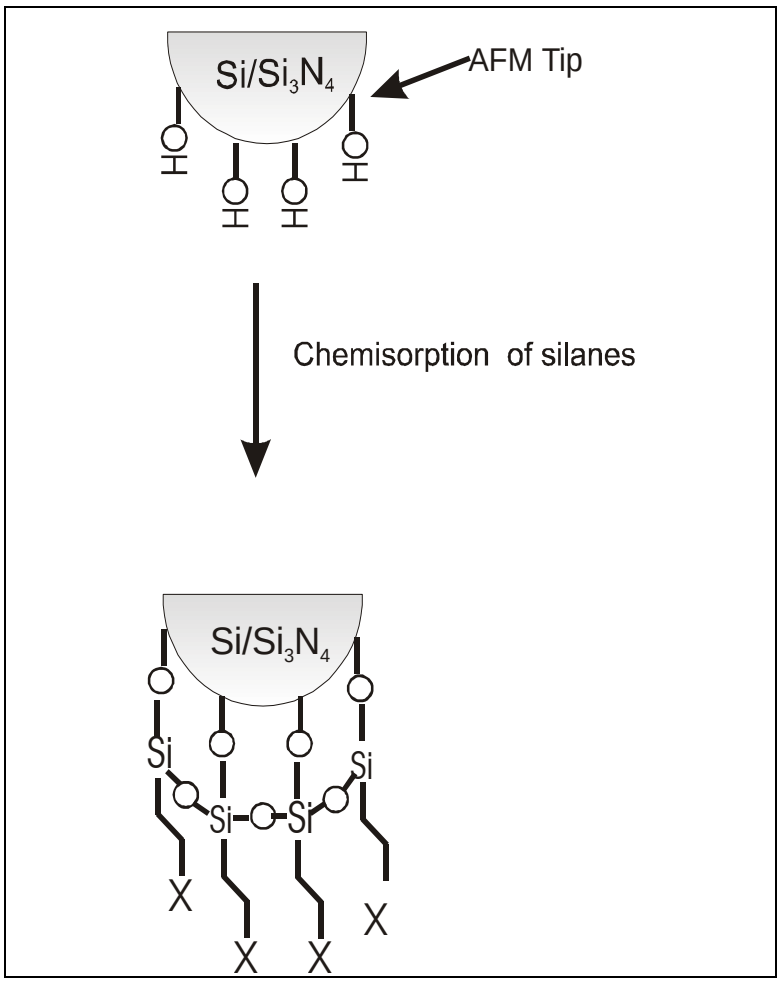

Figure 11: *Schematic of tip modification using silane based self-assembled films, where X represents different terminal groups.*

3.2.4 Colloidal particles

The AFM tip can also be functionalised by attaching micrometer-sized spheres directly onto the cantilever or tip [34]. This concept was first established by Ducker and coworkers, who used epoxy resin to adhere silica microspheres to tips with the assistance of micromanipulators [48]. Currently, silica microspheres are the most favoured of the particle based modifications because their surfaces are relatively smooth. The chemical surface composition of silica is well known and can be easily modified because of the wide range of covalent coupling reactions that can be used to attach chemical or biological materials to the surface of the sphere. A SEM image of a gold-coated silica sphere on the end of a rectangular cantilever is presented in Figure 12.

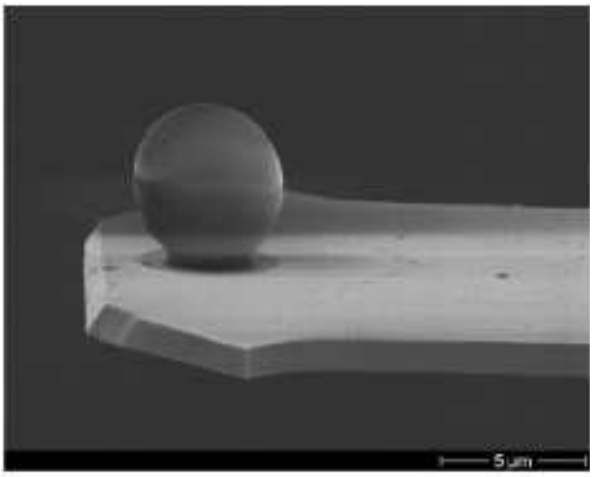

Figure 12: *SEM image of a gold-coated silica sphere on the end of a rectangular cantilever [34].*

3.2.5 Effect of the environment

The environmental conditions under which adhesion measurements are conducted are also an important consideration [44]. Under ambient laboratory conditions, surfaces are exposed to organic compounds contained in the air. Humidity might lead to a layer of condensed water. The water layer between the tip and sample will add a capillary force to the measured adhesion and its presence can overwhelm the adhesion originating from the interaction of the functionalised tip and the sample. This would emphasise the relative degree

of polarity (hydrophilicity) and can be the basis for discriminating between hydrophobic and hydrophilic groups when imaging under ambient conditions [40].

To reduce capillary forces, many studies are carried out in liquid or ultrahigh vacuum. In liquid environments, the nature of the solvent will influence the measured adhesion for a given pair of interacting surfaces, due to the effect of solvent exclusion. Furthermore, the pH and ionic strength of the water environment can control the measured adhesion in the presence of any surface-bound charges.

The effect of topography on the adhesive force in CFM was studied by Sato et al. [49] with PFM-AFM on two surfaces: (i) an Au(111)-terrace-rich gold film prepared by vacuum vapour deposition at high temperature and (ii) a gold film sputtered on a cover glass with different grain sizes obtained, using different deposition times. They found that a variation in the grain sizes and the change in the resulting multiple tip/sample contacts (e.g. if the grain size becomes too large at a close packing density) resulted in different distribution widths of the observed adhesion forces, although it did not change the average adhesion value.

The effect of the surface topography on the adhesive force arises when convex surface structures are in the same size range as the tip. This might increase the detected adhesive force on the side or between structures because of the multiple contacts. This problem did not occur with the samples investigated in this study.

Despite these shortcomings, the obvious advantage of AFM as a tool for the surface characterisation of pulp fibres is the simultaneous acquisition of a high resolution (<10 nm) topography images and spatial chemical information of the observed area.

3.3 Surface forces

The chemical nature of surfaces determines most of their characteristics, such as surface tension and adhesion. The outer atomic layers with a characteristic action radius determine the magnitude of the different interaction types that contribute to the excess free energy of a surface [50]. A typical atom in the bulk is surrounded by its neighbours and experiences forces in all directions due to interatomic interactions. The resulting interatomic force fluctuates in equilibrium around a zero value [50]. Atoms at the surface, on the other hand, are only interacting with the atoms below or beside them. The net resulting force is directed towards the interior and its value depends on pair- and multi-atomic forces within the action radius. Whereas the first neighbour atoms make the strongest contributions, there are also non-zero force contributions from second, third, etc. atoms below the particular surface atom that need to be considered. These make an effective contribution to acting surface forces (and to surface tension) up to a characteristic distance of a few atomic layers. Thus the determination of surface tension results in values averaged over a technique-characteristic action radius, typically in the range of a few nanometres in the AFM. In multi-component systems with different atoms and molecules all the different interaction types contribute to the macroscopic surface tension. Techniques determining surface tension therefore average over several types of atoms and several interaction radii [51].

Differences in surface tension or surface free energy and in adhesion for different substances are a result of different interatomic forces. These forces are, for example, responsible for the work required to separate two contacting bodies to infinite distance. These intermolecular forces could be ionic, dipole-dipole, ion-dipole interactions, induced dipolar forces, van der Waals interactions, hydrophobic and hydrophilic, structural, and hydration forces; and steric and fluctuation forces [52].

The thermodynamic work of adhesion (W_A) is defined as the reversible change in free energy required separating two phases from contact to infinity.

The corresponding work of adhesion (and cohesion for similar bodies) can then be expressed through the surface tension.
Generally, to separate the surfaces of two materials 1 and 2 in a medium 3, the work W_{132} is required [50, 53]. This can be expressed as:

$$W_{132} = W_{12} + W_{33} - W_{13} - W_{23}$$

This equation includes the creation of a new 1–3 and 2–3 interface at the expense of breaking up the contact area 1–2 and expanding the medium 3 by two unit areas to cover both sides of the originally contacting bodies.

The basic concept in CFM is to detect adhesive forces while scanning with a chemically specific contrast [40, 54]. For a full force characterisation, both the magnitude and direction of the force are needed. However, AFM typically records the lateral and the normal component separately [55]. It is also assumed that the usual measurement geometry applies, i.e. the sample surface is horizontal compared to the size range of the tip and the tip forms an angle about 45^{o} with the sample surface. The magnitude of the lateral component, i.e. the friction force, depends on the normal load, which is the sum of the vertical load and the normal component of the surface adhesion and elastic deformation forces, respectively.

In order to image with chemical sensitivity (either based on adhesion, or on friction force arising from chemical differences) it is necessary to understand the physical origins of the pull-off force, i.e. the separation of atoms from the sample surface and tip, detected in force–distance curves. During an AFM force–distance cycle, the contact between tip and sample is first established during approach and then broken during withdrawal [12]. The radius of the contact areas between AFM tip and sample are ideally small (depending on the tip quality), typically in the range of several tens of nanometers for imaging [52].

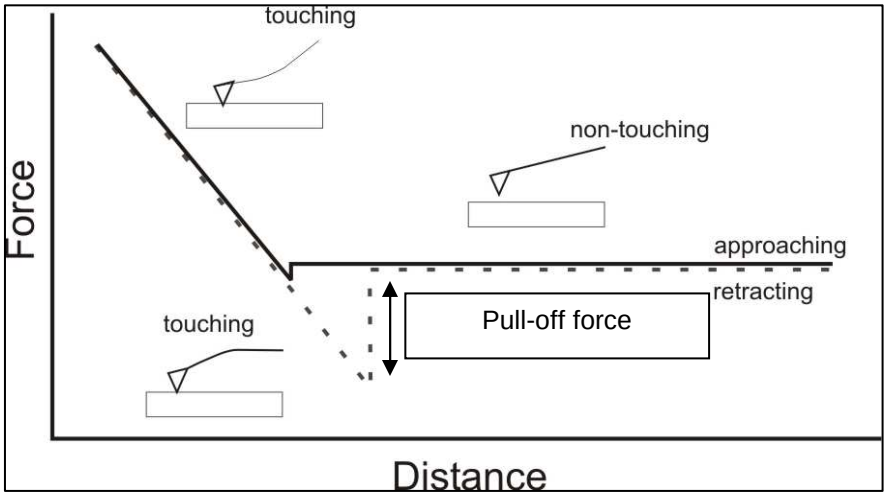

Figure 13: *Schematic diagram of a general approach and retract distance–force curve.*

To quantitatively describe the pull-on and pull-off forces, theories related to (continuum) contact mechanics and related work of adhesion are taken into account. It is also of interest to consider whether the macroscopic contact mechanics theories break down at a level of only a few contacting pairs of atoms or molecules [51]. The most relevant results of contact mechanics theories, relevant to AFM adhesion and chemical mapping studies, are summarised below.

To quantify adhesion energies from AFM measurements, the model developed by Johnson, Kendall, and Roberts (JKR model) is frequently used for the analysis of data obtained by force–distance spectroscopy [40]. In the JKR model the adhesion force (AFM pull-off force) is related to the work of adhesion, W_{adh}, and the reduced radius, *R,* of the tip-surface contact:

$$\mathbf{F_{adh} = -3/2(\pi R W_{adh})}$$

The work of adhesion is a combination of the tip-surface (γ_{ts}), tip-solvent (γ_{l}) and surface-solvent (γ_{sl}) interfacial energies ($W_{adh} = \gamma_{sl} + \gamma_{tl} - \gamma_{ts}$) and for tip surface combinations that have the same chemical composition the surface energy may be estimated directly from the adhesion measurement as W_{adh}. The effective contact radius at separation, r_s, from the JKR model is given as:

$$r_s = [3\pi(W_{adh}\, R^2/2K)]^{1/3}$$

where *K* is the reduced elastic modulus of the tip and surface [46]. Using the contact area at separation and the assumed packing density of the molecules at the surfaces in contact, an estimate of the adhesive force or interaction energy on a per molecule basis can be made.

The accuracy of the interfacial energies and the values per molecule obtained with this approach must, however, be carefully considered, due to the error accumulation given by the imprecise knowledge of the contact area, tip radius, molecular packing density of the modified surface, as well as the associated elastic properties of the contact at the monolayer level. As the details of the elastic properties of self-assembled monolayers are generally not known, the elastic properties are typically assumed to be dominated by the underlying substrate (Au, Si, mica, Si_3N_4, SiO_2).

Another model to quantify the adhesive interaction, based on Poisson statistics for the statistical evaluation of single bond forces without consideration of the tip sample contact details, was suggested by Beebe et al. [56]. The disadvantage of this model, however, is that an absolutely homogeneous chemical system is assumed with only one type of chemical interaction that contributes to the measured adhesion.

A number of other contact mechanics theories have been put forward. These are however not described in detail here, because of their limited relevance. These theories differ in their assumptions and limitations and yield different expressions for the pull-off force [4, 51].

The most important models for AFM application include:

- The Derjaguin-Muller-Toporov (DMT) theory, which assumes that the attractive force between the surfaces has a finite range and acts outside

the contact zone, where the surface shape is not affected by interfacial forces.

- The Burnham-Colton-Pollock (BCP) theory, which further improves the contact profile by adding a long-range attractive force outside the area of contact. The surfaces are assumed to bulge towards each other on approach.

- The Maguis theory, which models the interface as an opening crack. The influence of each parameter (surface energy or sphere radius and stiffness) on contact area is recognised in a dimensionless parameter.

Quantitative values of stiffness and surface energy are, however, difficult to obtain [57].

3.4 Scanning electron microscopy (SEM)

Topography or morphology is an important surface characteristic that influences the physical properties of materials such as wettability, adhesion, and biocompatibility. Electron microscopy provides valuable information about the three-dimensional microstructure of surfaces. Any type of dry specimen can be analysed by this technique [58].

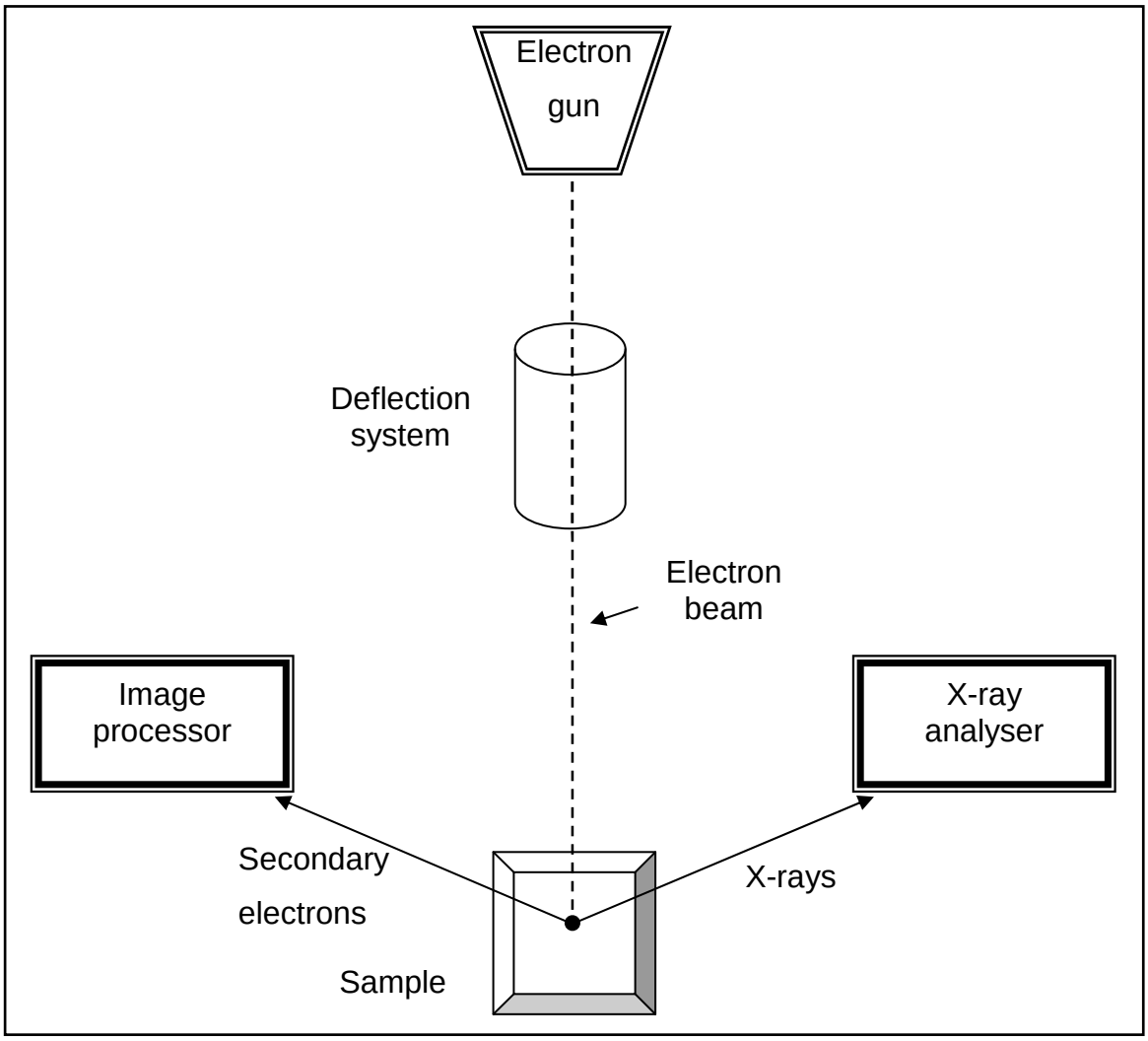

Figure 14: *Schematic diagram of scanning electron microscopy instrumentation with an X-ray detector for chemical composition analysis, EDX [22].*

SEM uses electrons as a source, which produces high resolution images. Figure 14 shows a typical SEM setup. Samples are placed in a vacuum chamber that contains an electron gun. The emitted electrons travel through a series of magnetic lenses designed to focus the electrons on a very fine spot on the sample. As the electron beam hits the sample secondary electrons are released, and these can be detected [22].

Because of the shallow penetration depth of the primary electrons only the secondary electrons generated near the surface can escape and be detected. A detector counts these electrons and sends the signal to an amplifier. The

final image is built from the number of electrons emitted from each scanned point.

Samples have to be electrically conductive to be suitable for SEM imaging. The surfaces of non-conductive samples, such as polymers, need to be coated with a thin layer of metal, typically gold, to minimise negative charge accumulation from the electron beam.

3.4.1 Energy dispersive x-ray (EDX) analysis

EDX is a very useful technique to determine the elemental composition of sample surfaces. The primary electron beam of the SEM causes the emission of X-rays from the sample atoms. EDX detects the energy of these emitted X-rays to identify the elements present in the sample [59, 60] (qualitative analysis). The rate of detection of these characteristic x-rays is used to measure the amount of the present elements (quantitative analysis). If the electron beam is raster scanned over an area of the sample, the EDX system can also acquire an X-ray map showing the spatial distribution of elements on the surface. EDX provides the elemental composition of the surface for elements from boron through to uranium [61]. The technique is sensitive to elements of approximately 0.1 wt % and can probe depths from 0.2 to 8 mm, depending on the energy of the electron beam used and the average atomic number of the sample.

SEM provides spatial resolution of the surface in the nanometer range. Together with the topography image, an elemental map of the same area can be acquired to aid the analysis. For unknown samples, this is frequently the analytical technique of choice for initial analysis.

SEM/EDX has become one of the most important techniques to analyse the morphology of wood materials [62]. It has also been used to analyse the distribution of metal in wood impregnated with aqueous solutions of metal salts [59]. A typical example of an EDX spectrum of a silicon AFM tip is shown in Figure 15.

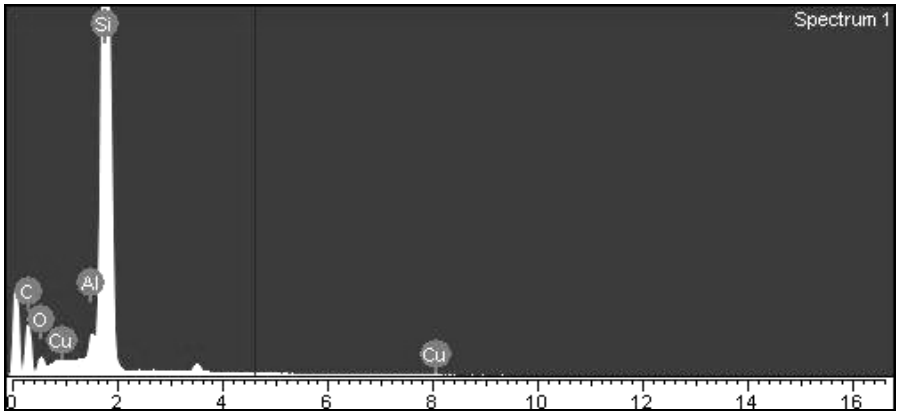

Figure 15: *An example of an EDX spectrum of a silicon AFM tip.*

3.5 Attenuated total reflectance Fourier-transform infrared spectroscopy (ATR-FTIR)

FTIR spectroscopy has been used extensively to analyse organic materials including polymers. Molecular structure, inter- and intra-molecular interactions, conformation, crystallinity as well as the orientation of organic compounds have all been studied using infrared spectroscopy (IR) for many decades [63 64]. It is also a powerful tool for wood analysis [65, 66]. In combination with ATR, FTIR analysis permits reproducible qualitative and quantitative analysis of solid samples with little or no sample preparation required [67]. ATR-FTIR has proven very useful for the analysis of solid sample surfaces making it one of the most widely used surface, characterisation techniques [68].

For many chemical compounds the infrared spectrum is a fingerprint, which may be used for identification of chemical constituents. As the beam of the infrared is passed through a sample (or reflected off a sample) certain frequencies are absorbed by the sample's inter-atomic bonds. The absorbed frequencies are measured by an interferometer and can be related to the chemical structures present in the sample. The energy absorbed can be expressed as in the following equation [69]:

$$E = (n + ½)\, h\, v$$

n = particular energy level (0, 1, 2,…), h = Planck's constant (6.63×10^{-27} P/s), v = vibrational frequency.

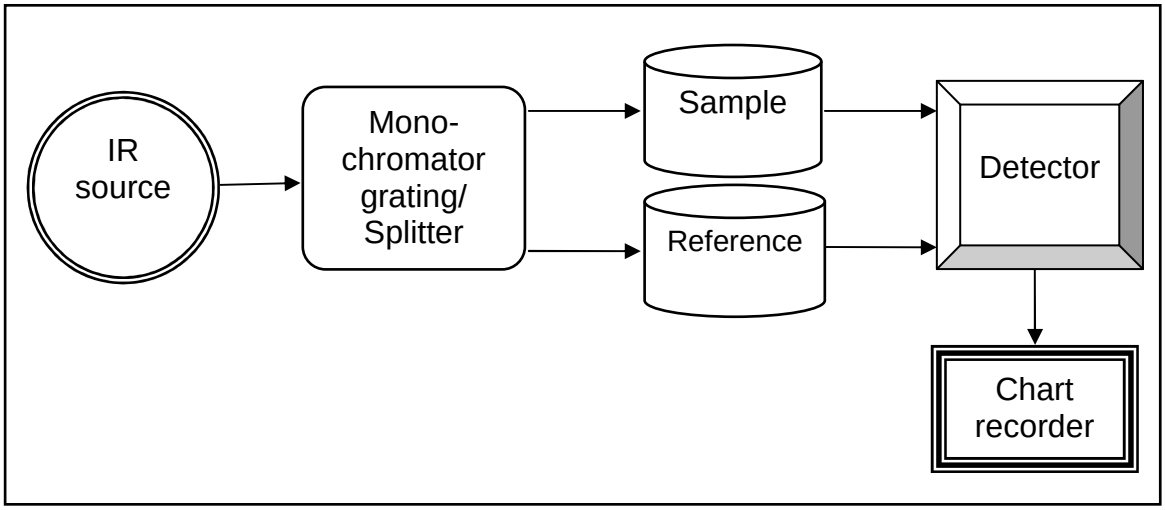

Figure 16: *Schematic representation of a modern FTIR spectrometer [69].*

The energies required to cause a vibrational transition can be found in the IR region of the electromagnetic spectrum, whereas rotational energies are several hundred times smaller (microwave and far IR region). IR spectroscopy is therefore a useful technique to analyse molecules containing polar groups [70]. Homo-nuclear diatomic molecules are IR inactive because their dipole moments remain zero. A schematic representation of a FTIR spectrometer is shown in Figure 16.

The main difference between FTIR and dispersive IR is the interferometer which replaces the monochromator and the slit found in dispersive IR instruments. The interferometer measures all the frequencies simultaneously and produces a unique type of encoded signal, which is called an interferogram. An interferogram contains the information for every data point (a function of the moving mirror point) which constitutes the signal for every infrared frequency from the source. This results in extremely fast measurements. Decoding of individual frequencies from the interferogram to a spectrum is operated by a mathematical technique called a Fourier

transformation. The Fourier transform converts an intensity versus time spectrum into an intensity versus frequency spectrum [70].

There are three basic sampling modes to study surfaces using FTIR techniques: transmission, internal reflection, and external reflection. ATR is one of the most widely used accessories for FTIR because of the ease of sampling and, of all the FTIR techniques, it is the most useful for the surface characterisation of solid samples [71]. A schematic diagram of an ATR element is shown in Figure 17.

When the infrared radiation passes through the ATR crystal it reflects at the surface of the sample. However, the sample in contact with the internal reflection elements (IRE) absorbs part of the radiation. The IRE are IR-transparent crystals such as iodide-thallium bromide (KRS-5), germanium (Ge), aluminum oxide (Al_2O_3), silicon (Si), zinc selenide (ZnSe) and diamond.

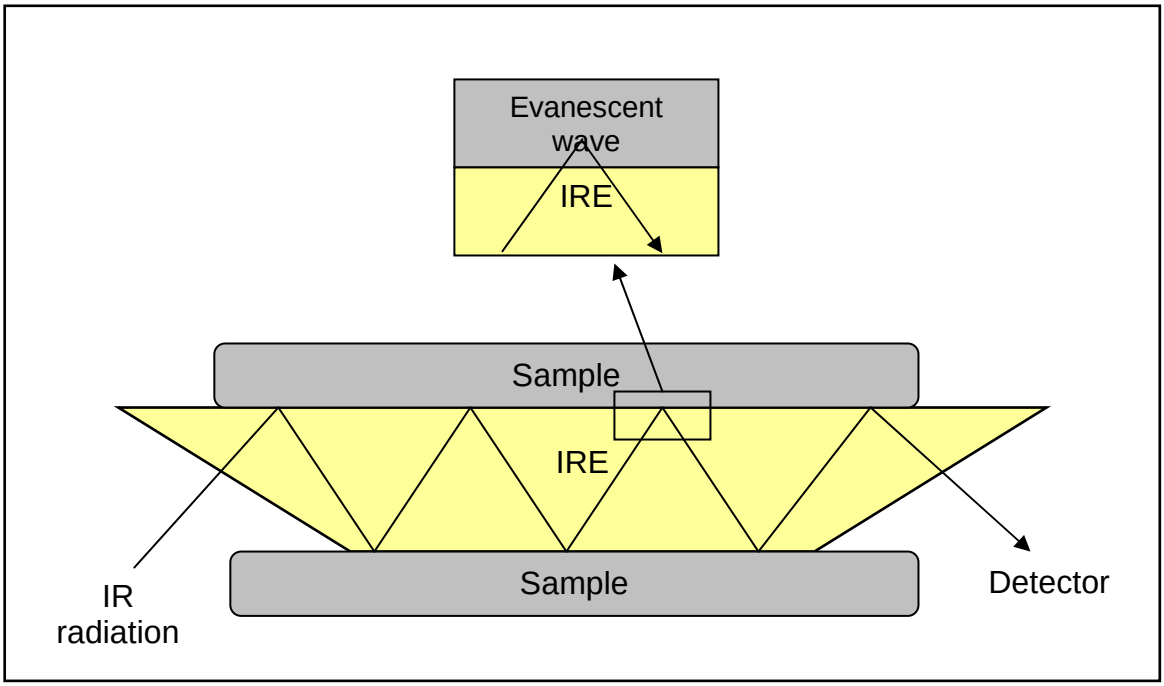

Figure 17: *Schematic diagram of ATR at the interface of an IRE [72].*

At each reflection, the absorbed radiation's electric field penetrates a small distance into the sample (evanescent wave). The penetration distance is determined by the following equation [72]:

$$d_p = \frac{\lambda}{2\pi n_{crystal}\left[\sin^2\theta - \left(\frac{n_{sample}}{n_{crystal}}\right)^2\right]^{\frac{1}{2}}}$$

λ is the wavelength, $n_{crystal}$ and n_{sample} are refractive indexes of the ATR crystal and sample, respectively, and θ is the angle of incidence. The depth of penetration can be altered by varying the wavelength and angle to achieve the depth profile. Although, little or no sample preparation is required for the ATR technique, it is however essential for samples to have a good contact with the crystal in order to obtain a high quality spectrum.

3.6 References

[1] G. Binnig, H. Rohrer, C. Gerber, and E. Weibel, *7 x 7 Reconstruction on Si (111) resolved in real space.* Physical Review Letters, 1983, **50**: p. 120-123.

[2] G. Binnig, C. F. Quate, and C. Gerber, *Atomic force microscope.* Physical Review Letters, 1986. **56**: p. 930-933.

[3] L. Xu, X. W. Yao, L. P. Zhang, M. Q. Li, and F.J. Yang, *Interpretations of atomic-resolution images in atomic-force microscop,.* Physical Review B, 1995. **51**: p. 10013-10017.

[4] S. N. Magonov, *Atomic force microscopy in analysis of polymers*, in *Encyclopedia of Analytical Chemistry*, R.A. Meyers, Editor. 2000, Wiley. New York, p. 7433-7490.

[5] L. A. Bottomley, E. D. Gadsby, and M. A. Poggi, *Microscopy techniques/atomic force and scanning tunneling microscopy*, in *Encyclopedia of Analytical Science*, P. Worsfold, A. Townshend, and C. Poole, Editors. 2005, Elsevier Academic Press: Maryland Heights, p. 397-408.

[6] H. Y. Nie, M. J. Walzak, and N. S. Mclntyre, *Atomic force microscopy study of biaxially-oriented polypropylene films.* International Surface Engineering Congress, 2003: p. 293-302.

[7] P. A. Maurice, *Applications of atomic-force microscopy in environmental colloid and surface chemistry.* Colloids Surface A, 1996. **107**: p. 57-75.

[8] M. C. Davies S. O. Vansteenkiste, C. J. Roberts, S. J. B. Tendler and P. M. Williams, *Scanning Probe Microscopy of Biomedical Interfaces.* Progress in Surface Science, 1998. **S7**(2): p. 95-136.

[9] M.J. Walzak H.-Y. Nie, B. Berno, N.S. Mcintyre, *Atomic force microscopy study of polyproylene surfaces treated by UV and ozone exposure: modification of morphology and adhesion force.* Applied Surface Science, 1999. **144-145**: p. 627-732.

[10] R. Erlandsson and P. Apell, *Progress in scanning probe microscopy: high resolution force microscopy and spectroscopy.* Current Science, 2000. **78**: p. 1445-1458.

[11] M. Meincken and R. D. Sanderson, *Advantages of scanning probe microscopy in polymer science.* South Africa Journal of Science, 2004. **100**: p. 256-260.

[12] P. A. Maurice, *Applications of atomic-force microscopy in environmental colloid and surface chemistry.* Colloids and Surfaces A, 1996. **107**: p. 57-75.

[13] O. Marti, T. Stifter, H. Waschipky, M. Quintus, and S. Hild, *Scanning probe microscopy of heterogeneous polymers.* Colloids and Surfaces A, 1999. **154**: p. 65-73.

[14] H. Krotil, T. Stifter, H. Waschipky, K. Weishaupt, S. Hild, and O. Marti, *Pulsed force mode: a new method for the investigation of surface properties.* Surface and Interface Analysis, 1999. **27**: p. 336-340.

[15] Nanoworld, product guide 2006. http://www.nanoworld.com. [cited 27/07/2009]

[16] W. A. Hofer, A. S. Foster, and A. L. Shluger, *Theories of scanning probe microscopes at the atomic scale.* Reviews of Modern Physics, 2003. **75**: p. 1287-1332.

[17] M. R. Jarvis, R. Pérez, and M. C. Payne, *Can atomic force microscopy achieve atomic resolution in contact mode?* Physical Review Letters, 2001. **86**: p. 1287-1291.

[18] U. D. Schwarz, H. Holscher, and R. Wiesendanger, *Atomic resolution in scanning force microscopy: concepts, requirements, contrast mechanisms and image interpretation.* Physical Review B, 2000. **62**: p. 13089-13098.

[19] F. M. Ohnesorge, *Intricate stepline artifact can mimic true atomic resolution in atomic force microscopy.* Physical Review B, 2000. **61**: p. 5121-5125.

[20] S. S. Sheiko, *Imaging of polymers using scanning force microscopy: from superstructures to Individual molecules.* Advances in Polymer Science, 2000. **151**: p. 61-174.

[21] F. J. Giessibl, *Advances in atomic force microscopy.* Reviews of Modern Physics, 2003. **75**: p. 949-984.

[22] S. M. Lindsay, *The scanning probe microscope in biology*, in *Scanning Probe Microscopy and Spectroscopy*, D. Bonnell, Editor. 2000, wiley. p. 290-330.

[23] F. Gittes. C. F. Schmidt, *Thermal noise limitations on micromechanical experiments.* European Biophysics Journal, 1998. **27**: p. 75–81.

[24] W. Stocker, S. N. Magonov, H. J. Cantow, J. C. Wittmann, and B. Lotz, *Contact faces of epitaxially crystallized α- and γ-phase isotactic polypropylene observed by atomic force microscopy.* Macromolecules, 1993. **26**(22): p. 5915-5923.

[25] P. West and N. Starostina. *A guide to AFM image artifacts*. Pacific Nanotechnology. 2002, http://www.cma.fcen.uba.ar/files/Guide_AFM. [cited 10/05/2005]; 1-12].

[26] D. V. Vezenov, A. Noy, and P. Ashby, *Chemical force microscopy: probing chemical origin of interfacial forces and adhesion.* Journal of Adhesion Science and Technology, 2005. **19**: p. 313-364.

[27] D. I. Kreller, G. Gibson, G. W. VanLoon, and J. H. Horton, *Chemical force microscopy investigation of phosphate adsorption on the surfaces of iron(III) oxyhydroxide particles.* Journal of Colloid and Interface Science, 2002. **254**: p. 205-213.

[28] J. C. Bastidas, R. Venditti, J. Pawlak, R. Gilbert, S. Zauscher, and J. F. Kadla, *Chemical force microscopy of cellulosic fibers.* Carbohydrate Polymers, 2005. **62**: p. 369-378.

[29] Y. Okabe, U. Akiba, and M. Fujihira, *Chemical force microscopy of –CH_3 and –COOH terminal groups in mixed self-assembled monolayers by pulsed-force-mode atomic force microscopy.* Applied Surface Science, 2000. **157**: p. 398-404.

[30] Y. Okabe, M. Furugori, Y. Tani, U. Akiba, and M. Fujihira, *Chemical force microscopy of microcontact-printed self-assembled monolayers by pulsed-force-mode atomic force microscopy.* Ultramicroscopy, 2000. **82**: p. 203-212.

[31] N. J. Brewer and G. J. Leggett, *Chemical force microscopy of mixed self-assembled monolayers of alkanethiols on gold: evidence for phase separation.* Langmuir, 2004. **20**: p. 4109-4115.

[32] M. Fujihira, Y. Tani, M. Furugori, U. Akiba, and Y. Okabe, *Chemical force microscopy of self-assembled monolayers on sputtered gold flms patterned by phase separation.* Ultramicroscopy, 2001. **86**: p. 63-73.

[33] S. C. Clear and P. F. Nealey, *Chemical force microscopy study of adhesion and friction between surfaces functionalized with self-assembled monolayers and immersed in solvents.* Journal of Colloid and Interface Science, 1999. **213**: p. 238-250.

[34] S. Gourianova, N. Willenbacher, and M. Kutschera, *Chemical force microscopy study of adhesive properties of polypropylene films: influence of surface polarity and medium.* Langmuir, 2005. **21**: p. 5429-5438.

[35] M. Fiorini, R. McKendry, M. A. Cooper, T. Rayment, and C. Abell, *Chemical force microscopy with active enzymes.* Biophysical Journal, 2001. **80**: p. 2471-2476.

[36] D. A. Smith, S. D. Connell, C. Robinson, and J. Kirkham, *Chemical force microscopy: applications in surface characterisation of natural hydroxyapatite.* Analytica Chimica Acta, 2003. **479**: p. 39-57.

[37] A. Noy, C. D. Frisbie, L. F. Rozsnyai, M. S. Wrighton, and C. M. Lieber, *Chemical force microscopy: exploiting chemically-modified tips to quantify adhesion, friction, and functional group distributions in molecular assemblies.* Journal of the American Chemical Society, 1995. **117**: p. 7943-7951.

[38] Y. Sugimoto, P. Pou, M. Abe, P. Jelinek, R. Pe´rez, S. Morita, and O. Custance, *Chemical identification of individual surface atoms by atomic force microscopy.* Nature, 2007. **446**: p. 64-67.

[39] A. Noy, C. H. Sanders, D. V. Vezenov, S. S. Wong, and C. M. Lieber, *Chemically-sensitive imaging in tapping mode by chemical force microscopy: relationship between phase lag and adhesion.* Langmuir, 1998. **14**: p. 1508-1511.

[40] A. Noy, D. V. Vezenov, and C. M. Lieber, *Chemical force microscopy.* Annual Review of Materials Science, 1997. **27**: p. 381-421.

[41] H. A. Mizes, K. G. Loh, R. J. Miller, S. K. Ahuja, and E. F. Grabowski, *Submicron probe of polymer adhesion with atomic force microscopy:*

dependence on topography and material inhomogeneities. Applied Physics Letters, 1991. **59**: p. 2901-2903.

[42] D. K. Schwartz, *Mechanisms and kinetics of self-assembled monolayer formation.* Annual Review of Physical Chemistry, 2001. **52**: p. 107–137.

[43] H. Takano, J. R. Kenseth, S. S. Wong, J. C. O'Brien, and M. D. Porter, *Chemical and biochemical analysis using scanning force microscopy.* Chemical Reviews, 1999. **99**: p. 2845-2890.

[44] B. Bhushan, ed. *Springer Handbook of Nanotechnology*. 2004, Springer-Verlag: Berlin Heidelberg: p. 618-630.

[45] G. G. Baralia, A. S. Duwez, B. Nysten, and A. M. Jonas, *Kinetics of exchange of alkanethiol monolayers self-assembled on polycrystalline gold.* Langmuir, 2005. **21**: p. 6825-6829.

[46] J. C. Love, L. A. Estroff, J. K. Kriebel, R. G. Nuzzo, and G. M. Whitesides, *Self-assembled monolayers of thiolates on metals as a form of nanotechnology.* Chemical Reviews, 2005. **105**: p. 1103-1169.

[47] D. K. Schwartz, *Mechanisms and kinetics of self-assembled monolayer formation.* Annual Review of Physical Chemistry., 2001. **52**: p. 107–137.

[48] W. A. Ducker, T. J. Senden, and R. M. Pashley, *Direct measurement of colloidal forces using an atomic force microscope.* Nature, 1991. **353**: p. 239-241.

[49] F. Sato, H. Okui, U. Akiba, K. Suga, and M. Fujihira, *A study of topographic effects on chemical force microscopy using adhesive force mapping.* Ultramicroscopy 2003. **97**: p. 303-314.

[50] G. J. Vancso, H. Hillborg, and H. Schönherr, *Chemical composition of polymer surfaces imaged by atomic force microscopy and complementary approaches.* Advances in Polymer Science, 2005. **182**: p. 55-129.

[51] H. J. Butt, B. Cappella, and M. Kappl, *Force measurements with the atomic force microscope: technique, interpretation and applications.* Surface Science Reports, 2005. **59**: p. 1-152.

[52] W. W. Gerberich and M. J. Cordill, *Physics of adhesion.* Reports on Progress in Physics, 2006. **69**: p. 2157-2203.

[53] D. L. Sedin and K. L. Rowlen, *Adhesion forces measured by atomic force microscopy in humid air.* Analytical Chemistry, 2000. **72**: p. 2183-2189.

[54] P. D. Ashby, L. Chen, and C. M. Lieber, *Probing intermolecular forces and potentials with magnetic feedback chemical force microscopy.* Journal of the American Chemical Society, 2000. **122**: p. 9467-9472.

[55] W. A. Ducker, T. J. Senden, and R. M. Pashley, *Measurement of forces in liquids using a force microscope.* Langmuir, 1992. **8**: p. 1831-1836.

[46] T. Han, J. M. Williams, and T. P. Beebe, *Chemical bonds studied with functionalized atomic force microscopy tips.* Analytica Chimica Acta, 1995. **307**: p. 365-376.

[57] C. Jacquot and J. Takadoum, *A study of adhesion forces by atomic force microscopy*, in *Atomic force microscopy in adhesion studies*, J. Drelich and K.L. Mittal, Editors. 2005, VSP: Leiden-Boston. p. 299-305.

[58] F. Fay, I. Linossier, V. Langlois, D. Haras, and K. Vallee-Rehel, *SEM and EDX analysis: two powerful techniques for the study of antifouling paints.* Progress in Organic Coatings, 2005. **54**: p. 216-223.

[59] S. Yata and K. Nishimoto, *Application of SEM-EDXA technique to the study of metal distribution in preservative-treated wood.* Wood Research, 1983. **69**: p. 71-79.

[60] M. Rabiller-Baudry, M. Le Maux, B. Chaufer, and L. Begoin, *Characterisation of cleaned and fouled membrane by ATR-FTIR and EDX analysis coupled with SEM: application to UF of skimmed milk with a PES membrane.* Desalination, 2002. **146**: p. 123-128.

[61] M. J. Walzak, R. Davidson, and M. Biesinger, *The use of XPS, FTIR, SEM/EDX, contact angle, and AFM in the characterization of coatings.* Journal of Materials Engineering and Performance, 1998. **7**: p. 317-323.

[62] F. Bettazzi, G. Giachi, G. Staccioli, and S. Chimichi, *Chemical characterisation of wood of Roman ships brought to light in the recently discovered ancient harbour of Pisa (Tuscany, Italy).* Holzforschung, 2003. **57**: p. 373-376.

[63] A. R. Hinda, S. K. Bhargavaa, and A. McKinnonb, *At the solid/liquid interface: FTIR/ATR - the tool of choice.* Advances in Colloid and Interface Science, 2001. **93**: p. 91-114.

[64] W. M. Cross, S. Ma, R. M. Winter, and J. J. Kellar, *FT-IR/ATR and SEM study of colloidal particle deposition.* Colloids and Surfaces A, 1999. **154**: p. 115-125.

[65] M. Kacurakova and R.H. Wilsonb, *Developments in mid-infrared FT-IR spectroscopy of selected carbohydrates.* Carbohydrate Polymers, 2001. **44**: p. 291-303.

[66] R. Rana, G. Muller, A. Naumann, and A. Polle, *FTIR spectroscopy in combination with principal component analysis or cluster analysis as a tool to distinguish beech (Fagus sylvatica L.) trees grown at different sites.* Holzforschung, 2008. **62**: p. 530-538.

[67] G. Müller, M. Bartholme, A. Kharazipour, and A. Polle, *FTIR-ATR spectroscopic analysis of changes in fiber properties during insulating fiberboard manufacture of beech wood.* Wood and Fiber Science, 2008. **40**: p. 532 - 543.

[68] Y. I. Malakhov, A. L. Kalabekov, and Y. N. Korolev, *Application of methods of spectroscopy of attenuated total internal reflection for analysis of biological objects.* Measurement Techniques, 2002. **45**: p. 843-851.

[69] B. C. Smit, *Fundamentals of Fourier transform infrared spectroscopy*. 1996, CRC Press: New York. 1-50.

[70] J. Coates, *Interpretation of infrared spectra, a practical approach*, in *Encyclopedia of Analytical Chemistry*, R.A. Meyers, Editor. 2000, John Wiley & Sons, Chichester. p. 10815–10837.

[71] N. J. Harrick, *Surface chemistry from spectral analysis of totally internally reflected radiation.* Physical Review Letters, 1960. **4**: p. 1110-1114.

[72] K. K. Chittur, *FTIR/ATR for protein adsorption to biomaterial surface.* Biomaterials, 1998. **19**: p. 357-369.

4 Experimental Setup

4.1 Sample and tip preparation

4.1.1 Chemical tip modification

Silicon force modulation cantilevers from Nanosensors (Switzerland) were used for the tip modifications according to Bastidas *et al.* [1]. Tips with the following functional groups were prepared:

- methyl (-CH_3) groups, from 1-octadecanethiol, $H_3C(CH_2)_{17}SH$ (Acros)
- hydroxyl (-OH) groups, from 11-mercapto-1- undecanol, $HO(CH_2)_{11}SH$ (Aldrich)
- carboxylic (-COOH) groups, from 11-mercaptoundecanoic acid, $HOOC(CH_2)_{10}SH$ (Aldrich)
- amine (-NH_2) groups, from 11-amino-1-undecanethiol hydrochloride, $H_2N(CH_2)_{10}SH$ (Aldrich)
- carboxylic-starch groups, from 11-mercaptoundecanoic acid, $HOOC(CH_2)_{10}SH$ (Aldrich)
- amine-starch groups, from 11-amino-1-undecanethiol hydrochloride, $H_2N(CH_2)_{10}SH$ (Aldrich).

The starch was supplied by the Mondi Research Group.

The silicon tips were first coated with gold using an Edwards S150B Gold Sputter Coater (standard gold coating for routine SEM analysis) and cleaned under a 254 nm UV lamp for one hour to ensure that all organic material was removed. The gold-coated tips were subsequently immersed in reagent alcohol for 30 minutes and then in an alcoholic solution 3 mM concentrating of the chosen functional group in for two hours at room temperature. The coated tips were then rinsed with n-heptane (Aldrich) and alcohol, and gently dried in an argon stream.

4.1.2 Substrate films

Films of α-cellulose (Sigma), lignin alkali (Aldrich) and wood extractives (hot water and benzene/ethanol extractives from Acacia) were prepared from solution by spin coating and film casting. For the cellulose film, a mixture of α-cellulose (1.333 g, 8.21 mmol based on glucose units) and *N*,*N*-dimethylacetamide (DMAc) (50 mL) was heated to 150 ℃ for 30 min in a round bottomed flask equipped with a condenser. Then LiCl (1.08 g, 25.5 mmol) was added and the mixture was heated to 166 °C for 8 min. The reaction mixture was subsequently cooled to room temperature and stirred overnight for dissolution [2]. The lignin alkali (2% wt/v) was dissolved in deionised water. For the extractive solution a combination of hot water and ethanol/cyclohexane extractive was used as obtained from prior wood extractions. The starch and starch-pcc (starch and $CaCO_3$ particles) films were prepared by dissolving 5% wt/v of the material in dimethylsulphoxide. The dissolved materials were spin-coated on freshly cleaved mica surfaces at 1,500 rpm for 7 min to accomplish a uniform distribution and film thickness.

Substrate films with functional –OH, –COOH, $–CH_3$ and $–NH_2$ groups were prepared on freshly cleaved mica in the same way as the tip coatings. The mica was coated with gold and subsequently immersed in reagent alcohol for 30 minutes and then in an 3 mM solution containing the chosen functional group in for two hours at room temperature. The coated substrates were then rinsed with n-heptane (Aldrich) and alcohol, and gently dried in an argon stream.

4.1.3 Wood preparation

Wood chips received the following pre-treatments before maceration or pulping: no treatment, hot water extraction (HWE) for one hour at 140 ℃, hot water extraction for one hour at 140 ℃ with subsequent biopulping (HWE&BP). Biopulping using cocultures of *Pycnoporus sanguineus* and *Aspergillus flavipes* was carried out, to loosen the wood structure and facilitate lignin removal in the subsequent chemical pulping process. *P. sanguineus* is a lignin-digesting fungus, while *A. flavipes* is known to utilise readily available

sugars, and does not alter the wood structure extensively. Cultures of *A. flavipes* and *P. sanguineus* were inoculated on 1 kg of wood chips. The chips were placed on a grid, 5 cm from the bottom of a closed, cylindrical, plastic bioreactor. The bioreactor was incubated for 14 days at 30 ℃ and aerated from below the grid with 10 L/min sterile, moist air, blown through a water trap. The chips were then harvested.

Sulphite pulping

80 g of oven-dry wood chips were pulped in a micro-bomb for 12 hours at 140 ℃ with magnesium bisulphite (sulphite concentratio n of 5%). Before pulping, the chips were impregnated at 100 ℃ for 2 hours. T he filled micro-bomb was then placed in a 15 L digester and covered with water. The temperature of the water was monitored with a thermocouple. After pulping the rejects were separated from the pulp fibres. The latter were kept for analysis.

4.1.4 Fibre preparation

Fibres from *Acacia mearnsii* and various eucalyptus species were investigated. If the samples had not already disintegrated into single fibres during pulping they were separated into single fibres by a mild maceration method in Jeffery's solution [3] at 40 ℃ for 4 hou rs. The fibres were kept in distilled water, from which they were spread onto a glass slide for AFM analysis, and left to dry for 12 hours. The adhesion due to capillary forces between the cells and the mica substrate was sufficient to keep the fibres in position for AFM analysis. The fibres were well dispersed and formed a single layer on the substrate, in order to allow imaging of individual fibres. After this time they reached an equilibrium moisture content of about 8-10%, which means that water is definitely still present at the fibre surface.

AFM images were acquired with the fast scan axis parallel to the fibre axis, in order to minimise shear forces.

Fibres prepared for chemical analysis by FTIR were spread into a thick layer to avoid any absorption peaks originating from the substrate.

4.2 AFM imaging and adhesive force determination

AFM images were acquired with a multimode AFM from Veeco combined with a digital pulsed force mode (DPFM) controller from Witec. The z-piezo was modulated sinusoidally with a frequency of 1 kHz. Images were acquired with a scan range of 2 x 2 μm^2 and a scan speed of 0.7 lines/s. All the adhesive force measurements were obtained under ambient conditions. In order to compensate for the environmental effect (varying humidity and temperature), which could lead to a change in surface polarity and therefore the detected adhesive forces, the adhesive force was calibrated on a mica surface before each measurement. This was used as an internal reference. Any difference to this reference value was then added or subtracted from the actual adhesive force value determined for the investigated samples. The correction value was typically below 5%.

The average polarity of the substrate films was measured from adhesion images – each of which consisted of 256 x 256 = 65536 adhesion values – obtained at ten different locations for each sample. The average fibre polarity was determined from adhesion images obtained on ten different, random fibres. The z-range was 0–2V for all images.

4.3 Infrared spectroscopy

The removal of lignin due to pulping was confirmed by ATR-FTIR. It consists of a Smart Golden Gate ATR from Thermo Nicolet attached to a FTIR from Nexus. Each spectrum consisted of 16 scans, which were recorded with a penetration depth of about 1.2 μm at a resolution of 8 cm^{-1}. The spectra were normalised on the peak originating from the C–O stretching in cellulose at 1029 cm^{-1} and the intensity of the aromatic C=C peak at 1507 cm^{-1} was used to determine the presence of lignin.

4.4 SEM/EDX analysis

In order to verify that the AFM tip had indeed been chemically modified and that the desired functional groups were present, SEM images and EDX

spectra were acquired of the tips. Imaging of the samples and analysis of the phase compositions was accomplished using a Leo® 1430VP scanning electron microscope at Stellenbosch University. The sample was mounted on a stub with double sided carbon tape, which was then mounted onto the SEM stage. Sample and stub were sputter coated with a thin layer 15–20 nm of gold prior to imaging, in order to make the sample surface conductive. The sample was placed on the SEM stage in a chamber under high vacuum and images were acquired with a beam energy of 7–10 keV.

Chemical components in the imaged area were identified and quantified by EDX analysis using an Oxford Instruments® 133 keV detector and Oxford INCA software. Beam conditions during the quantitative analysis were 20 kV and approximately 1.5 nA, with a working distance of 13 mm and a specimen beam current of –3.92 nA. Despite the relatively low energy of the beam, X-ray counts with the setup used were typically ~ 5000 cps.

4.5 Investigated wood fibres

Two sets of samples were investigated in this project. The first set was supplied by TWK Agricultural Ltd, South Africa, and consisted of fibres from *Acacia mearnsii*, *Eucalyptus dunnii*, *E. grandis* and *E. macarthurii.* This wood originated from the escarpment around Piet Retief in Mpumalanga. This area can be regarded as cool and moist. These fibres were used for the experiments that compared fibre surfaces of different species from comparable growth sites as well as fibre surfaces after different pre-treatments and pulping.

The second set was supplied by Mondi, South Africa, and consisted of samples from different Eucalyptus species and genotypes, namely *E. dunnii*, *E. macarthurii, E. grandis* (grown from genetically variable seedlings), *E. grandis* (clonal material) as well as *E. grandis x nitens* and *E. grandis x camaldulensis.* They were collected from different growth sites with either cool temperate, warm temperate or subtropical (hot) mean annual temperature (MAT), and on sites with a mean annual precipitation (MAP) that was either

dry, moist or wet according to the classification by Smith [4, 5]. Not all species were available from all growth sites. These samples were used for the experiments, in which the effect of growth site and genotype was studied.

The MAT, MAP, average age, diameter at breast height (DBH), site index at 5 years (SI_5), basal area (BA) and mean annual increment (MAI) of the investigated species are given in Table 4.

The trees were between six (fast growing species) and eight (slower growing species) years old when harvested. Only straight trees without any reaction wood (compression wood) that would result in a different cellulose and lignin content were cut on each sample site and disks were cut at DBH directly after harvesting. These disks were chipped and fibres were prepared by maceration. In order to verify the reproducibility of results, two independent sample sets were prepared from randomly chosen wood chips and analysed in separate experimental steps. This was, however, only possible where enough material was available.

Table 4: Site and tree properties of the sampled Eucalyptus genotypes

Species	**MAT**	**MAP**	**Age [years]**	**DBH [cm]**	**SI_5 [m]**	**BA [m^2/ha]**	**MAI [m^3/ha/ year]**
E. grandis	Warm	Moist	6	14.5	18.1	17.8	23.5
E. grandis clone	Cool	Moist	8	19.9	19.9	12.4	14.9
E. dunnii	Warm	Moist	8	14.0	13.8	17.8	15.2
E. dunnii	Warm	Wet	7	18.0	17.4	16.8	21.0
E. grandis x camaldulensis	Cool	Moist	8	13.2	15.3	18.7	17.5
E. grandis x nitens	Cool	Moist	7	20.6	21.0	21.4	41.4
E. grandis x nitens	Warm	Moist	7	15.6	16.2	10.7	24.1
E. grandis x nitens	Hot	Dry	7	17.7	17.0	11.8	12.9

References

[1] J. C. Bastidas, R. Venditti, J. Pawlak, R. Gilbert, S. Zauscher, and J. F. Kadla, *Chemical force microscopy of cellulosic fibers.* Carbohydrate Polymers, 2005. **62**: p. 369-378.

[2] B. Tosh, C. N. Saikia, and N. N. Dass, *Homogeneous esterification of cellulose in the lithium chloride-N,N-dimethylacetamide solvent system: effect of temperature and catalyst.* Carbohydrate Research, 2000. **327**: p. 345-352.

[3] J. S. Han, T. Mianowski, and Y. Lin, *Validity of plant fiber length measurement, forest products laboratory.* International Journal of Agricultural and Biological Engineering, 1999: p. 149-167.

[4] C. W. Smith, R. N. Pallett, R. P. Kunz, R. A. Gardner, and M. Du Plessis, *A strategic forestry site classification for the summer rainfall region of southern Africa based on climate, geology and soils.* ICFR Bulletin Series 03/05, Pietermaritzburg, South Africa, 2005.

[5] D1105-96, *Standard test method for preparation of extractive free wood.* ASTM, 2001.

5 Results and Discussion

5.1 Tip characterisation

Functionalised atomic force microscopy (AFM) tips were characterised using scanning electron microscopy (SEM) and energy dispersive X-ray (EDX) to verify the tip modification and ensure that the shape of the tip had not been changed significantly during the coating. Images with a magnification of 3000x showed that the aspect ratio had not changed significantly after any of the coatings (see Figure 18) and that the resolution of resulting AFM images should therefore not be much lower than with uncoated tips.

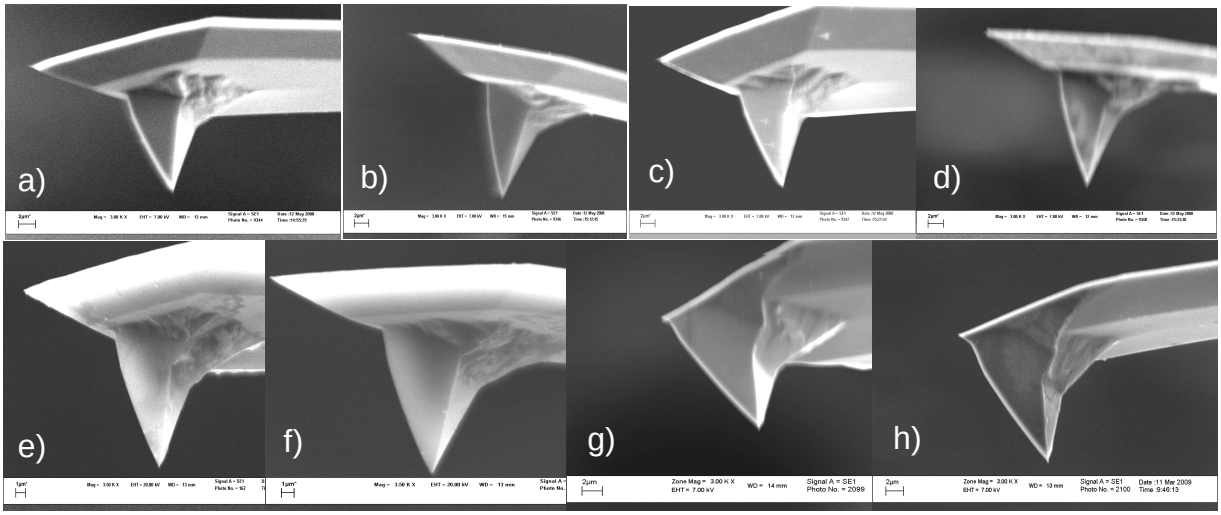

Figure 18: *SEM images of a) silicon AFM tip, b) gold coated tip, c) –OH functionalised tip, d) –COOH functionalised tip, e) –CH_3 functionalised tip, f) –NH_2 functionalised tip, g) –COOH-starch functionalised tip and h) –NH_2-starch functionalised tip.*

EDX spectra, displayed in Figure 19, were used to detect the presence of organic elements and ensure that the tip was really modified. The presence of C, O, N and Au confirmed that the tips had indeed been coated with the desired functional groups.

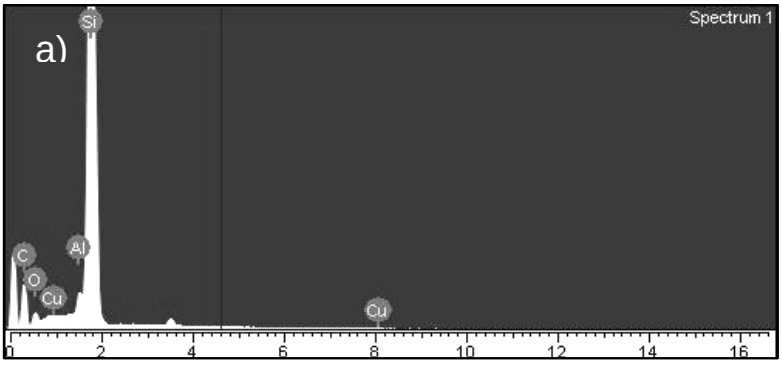
a)
Spectrum 1
Si
Al
C
O
Cu
Cu
0
2
4
6
8
10
12
14
16

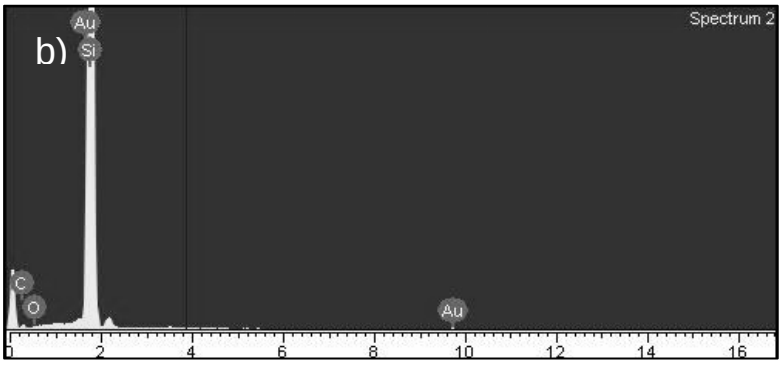
b)
Spectrum 2
Au
Si
C
O
Au
0
2
4
6
8
10
12
14
16

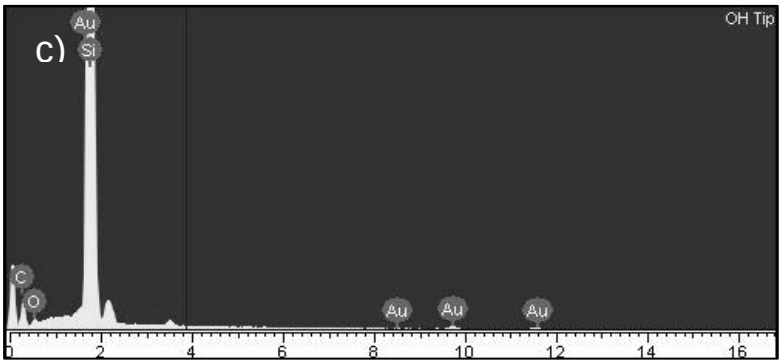
c)
OH Tip
Au
Si
C
O
Au
Au
Au
0
2
4
6
8
10
12
14
16

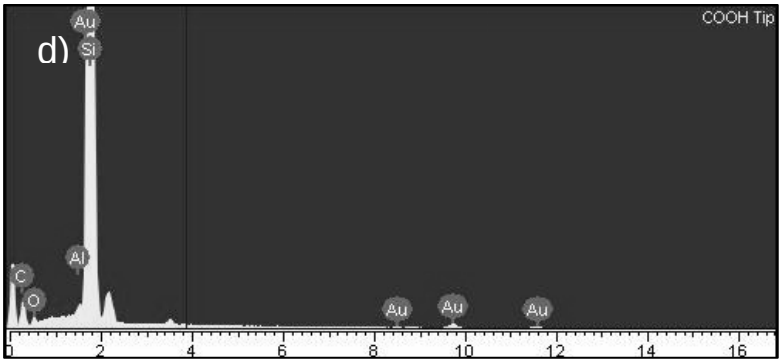
d)
COOH Tip
Au
Si
Al
C
O
Au
Au
Au
0
2
4
6
8
10
12
14
16

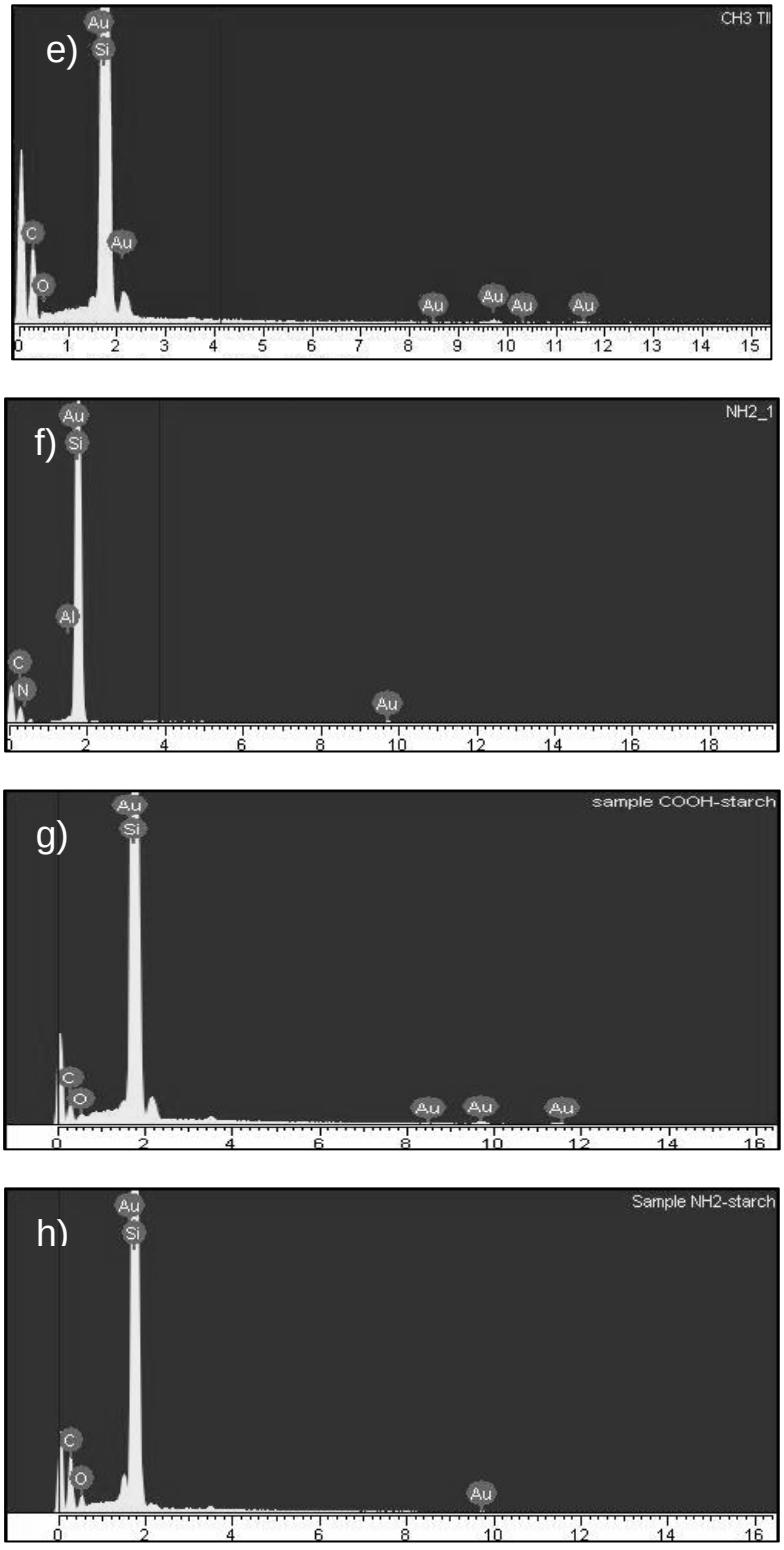

Figure 19: *EDX spectra of a) silicon AFM tip, b) gold coated tip, c) –OH functionalised tip, d) –COOH functionalised tip, e) –CH_3 functionalised tip, f) –NH_2 functionalised tip, g) –COOH-starch functionalised tip and h) –NH_2-starch functionalised tip.*

Even on the unmodified tip traces of oxygen and carbon were found. The silicon tip had probably formed a silicon oxide layer. The amount of carbon, oxygen and nitrogen did however, increase significantly after tip modification. The quantities of the detected elements are tabulated in Table 5.

Table 5: Quantities (wt %) of the elements found on the modified AFM tips

Tips	wt% C	wt% N	wt% O	wt% Si	wt% Au
Si tip	13.10	0.00	24.70	62.20	0.00
Gold tip	0.80	0.00	0.60	55.60	43.00
–COOH tip	44.30	0.00	9.00	41.10	5.60
–CH_3 tip	46.10	0.00	1.60	45.50	7.80
–OH tip	46.50	4.40	5.90	38.10	4.90
–NH_2 tip	48.70	3.20	4.60	39.70	3.80
–starch-COOH tip	46.90	0.00	2.50	44.00	6.50
–starch-NH_2 tip	41.00	1.30	5.70	45.20	6.80

From the SEM images and the EDX spectra it can be concluded that the tip modifications were successful. These tips, or tips prepared in a similar way, were used for subsequent analyses of model films and wood fibres.

5.2 The adhesive forces between modified tips and model films

5.2.1 Functionalised substrates

The adhesive force between the functionalised tips and different substrate films, prepared on mica in the same way as the tip coatings, was determined to detect a difference in sensitivity.

The adhesion force measured for the various tip/sample combinations reflect different interactions, such as hydrogen bonds (–COOH/–COOH, –OH/–NH_2, etc.) or van der Waals interactions (–CH_3/–OH, –CH_3/–CH_3, etc.).

The average adhesive force values determined for all possible tip/sample combinations are summarised in Table 6. The highest adhesive force values determined for each tip are given in bold. As expected, the highest affinity was found between the same tip coating and film composition, although a differentiation between carboxyl and hydroxyl groups was difficult; these values were very similar.

Table 6: Adhesive forces (in nN) determined between the different substrates and a) –COOH, b) –CH_3, c) –OH and d) –NH_2 coated tips. The standard deviation is given in brackets.

Substrate	Tip coating			
	–COOH	–CH_3	–OH	–NH_2
	Adhesive force (nN)	Adhesive force (nN)	Adhesive force (nN)	Adhesive force (nN)
–COOH	**426.73 (25.92)**	125.41 (23.58)	**489.79 (18.10)**	217.59 (17.69)
–CH_3	171.60 (17.12)	**234.18 (9.42)**	110.60 (17.93)	92.14 (14.72)
–OH	351.98 (23.68)	89.38 (17.98)	373.39 (16.46)	145.56 (16.53)
–NH_2	381.24 (19.72)	109.79 (21.32)	472.29 (27.21)	**329.73 (27.43)**

For all modified tips, the expected trend was qualitatively observed depending on the nature of the interactions: for the –CH_3 modified tip, where only van der Waals interactions play a role, all adhesive force values were smaller compared to the tips in which hydrogen bonding take place, such as –OH, –COOH and –NH_2 tips. The cohesive –CH_3/–CH_3 van der Waals interaction was found to be larger than the van der Waals forces between, such as –CH_3/–COOH.

In the case of tip coatings where the formation of hydrogen bonds was possible, e.g., –COOH or –NH_2 tips, the van der Waals interaction with the –

CH_3 model surface resulted in the lowest adhesive force, whereas adhesive forces due to hydrogen bond formation on –OH, –COOH and $–NH_2$ model surfaces were higher.

Quantitative comparisons can only be made for the same tip on different substrates; comparing different tips with each other is not possible. This is because each tip has a different radius of curvature, which means a different contact area between tip and sample, and hence the number of interacting molecules contributing to the measured adhesive force varies for each tip. Mechanical factors, such as the spring constant of the cantilever, also vary between tips. A quantitative comparison between the different substrates for each tip is shown in Figure 20.

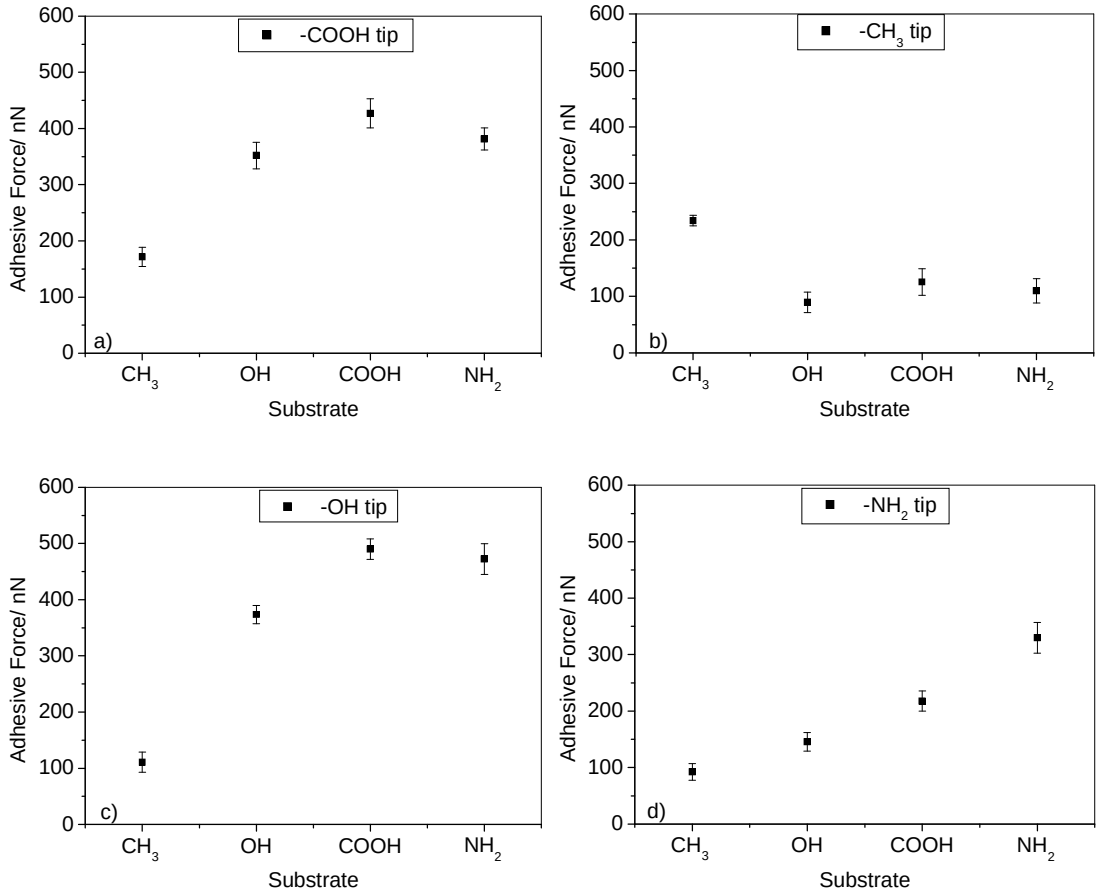

***Figure 20**: Adhesive forces determined between the different model substrates and a) –COOH, b) –CH_3, c) –OH and d) –NH_2 coated tips.*

It can be seen that a distinction between –OH, –COOH and $–NH_2$ substrates is very difficult with the –OH, –COOH, or $–NH_2$ coated tips, as the determined adhesive force values for these groups were not very different from each other, as can be seen in Figure 20. A clear distinction was, however, possible between $–CH_3$ and the other functional groups.

5.2.2 Wood components

FTIR of model substrates

The charcteristic ATR-FTIR spectra of cellulose and lignin films are displayed in Figure 21.

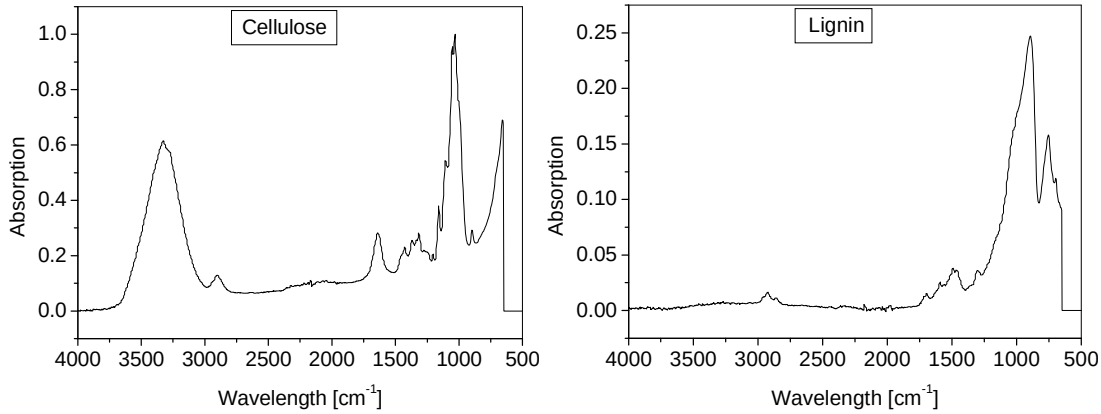

Figure 21: *FTIR spectra of a) cellulose and b) lignin films.*

The major peaks associated with cellulose are at 3300 cm^{-1} (bonded OH stretch), 2930 cm^{-1} (CH stretch), 1660 cm^{-1} (Keto-carbonyl conjugated with a benzene ring), 1370 cm^{-1} (CH_2 bending) and 1160 cm^{-1} (C–O–C asymmetric band). The major peaks characteristic for lignin are 1505 cm^{-1} (benzene ring aromatic stretch) and 1460 cm^{-1} (CH_3 deformation) [1]. All these peaks appear in the spectra.

No FTIR spectra were obtained from films containing extractives, as extractives contain a large variety of organic compounds.

CFM on model substrates

The sensitivity of tips coated with free –COOH, $–CH_3$ and –OH groups toward films consisting of the major components found in wood fibres (cellulose, lignin and extractives) were determined on spin-coated films. The aim of this experiment was to determine differences in sensitivity of the various tip coatings towards the different wood constituents and subsequently determine which tip coating could be used to identify a certain component. The results are displayed in Figure 22.

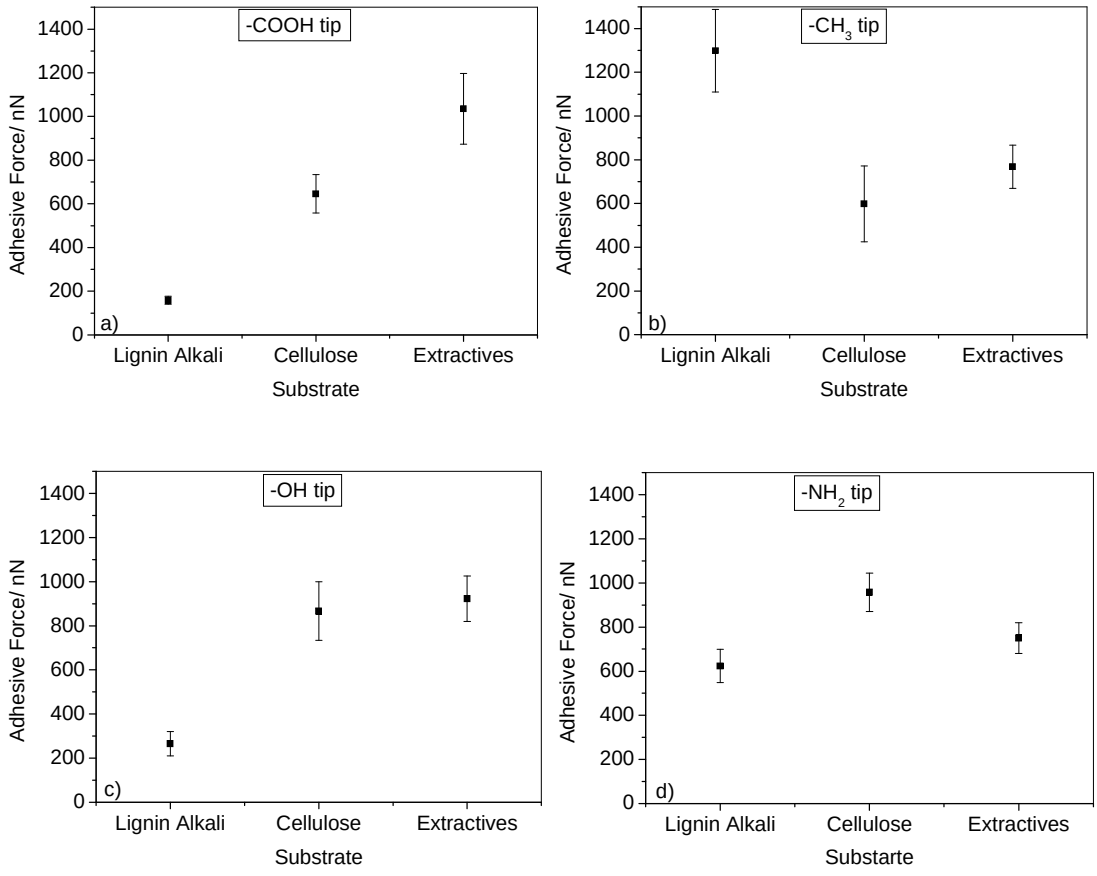

Figure 22: *Adhesive forces determined on films made from model compounds, and a) –COOH, b) $–CH_3$, c) –OH and d) $–NH_2$ coated tips.*

The –COOH coated tip showed the highest sensitivity towards extractives, followed by cellulose and lignin (Fig. 22 a). The $–CH_3$ coated tip (Fig. 22 b) showed a higher sensitivity towards lignin than to cellulose and extractives. This can be explained by methyl groups in the lignin molecules. The –OH coated tip (Fig. 22 c) showed similar behaviour to the –COOH coated tip, but

there was no significant difference between the adhesive forces determined on cellulose and extractives. In fact, the –OH coated tip provided very similar adhesive forces values to those measured with an uncoated SiO_x tip [2]. The high affinity of –COOH and –OH towards cellulose and extractives can be explained by the hydroxyl groups that are abundant in both components.

The $–NH_2$ coated tip showed the highest affinity to cellulose, followed by extractives and lignin, but no significant difference could be detected between the three substrates, as all the error bars overlap. It was hoped that the $–NH_2$ coated tip would show a higher affinity to extractives than to the other components, in order to be able to identify areas on wood fibres that are rich in extractives. Unfortunately this distinction was not possible.

These results suggest that a $–CH_3$ coated tip can be used to detect lignin-rich areas on fibre surfaces, while –COOH and –OH coated tips will be more sensitive to polar areas, such as cellulose, hemicelluloses and extractives. The presence of water molecules associated to cellulose would not affect this result, as it would simply amplify the adhesive force detected on this polar area.

A clear distinction between cellulose and extractives was not possible with any of the four evaluated tip coatings. The development of a coating that contains functional groups that are only sensitive to some of the more common extractives found in wood forms part of an ongoing project.

The cellulose, lignin and extractives films served, however, only as model components for wood fibres, in order to prove that the technique could deliver the necessary material contrast. On wood fibres, cellulose, hemicelluloses, lignin and extractives are blended together in various ratios.

5.3 CFM of wood fibres

5.3.1 The effect of topography on the adhesive force image

The adhesive force can be affected by the surface topography when the small convex structures are in the same size range as the tip and closely packed, which could lead to multiple tip/sample contacts (see Section 3.3).

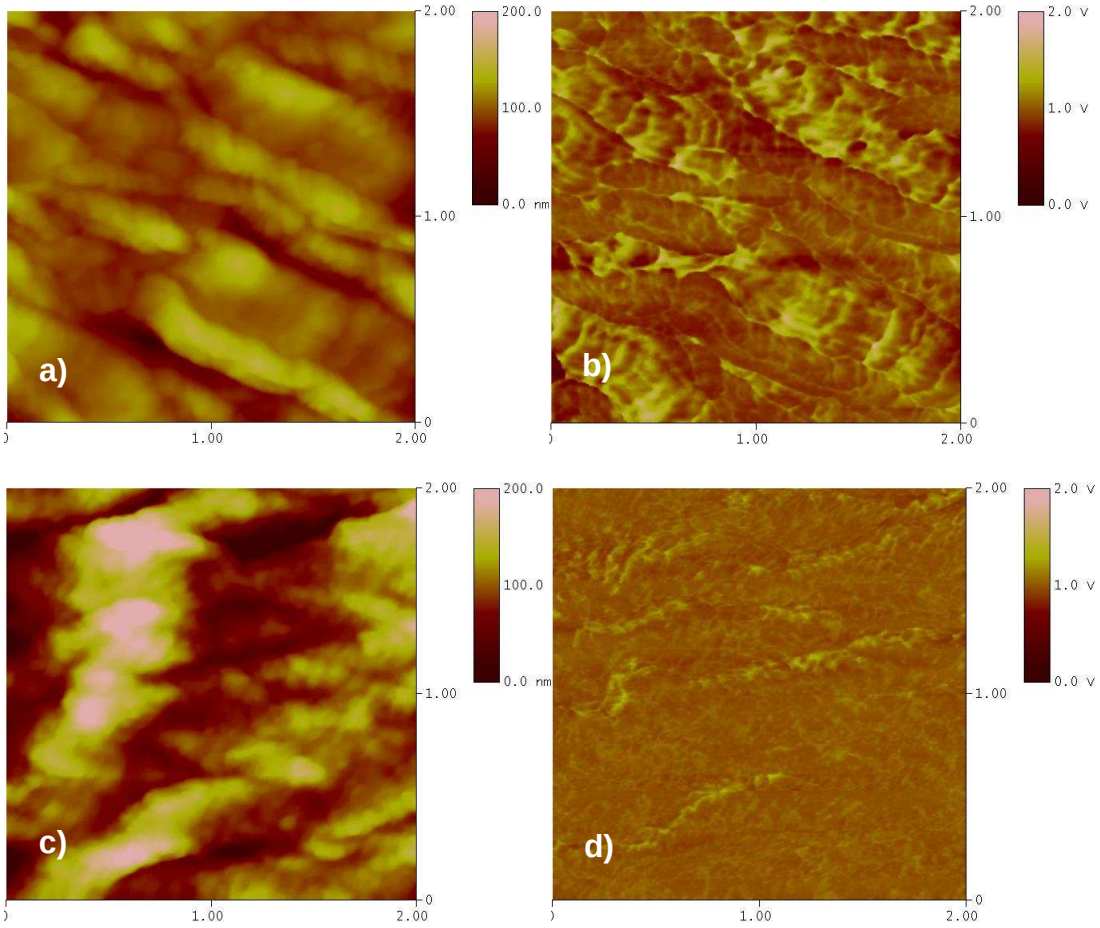

Figure 23: *AFM images of the fibre surface of untreated E. grandis obtained with a –CH_3 coated tip, (a) height and b) adhesive force image, and on the pulped fibre surface, (c) height and d) adhesive force image.*

The effect of topography on the adhesive force for typical results obtained by PFM-AFM measurements in this study was investigated with a –CH_3 coated tip. Figure 23 shows the a) topography and b) simultaneously obtained adhesive force map of a fibre surface of untreated *E. grandis and* (c) the topography and (d) adhesive force of pulped *E. grandis*. The fibrillar structures were widely spaced compared to the tip diameter; therefore the effect of

topography on the adhesive force can be assumed to be insignificant. These results are in good agreement with the results obtained by Sato et al. [3]. They found that a variation in the sample grain size and the resulting change in tip/sample contacts (e.g. if the grain size becomes too large at a close packing density) resulted in different distribution widths of the observed adhesive forces, although it did not change the average adhesion value.

5.3.2 The effect of pulping

In order to show that CFM technique can be used to determine, for example, the lignin removal due to pulping on different wood fibres, –COOH and $–CH_3$ coated tips, which were found to be more sensitive to cellulose and lignin, respectively, were chosen for the subsequent evaluation of wood fibres and pulped fibres from two different wood species. The surfaces of untreated and pulped fibres from eucalyptus (*E. grandis*) and acacia (*A. mearnsii*) wood, two species commonly used for paper manufacturing, were investigated.

As before, the –COOH coated tip showed a higher affinity for cellulose, hemicelluloses and extractives, which appeared as light areas in the adhesion images (Fig. 24 a and c). The $–CH_3$ coated tip showed a higher affinity for lignin, which was also represented by the lighter areas in the adhesion images (Fig. 24 b and d). Figures 24 a and b show typical adhesion images obtained for the fibre surface of untreated *E. grandis*, while Figures 24 c and d show the adhesion images obtained for untreated *A. mearnsii*.

The images acquired with the –COOH and $–CH_3$ coated tips showed a bright colour contrast on both wood species, which suggests the presence of cellulose, hemicelluloses, extractives and lignin on the fibre surfaces. The histograms showed a value distribution around 0.9 V for the –COOH coated tip and around 1.4 V for the $–CH_3$ coated tip for both species.

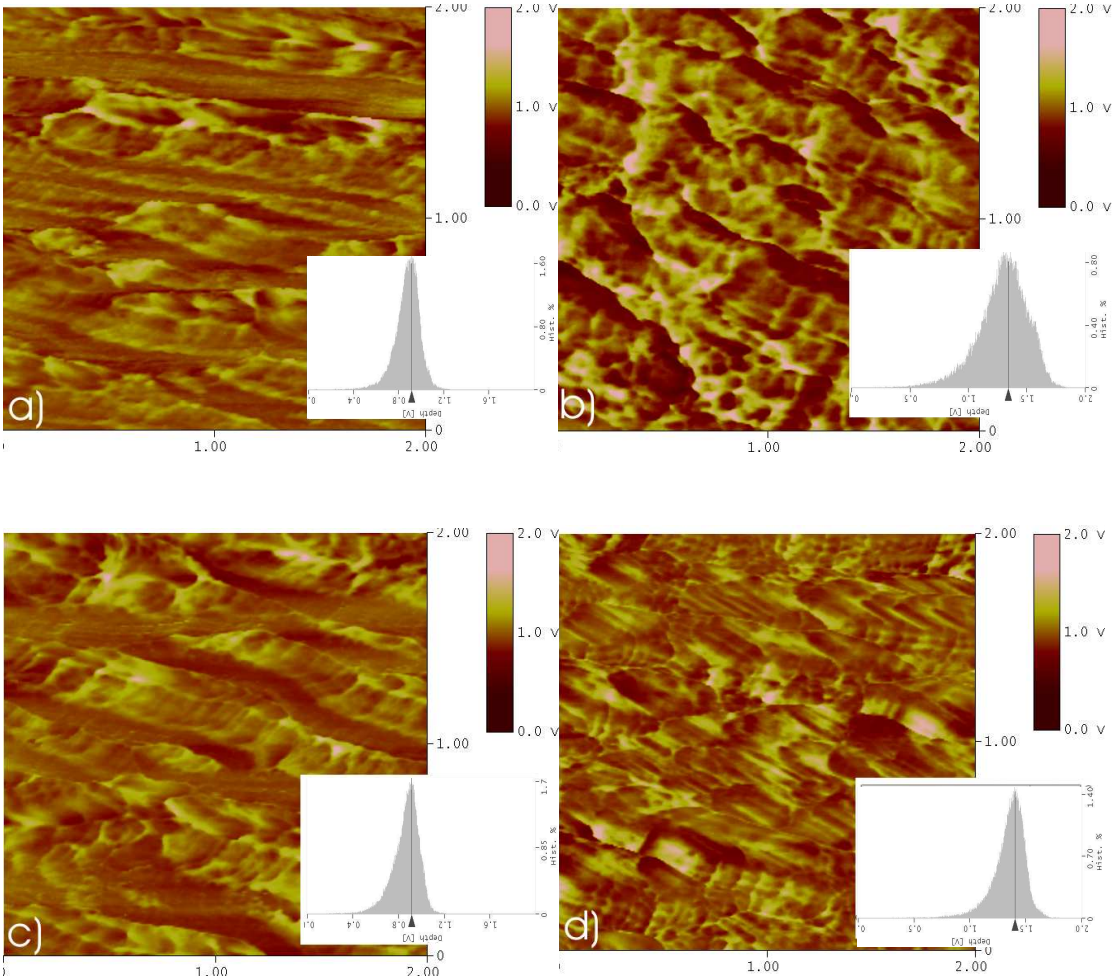

Figure 24: *Adhesive force images and histograms of colour values obtained for the fibre surface of untreated E. grandis with (a) –COOH and (b) –CH_3 coated tips and on the fibre surface of untreated A. mearnsii with (c) –COOH and (d) –CH_3 coated tips.*

Figure 25 (a – d) shows fibres from the same species after sulphite pulping. The images acquired with a –CH_3 coated tip (b and d) showed a low colour contrast with a narrow colour distribution and the absence of bright areas, which is consistent with the successful removal of most of the lignin by the pulping. No functional groups, to which the –CH_3 coated tip would be especially sensitive, remained on the fibre surface, resulting in a lower average adhesive force value.

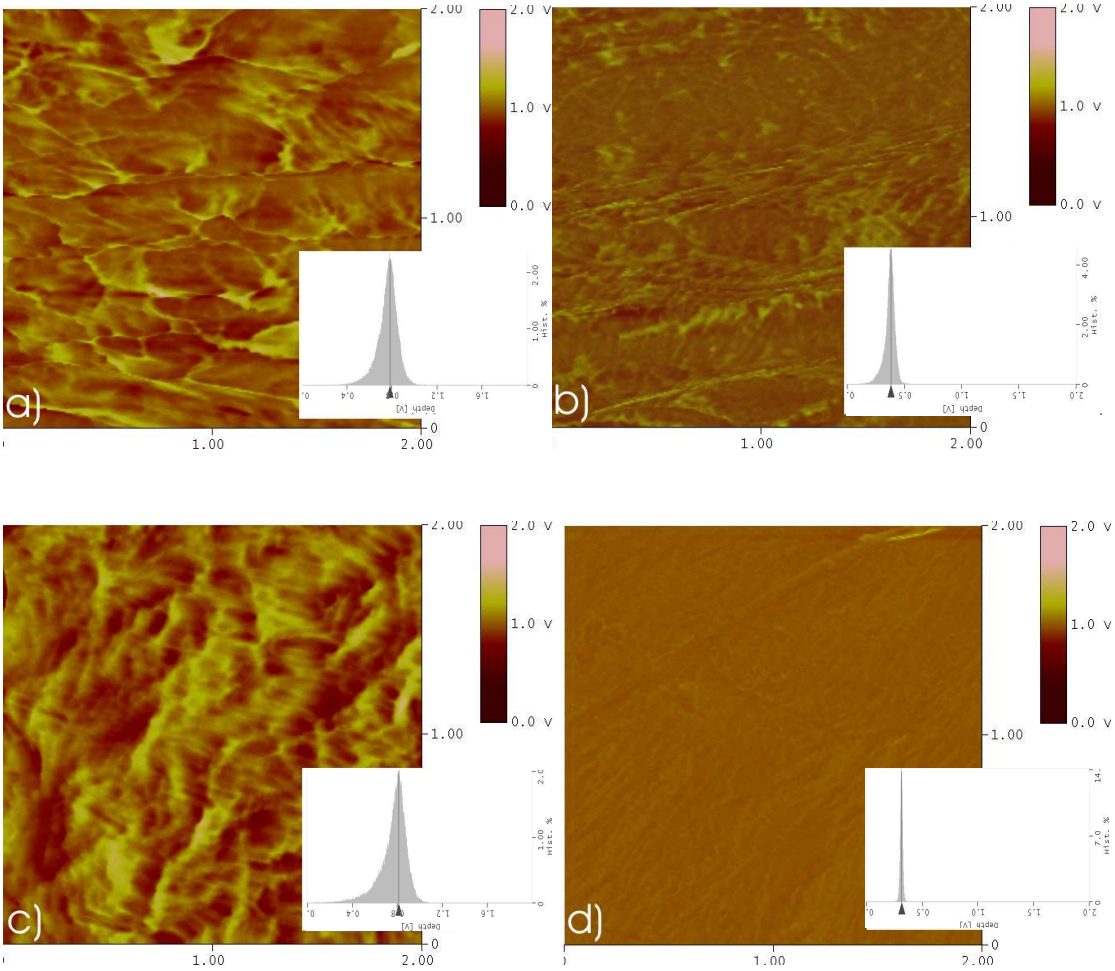

Figure 25: *Adhesive force images and histograms of colour values obtained for the fibre surface of pulped E. grandis with (a) –COOH and (b) –CH_3 coated tips and on the fibre surface of pulped A. mearnsii with (c) –COOH and (d) –CH_3 coated tips.*

The images acquired with a –COOH coated tip (a and c) showed a similarly high colour contrast, as for before pulping, with many bright areas. Areas without free hydroxyl groups were, however, still displayed as darker areas, resulting in the larger colour deviation within the images. The absence of free hydroxyl groups can be explained by the fact that after pulping many of the free hydroxyl groups from cellulose associate with each other.

The histograms showed a distribution value of about 0.9 V for the –COOH coated tip for the two wood species, whereas the values were about 0.35 V for the –CH_3 coated tip for both species. This significant shift to a lower value – from about 1.4 V in the images of untreated fibres to about 0.35 V in the

images of pulped fibres–clearly showed that the adhesive force determined between the $–CH_3$ coated tip and the sample surface had been reduced. This can be attributed to a decrease in free methyl groups, which in turn is a measure for the decreased lignin content in the imaged area.

For each image the average adhesive force value was determined with its standard deviation. The average value (obtained from 1250 measurements for each image) was measured for 10 images. The standard deviation was calculated from these averages and was used to describe the average adhesion determined for fibres of one wood species. The average standard deviation obtained for the ten individual images, which is a measure for the distribution of values within one sample, is given in brackets in Table 7. As Figure 25 suggested, this average value is proportional to the amount of lignin present on the fibre surface when a $–CH_3$ coated tip was used and to the amount cellulose, hemicelluloses and extractives present on the surface when a –COOH coated tip was used.

It was observed that the untreated fibre surfaces of the two wood species differed in the adhesive force detected with the –COOH coated tip. This can be explained by their different degrees of crystallinity of the cellulose and the different chemical composition. The –COOH coated tip is sensitive to cellulose, hemicelluloses *and* extractives, all of which are known to differ between the two species.

Table 7: The average adhesive force (in nN) and standard deviation determined between the functionalised tips and various wood samples.

Tip coating / Sample	$-CH_3$ (lignin)		–COOH (cellulose + extr.)	
	Adhesive force/ nN	STD	Adhesive force/ nN	STD
A. mearnsii	1434.22	178.16 (89)	1303.81	122.12 (93)
Pulped *A. mearnsii*	338.50	155.01 (12)	1275.30	153.17 (89)
E. grandis	1492.06	166.08 (121)	1049.74	144.43 (87)
Pulped *E. grandis*	476.54	83.03 (32)	942.82	90.24 (50)

Similar results were found in a previous study in which the polarity of fibre surfaces was characterised with un-modified SiO_x AFM tips [2]. The effect of sulphite pulping on the surface composition was considerable. The reduction of lignin in the fibres was clearly reflected by the decreased average adhesive force, detected with the $-CH_3$ coated tip (see Figures 25 b and d). The average adhesive force determined with the –COOH coated tip remained constant within the range of the standard deviations after pulping.

The fact that the adhesive force between the –COOH coated tip and the fibre surface did not increase after pulping, although a higher percentage of cellulose should now be present on the surface, can be explained by the fact that the increase in the cellulose content does not necessarily lead to an increase in hydroxyl groups on the fibre surface, as they will also associate with themselves. Furthermore, the extractives content, which previously added to the adhesive force value, can be expected to be lower after pulping.

The reduction of lignin due to pulping was confirmed by ATR-FTIR. Figure 26 shows spectra of untreated and pulped fibres from *E. grandis* (Fig. 26 a) and *A. mearnsii* (Fig. 26 b).

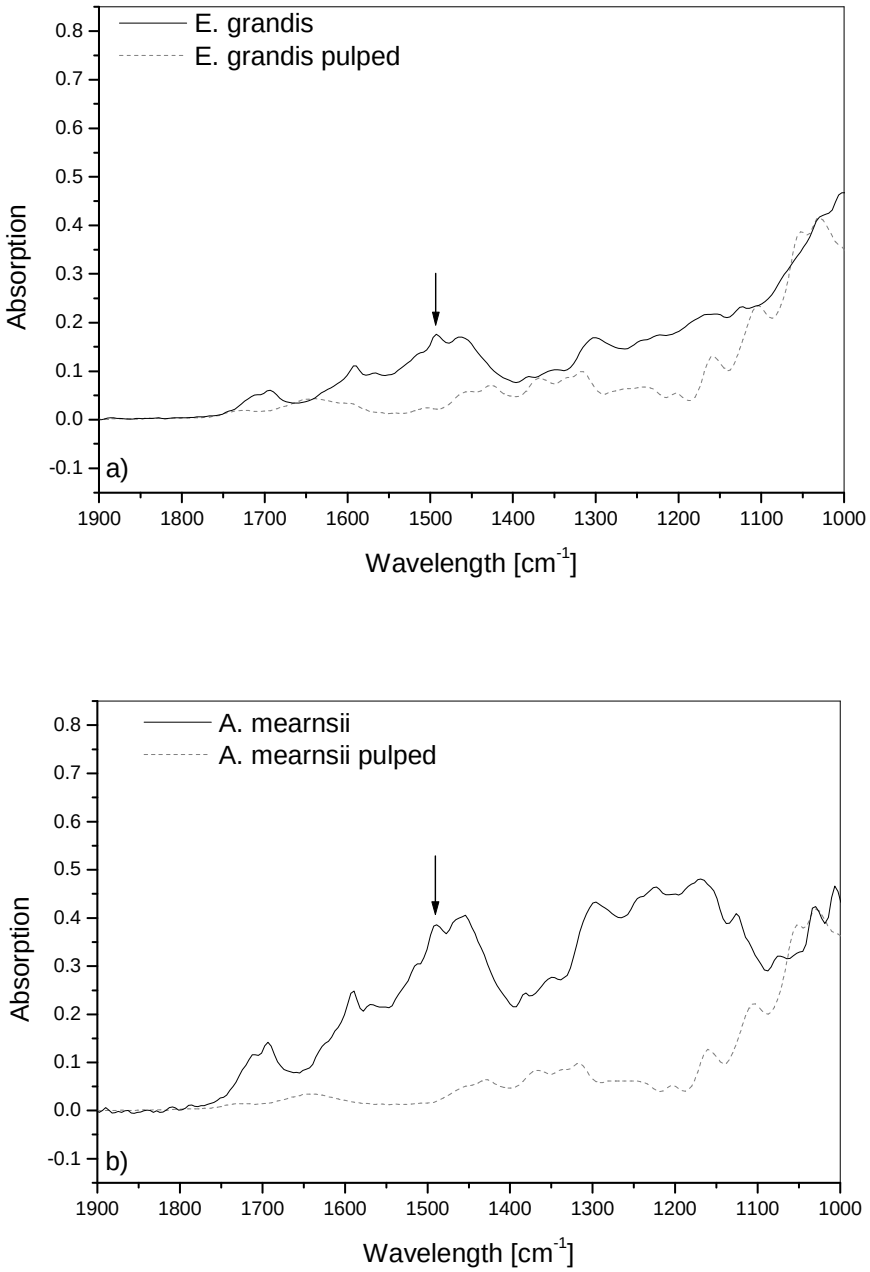

Figure 26: *ATR-FTIR spectra of a) untreated and pulped E. grandis fibres and b) untreated and pulped A. mearnsii fibres.*

The spectra clearly show a decrease in the peak at 1505 cm^{-1}, which is characteristic for the C=C bond in the aromatic rings of lignin**.** This is consistent with the fact that the amount of lignin was decreased by pulping.

5.3.3 The effect of pre-treatments: hot water extraction and bio-pulping

In order to establish whether the CFM technique could detect less severe changes to the fibre composition than those caused by pulping, the adhesive forces between functionalized tips and pre-treated fibres were determined. Pre-treatments that are often performed before pulping to loosen the fibrillar structure are hot water extraction (HWE) and bio-pulping.

The effect of HWE on the surface composition of wood fibres from *E. grandis* and *A. mearnsii* was very small and not statistically significant, but HWE treatment led to a slight decrease in the average adhesive forces detected with both tip coatings (see Figure 27). The decreased average adhesive force detected with the –COOH coated tip can be ascribed to the reduction of hydrophilic extractives in the fibres due to the HWE. The decrease in the average adhesive force determined with the $–CH_3$ coated tip can be ascribed to the removal of lipophilic extractives and the partial degradation of lignin.

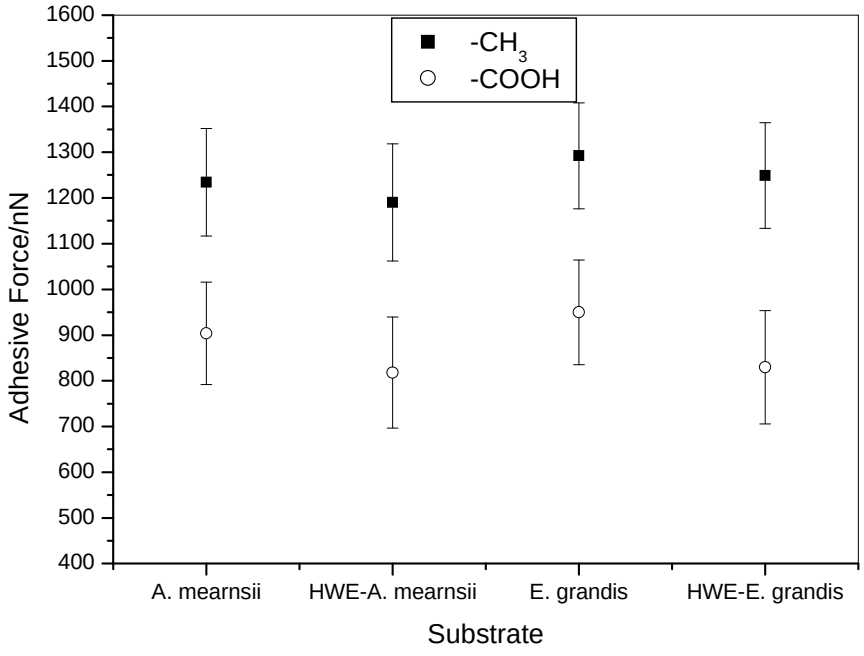

Figure 27: *The adhesive force determined for untreated and HWE wood fibres from A. mearnsii and E. grandis.*

Figure 28 shows a more significant effect of bio-pulping on the surface composition of fibres from *E. grandis* and *A. mearnsii.* The reduction of lignin in the fibres is clearly revealed by the decreased average adhesive force detected with the $–CH_3$ coated tip. The average adhesive force determined with the –COOH coated tip is slightly decreased, but remains constant within the range of the standard deviations after bio-pulping. Compared to sulphite pulping, however, bio-pulping has less of an effect on the chemical composition of fibre surfaces.

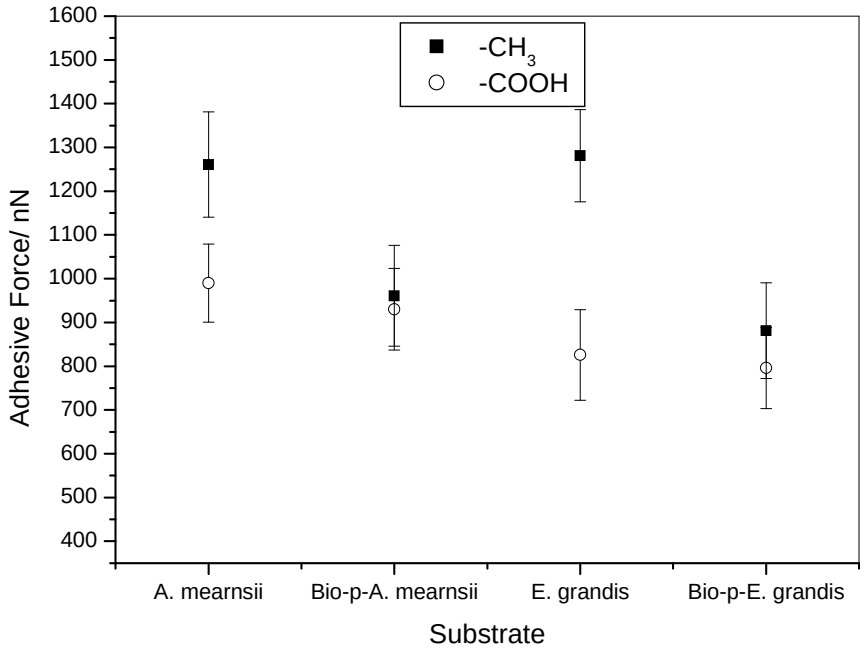

***Figure 28**: The adhesive force determined on bio-pulped wood fibres.*

As CFM proved to be sensitive enough to differentiate between native and pulped or pre-treated fibres, it was then used to try to determine differences in wood species and wood from different growth sites.

5.4 Variation of fibre surface composition depending on wood species and growth site

5.4.1 The effect of species and genotype

Fibres from four different wood species, *E. grandis*, *E. dunnii*, *E. macarthurii* and *A. mearnsii,* originating from cool, moist growth sites were compared. These investigated species are commonly used in the South African paper industry for pulping. *A. mearnsii* and *E. grandis* are commonly blended to attain a good pulp quality. Although *E. dunnii* and *E. macarthurii* produce a different pulp quality they are often used together with the former two wood species to augment available material for paper manufacture. The difference in surface properties may, be related to differing pulp qualities and a better understanding of the surface characteristics could enable the optimisation of pre-treatment and pulping conditions for different pulpwood fibres with the aim to maximise both the pulp yield and its quality.

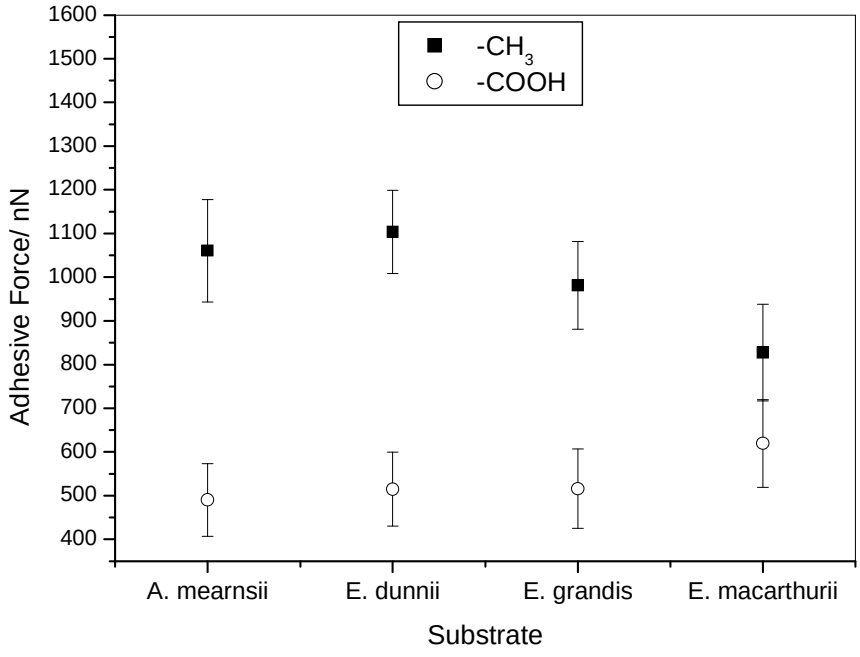

Figure 29: *The adhesive forces determined on fibres from different wood species.*

Figure 29 shows the amount of cellulose (–COOH) and lignin ($–CH_3$) detected on the fibre surfaces by CFM. *E. macarthurii* has on average the highest surface cellulose content. Although the amount of cellulose does not differ

significantly between the four species, the amount of lignin is considerably less on the surfaces of fibres from *E. macarthurii* and comparably the highest on fibres from *E. dunnii*.
Whereas *A. mearnsii* and *E. grandis* show comparable values, *E. dunnii* and *E. macarthurii* deviate to higher and lower values, respectively, in their cellulose / lignin surface content.

In a second study, various genotypes of Eucalyptus from various growth sites were compared. Based on the effects of site quality and the fibre properties, this study provides further ways of analysing the fibre quality. This was done by using CFM to characterise the chemical surface composition of pulpwood fibres and then comparing this to the chemical bulk composition, which might differ considerably. It is however, typically the determined bulk chemical composition that is used to describe pulpwood fibres.

The bulk chemical compositions of Eucalypt genotypes from cool (c) or medium (m) MAT sites with medium MAP are tabulated in Table 8.

Table 8: Chemical bulk compositions of various Eucalyptus genotypes from cool (c) or warm (w) MAT sites, with standard deviation in brackets

Species	**Lignin (%)**	**Cellulose (%)**	**E/C extractives (%)**	**H_2O extractives (%)**
E. grandis (m)	14.8 (4.5)	45.6 (2.2)	2.2 (0.7)	1.9 (0.9)
E. grandis clone (c)	20.9 (1.3)	47.6 (2.5)	3.3 (1.7)	2.0 (2.0)
E. dunnii (m)	12.7 (3.1)	44.1 (2.2)	5.4 (0.1)	2.7 (1.4)
E. grandis x nitens (m)	16.5 (1.2)	45.2 (2.8)	4.3 (2.3)	1.8 (1.5)
E. grandis x camaldulensis (c)	15.5 (0.7)	45.9 (3.0)	4.7 (1.7)	3.6 (1.7)

The amount of cellulose ranged from 44 to 48%, and did not differ significantly between the investigated genotypes. The *E. grandis* clone had the highest cellulose content (48%), followed by *E. grandis* and the two hybrids, *E. grandis x nitens* and *E. grandis x camaldulensis* (about 46%). The lowest

cellulose content was found in *E. dunnii* (44%). The lignin content followed the same trend: the *E. grandis* clone had the largest amount of lignin (21%) and *E. dunnii* the lowest (13%). The maximum variation in the bulk lignin content between the species was 8%.

The chemical surface composition of the fibres determined by CFM had considerably larger differences between the species than the bulk composition did. Figure 28 displays the adhesive forces and 95% confidence intervals determined with –COOH or $–CH_3$ functionalised tips on the fibre surfaces of wood originating from similar growth sites but from different species. The determined adhesive force values give a good estimation of the amount of cellulose or lignin present on the surface.

The adhesive forces of different *Eucalyptus* genotypes from comparable sites with a cool/moist MAT/MAP are shown in Figure 30a. It shows that similar adhesive force values were obtained with the $–CH_3$ coated tip on fibres from *E. grandis* clone and *E. grandis x camaldulensis* and they were significantly higher than the values observed on fibres from *E. grandis x nitens.* This indicates that fibres of *E. grandis x nitens* have a lower lignin content on the surface than *E. grandis* clone and *E. grandis x camaldulensis*, although the bulk lignin content was lower in *E. grandis x camaldulensis* compared to the other two genotypes. This result could be confirmed in a second set of measurements on *E. grandis x nitens* fibres.

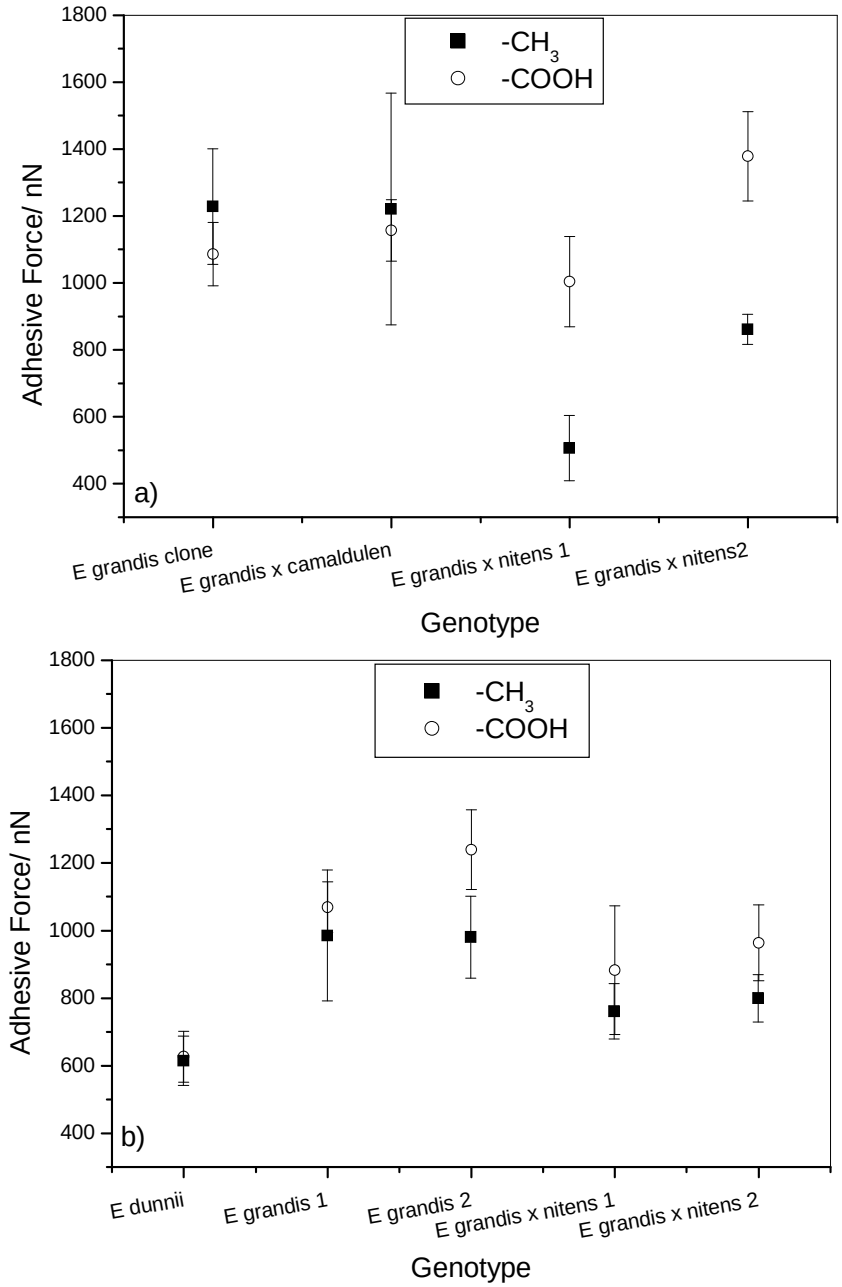

Figure 30: *The adhesive forces determined on different Eucalyptus genotypes from comparable sites a) with a cool/moist MAT/MAP, b) with warm/moist MAT/MAP.*

The adhesive forces determined with a –COOH coated tip showed similar values for all four species within the 95% confidence interval. Although the adhesive forces determined for *E. grandis x nitens* in the two measurement sets differ, the –COOH coated tip showed a higher sensitivity towards the fibre surfaces than the $–CH_3$ coated tip for both measurements. This suggests a higher cellulose content on the fibre surfaces compared to the lignin content.

Fibres from *E. grandis* clone and *E. grandis x camaldulensis,* on the other hand, showed a comparable cellulose and lignin content on the surface.

Comparison between the chemical surface compositions of the fibres determined by CFM and the bulk compositions showed that the amount of cellulose did not differ significantly between the examined genotypes for both methods. There was however, a considerable difference in the amount of lignin on the surface between the species with a higher (and similar) lignin content, on fibres from *E. grandis* clone and *E. grandis x camaldulensis,* than for *E. grandis x nitens*.

Figure 30b shows the surface functionality of different Eucalyptus genotypes from comparable sites with a warm/moist MAT/MAP. Note that where two sets of measurements were performed (labelled as 1 and 2 on the x axis), the adhesive force values were well reproducible.

For sites with a cool/moist climate, *E. grandis* and *E. grandis x nitens* displayed a slightly higher sensitivity towards the –COOH coated tip than towards the $–CH_3$ coated tip, although this was only significant in the second measurement set. This can be attributed to higher cellulose content on the fibre surface. Both, the cellulose and lignin content were significantly lower in *E. dunnii* than in *E. grandis* and *E. grandis x nitens.* This distribution was confirmed, although not quite as pronounced, by the bulk chemical composition. The lignin content on the surfaces of *E. grandis* fibres was significantly higher than on the fibres surfaces of *E. dunnii* or *E. grandis x nitens* fibers. This agrees well with the results displayed in Figure 30a, which showed a higher surface lignin content for *E. grandis* clone than for *E. grandis x camaldulensis.*

5.4.2 The effect of growth site

The adhesive forces determined on fibres from the same species *Eucalyptus genotypes* but from different growth sites are presented in Figure 31.

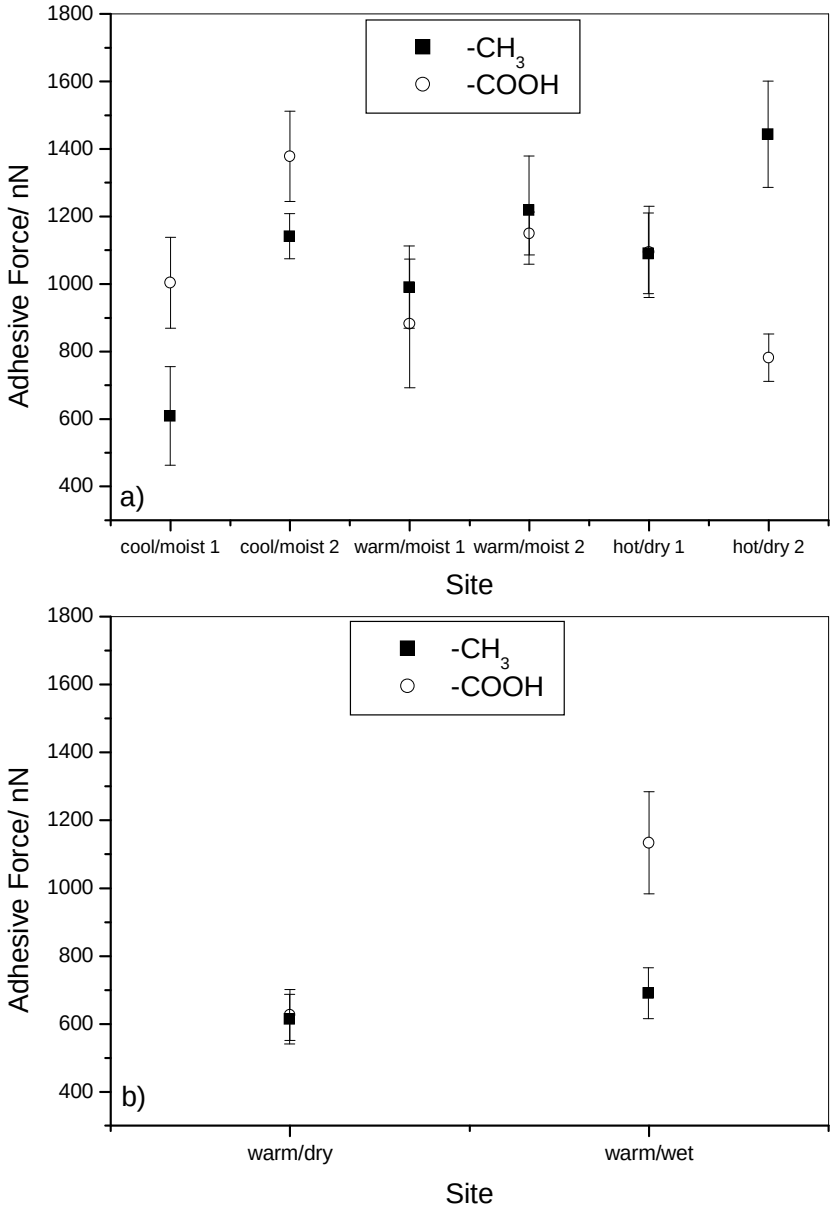

Figure 31: *The adhesive forces determined on fibres from the same Eucalyptus genotypes taken from different climatic sites: a) E. grandis x nitens hybrid and b) E.dunnii.*

The adhesive forces determined on fibres from *E. grandis x nitens* hybrids across an MAT/MAP gradient are displayed in Figure 31a. Most fibres showed a higher sensitivity towards the –COOH coated tip than the $–CH_3$ coated tip, which means that the cellulose content on the surface was higher than the lignin content in these samples. The only exception was the second set of fibres originating from a hot and dry site, where the results were contradictory. The highest cellulose content was found for cool and moist growth conditions and it decreased with increasing MAT and decreasing MAP. Simultaneously,

the lignin content at the fibre surface increased slightly with increasing MAT and decreasing MAP. Higher temperature and precipitation conditions lead to the faster growth of wood, which is known to increase the lignin content in many wood species.

The adhesive forces determined on fibres from *E. dunnii* across a MAP gradient are displayed in Figure 31b. Fibres originating from the warm/dry site showed similar sensitivity to the $–CH_3$ and –COOH coated tips, whereas the fibres from the warm/wet site had a considerably higher affinity to the –COOH coated tip. This means that the cellulose content on the surface of fibres originating from moist sites is significantly higher than that from dry sites, whereas the surface content of lignin remains the same.

The results showed that the chemical composition on the fibre surface differs in some cases from that of the bulk. Differences in composition between genotypes and growth site were more pronounced on the fibre surface than in the bulk. It is however the surface composition affects further processing of the fibres, such as pulping and paper formation. Statistically significant differences with regards to genotype were found in *Eucalyptus grandis x nitens*, which showed a lower lignin content on the fibre surface, and *Eucalyptus dunnii*, which had a considerably lower lignin and cellulose content on the fibre surface, compared to *Eucalyptus grandis* and *grandis x camaldulensis*.

The differences due to growth site were less significant, but the trend in data showed that the cellulose content on the fibre surface decreased with increasing temperature and decreasing moisture, whereas the lignin content on the fibre surface increased.

If a blend of fibres is pulped together a comparable fibre composition is desirable so that the amount of pulping chemicals can be adjusted accordingly and evenly distributed. Large differences in the fibre stock could result in uneven pulping and consequently in a lower pulp yield.

5.5 The adhesive force between wood fibres and a starch coated tip

Cellulose and starch consist of glucose units. Native starch is branched and composed of two different types of glucose polymers: amylose and amylopectin. The main glucosidic linkage between the glucose units in amylose is an α-1,4 configuration, while in amylopectin additional α-1,6 glucosidic bonds create branch points in the macromolecule [4, 5].

Starch plays a major role as a chemical additive; it is used for the manufacturing and upgrading of paper and board. It was used in papermaking even before the invention of handmade papers; it was detected in sheets of papyrus. Starch derivatives are mainly used to improve the dry strength of paper and board, and as a binder for pigment coating. Because it is a bio-polymer, starch can be provided in sufficient quantities. The dominant raw material for starch production is corn (maize) with a share of 75%, followed by 10% tapioca, 8% wheat and 7% potato [6, 7].

Starch is added as filler, to improve dry strength, for fine retention and surface sizing. Starch is very suitable for these purposes, because it contains free hydroxyl groups, which can form strong hydrogen bonds to the free hydroxyl groups of the cellulose. A difference in adhesive force between a starch coated tip and cellulose- or lignin-rich areas on wood fibres can therefore be expected. Images acquired with a starch coated tip could indicate possible binding sites for starch molecules on the wood fibres.

The images acquired for untreated *A. mearnsii* and *E. grandis*, with –COOH-starch coated tips, shown in Figure 32, reveal a bright colour contrast which suggests the presence of possible binding sites for starch, i.e. cellulose on the fibre surfaces. As mentioned earlier, the lighter areas of the adhesion image obtained with a –COOH-starch coated tip are due to a higher affinity of starch to cellulose, hemicelluloses and extractives. The darker areas can be correlated to lignin present on the surface.

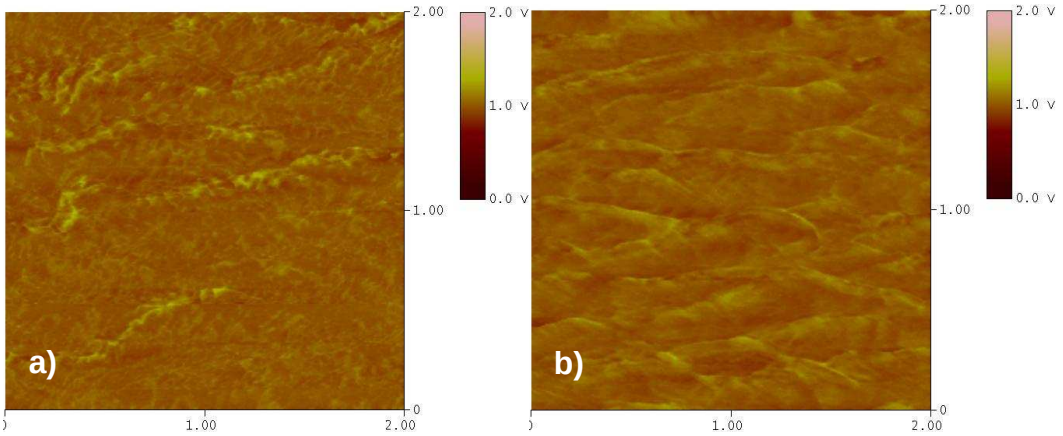

Figure 32: *Adhesive force images of the surface of wood fibres of a) A. mearnsii and b) E. grandis obtained with a –COOH-starch coated tip.*

Adhesive forces determined on films made from model compounds with carboxylic-starch and amino-starch coated tips, respectively are shown in Figure 33. Similar adhesive forces were obtained for both tips on all substrates, with the exception of films made from starch and hot water extractives.

This is surprising as the starch coated tip could be expected to show the highest affinity to a starch substrate. A possible explanation is the fact that the starch is coupled to the tip via carboxyl or amino groups. The hydrogen bonds between the starch and amino groups seem to be weak, which might have led to a dissociation and subsequent loss of the starch molecules. In comparison the hydrogen bonds between carboxyl groups and starch seem to be stronger and more stable. The adhesive force determined with the –COOH-starch coated tip showed the highest affinity for films made from hot water extractives, followed by starch and a similar affinity for cellulose and ethanol extractives. The lowest affinity was found for lignin films, as could be expected.

For this reason, a –COOH-starch coated tip was chosen to detect possible differences in the ability to bind starch onto the fibre surface between fibres originating from different wood species, as shown in Figure 34.

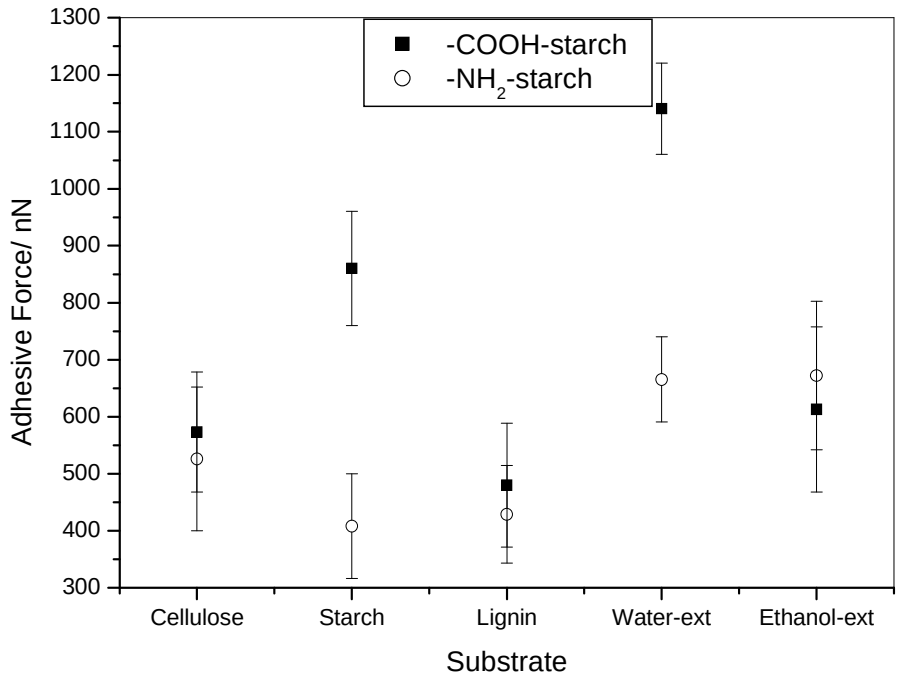

Figure 33: *Adhesive forces determined on films made from model compounds with –COOH-starch and –NH_2-starch coated tips.*

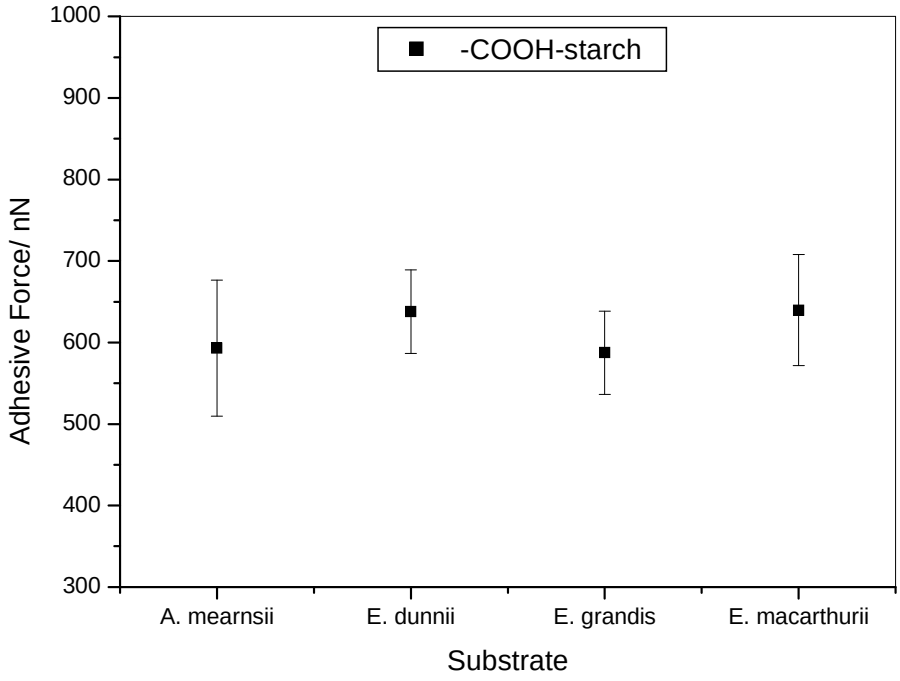

Figure 34: *The adhesive force determined on fibre surfaces of four different wood species with a –COOH-starch coated tip.*

No significant difference could be found in the adhesive force determined on the surface of fibres from *A. mearnsii*, *E. dunnii*, *E. grandis* and *E. macarthurii.* Use of a –COOH-starch coated tip for *E. dunnii* and *E. macarthurii* showed only slightly higher than average values, which could be attributed to a lower surface lignin content found in these species.

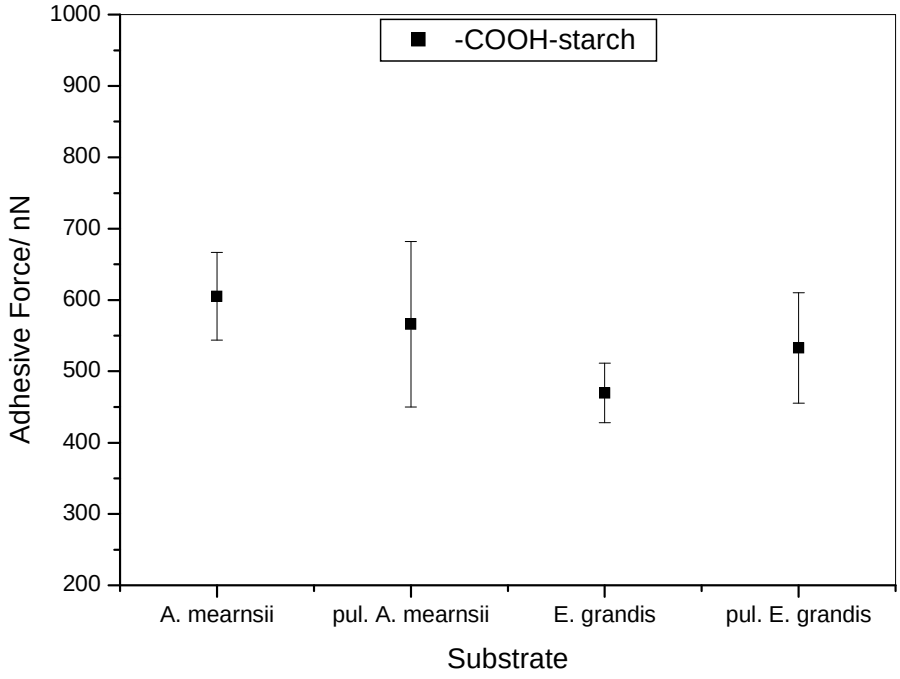

Figure 35: *The adhesive force determined on untreated and pulped wood fibres from A. mearnsii and E. grandis with a –COOH-starch tip.*

The average adhesive force determined with a –COOH-starch coated tip did not change significantly after pulping, as displayed in Figure 35.

In conclusion, taking above results into account, this technique was not found to be suitable to detect possible binding sites for starch molecules on wood fibres or detect differences between wood species. The reason for the decreased sensitivity towards different functional groups on the fibre surface is probably the weak link between the primary tip coating (carboxyl or amino groups) and the starch, and also the decreased lateral resolution of the adhesive force images due to this tip coating.

5.6 References

[1] R. M. Rowell, *Handbook of Wood Chemistry and Wood Composites*. 2005, CRC Press. New York: 36-74.

[2] M. Meincken, *Atomic force microscopy used to determine the surface roughness and surface polarity of different cell types of hardwoods commonly used for pulping* South African Journal of Science, 2007. **103**: p. 4-6.

[3] F. Sato, H. Okui, U. Akiba, K. Suga, and M. Fujihira, *A study of topographic effects on chemical force microscopy using adhesive force mapping.* Ultramicroscopy 2003. **97**: p. 303-314.

[4] A. Blennowa, S. B. Engelsenb, L. Munckb, and B. L. Møllera, *Starch molecular structure and phosphorylation investigated by a combined chromatographic and chemometric approach.* Carbohydrate Polymers, 2000. **41**: p. 163-174.

[5] D. J. Manners, *Recent developments in our understanding of amylopectin structure.* Carbohydrate Polymers, 1989. **11**: p. 87-112.

[6] T. Galliard, *Starch: properties and potential*. 1987, Wiley. New York: 1-60.

[7] R. P. Ellis, M. P. Cochrane, M. F. Dale, C. M. Duþus, A. Lynn, I. M. Morrison, R. D. M Prentice, J. S. Swanston, and S. A. Tiller, *Starch production and industrial use.* Journal of the Science of Food and Agriculture, 1998. **77**: p. 289-311.

6 Conclusions and Recommendations

6.1 Conclusions

It was successfully demonstrated that AFM with functionalised tips can be used to localise, identify and, to a degree quantify different chemical components on wood fibres. Adhesive force images acquired with an additional DPFM controller can show areas of different composition, with different colour contrast. The adhesive force images obtained with an –OH or –COOH coated tip show areas containing cellulose, hemicelluloses and extractives in lighter colours, whereas an adhesive force image obtained when using a $–CH_3$ coated tip will show areas containing lignin in lighter colours. A distinction between polar and non-polar wood components, such as cellulose and lignin was achieved, but the distinction between cellulose, hemicelluloses and extractives was not possible with tips comprising the evaluated functional groups. This is subject to ongoing studies. The average values of the adhesive force determined from the entire image could be used to compare wood fibres that had been subjected to different treatments, such as pulping and the removal of lignin could be confirmed. Despite some shortcoming this technique could be successfully used to characterise the surface topography and polarity of pulpwood surfaces. Together with other analytical techniques, such as FTIR, it can be used to describe fibre surfaces and determine the effects of various surface treatments.

It was found that the surface composition of the fibres followed the trend of the bulk composition in some, but not all cases. The cellulose content of fibres from different species but various growth sites was comparable within the standard deviations in the fibre bulk, as well as on the fibre surface. The lignin content, on the other hand, showed considerably more variation on the fibre surface than in the fibre bulk. While *E. grandis*, *E. grandis* clone and *E. grandis x camaldulensis* showed comparable values, *E. grandis x nitens* and *E. dunnii* had a significantly lower surface lignin content than suggested by the

bulk composition. These results could prove useful for the pulp and paper industry as they indicate why some species produce pulp of lower quality and also why some species cannot be pulped well together.

The effect of MAT and MAP on the surface composition on pulpwood fibres was recognisable. The surface cellulose content of *E. grandis x nitens* hybrids decreased with increasing MAT and decreasing MAP, while in turn the surface lignin content increased with increasing MAT and decreasing MAP. This was confirmed by the increasing surface cellulose content on fibres from *E. dunnii* with increasing MAP.

The attempt to map possible starch-binding sites on the wood fibres and determine differences between the species did not produce any conclusive results. No differentiation between wood species or treatment (such as pulping) was possible.

6.2 Recommendations

It will be interesting to correlate the results of the chemical surface composition determined on the wood fibres with their actual strength properties measured in hand-sheets. This would also add significance to the overall value of the results.

Appendix A: Element analysis of wood extractives by EDX

In order to determine possible functionalities of typical extractives that are NOT also present in cellulose or lignin, EDX spectra of H_2O and ethanol/cyclohexane extractives were obtained. They are shown in Figures 29-32. On the grounds of these results an amino ($–NH_2$) coating was chosen to detect extractive rich areas. This seemed a suitable tip coating to use to detect the H_2O extractives from Acacia. Unfortunately no clear distinction between extractives and cellulose/lignin was achieved, as was described in the results section.

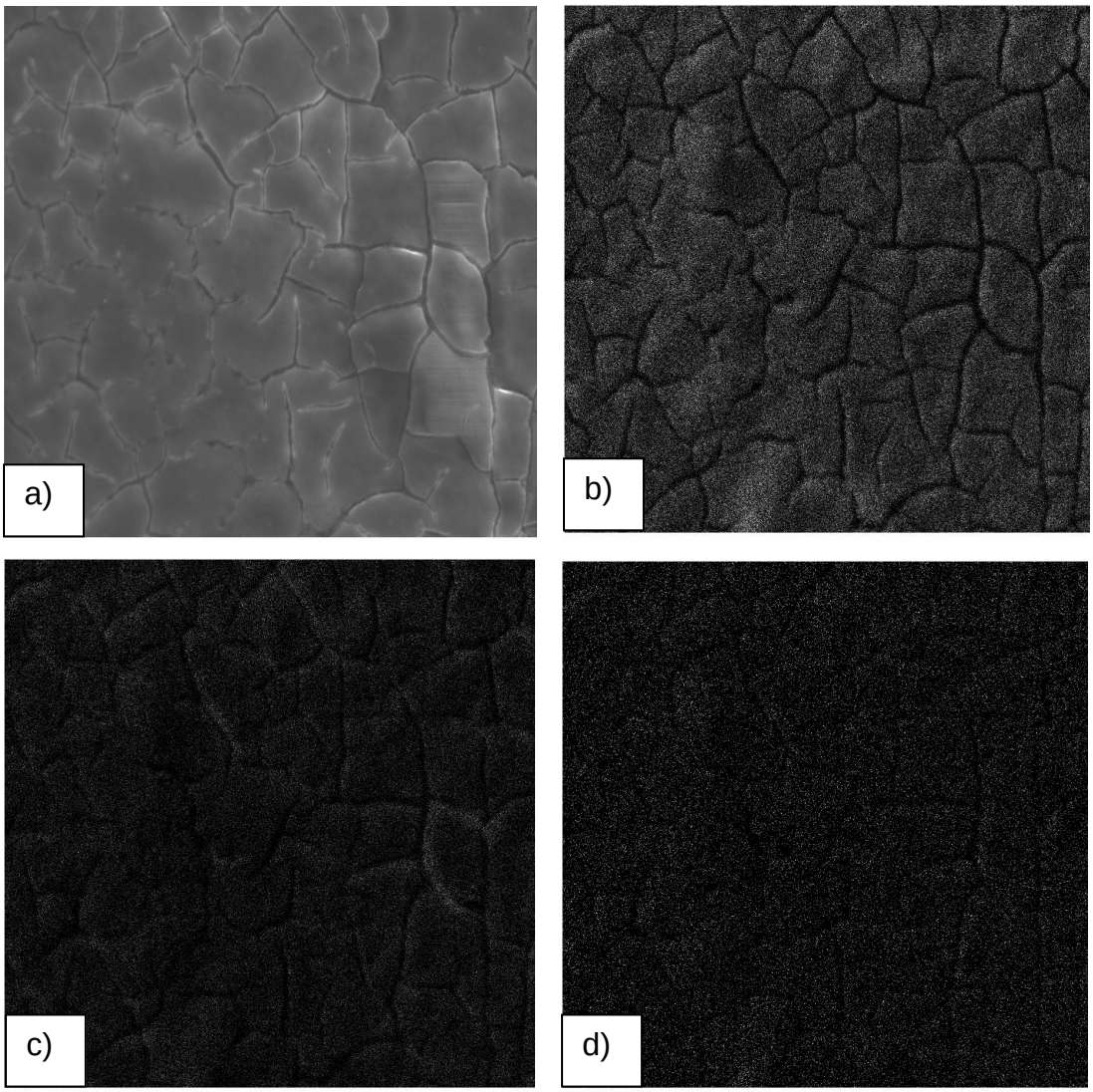

Figure 36: *EDX images of H_2O Extractives from A. mearnsii showing a) the topography, b) the distribution of carbon, c) the distribution of oxygen and d) the distribution of nitrogen.*

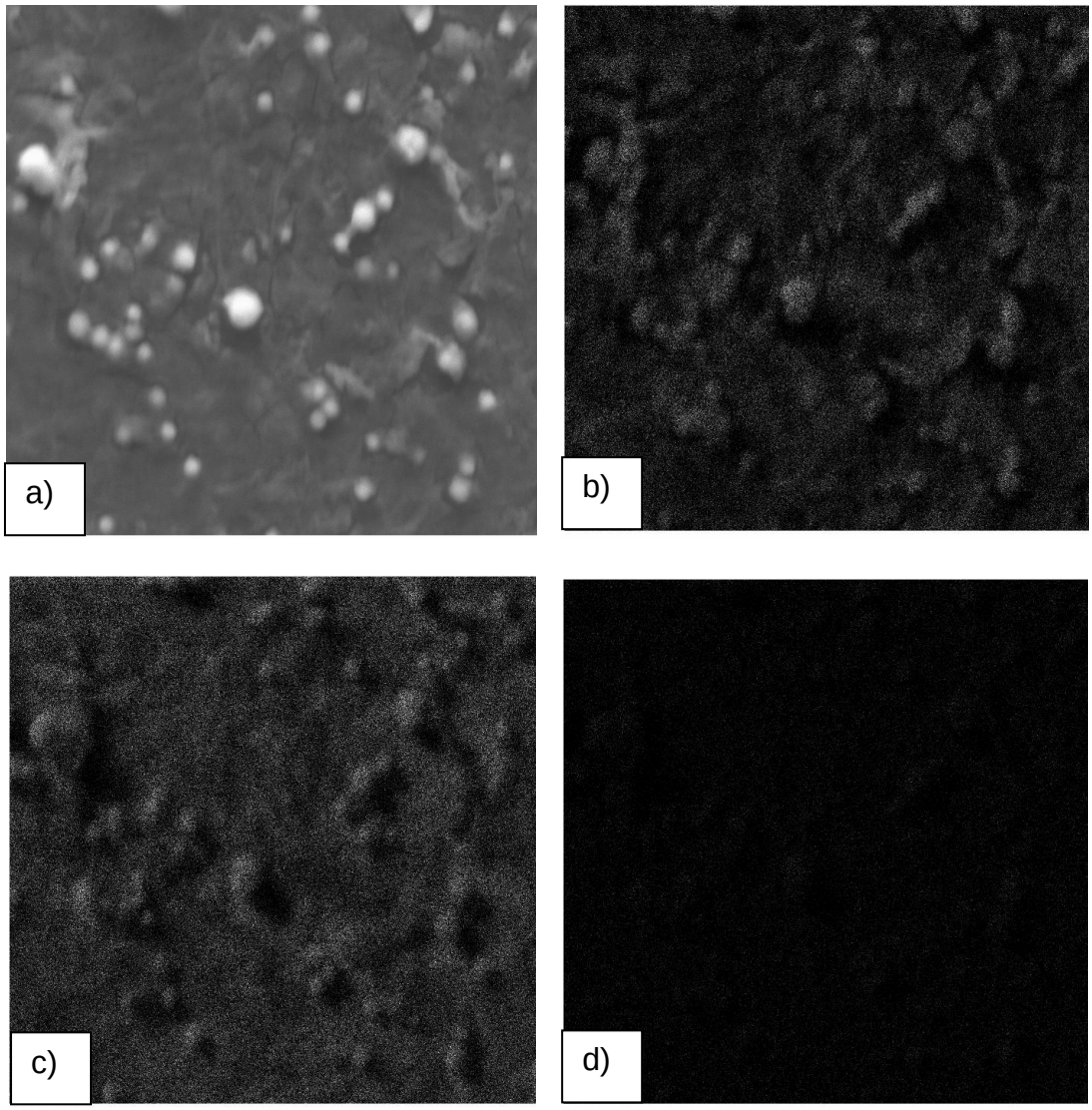

Figure 37: *EDX images of E/C extractives from A. mearnsi showing a) the topography, b) the distribution of carbon, c) the distribution of oxygen and d) the distribution of nitrogen.*

.

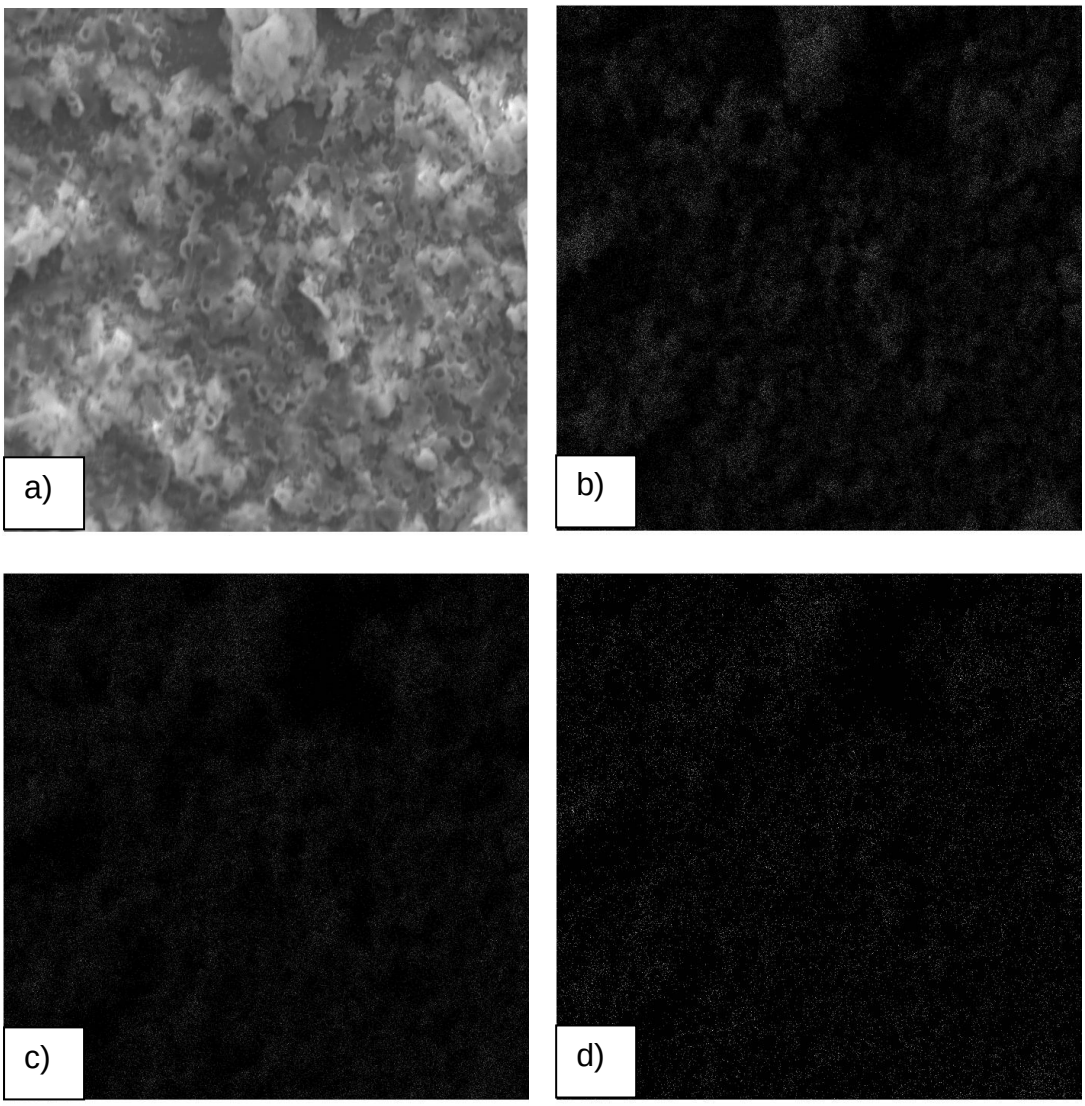

Figure 38: *EDX images of H_2O extractives from E. grandis showing a) the topography, b) the distribution of carbon, c) the distribution of oxygen and d) the distribution of nitrogen.*

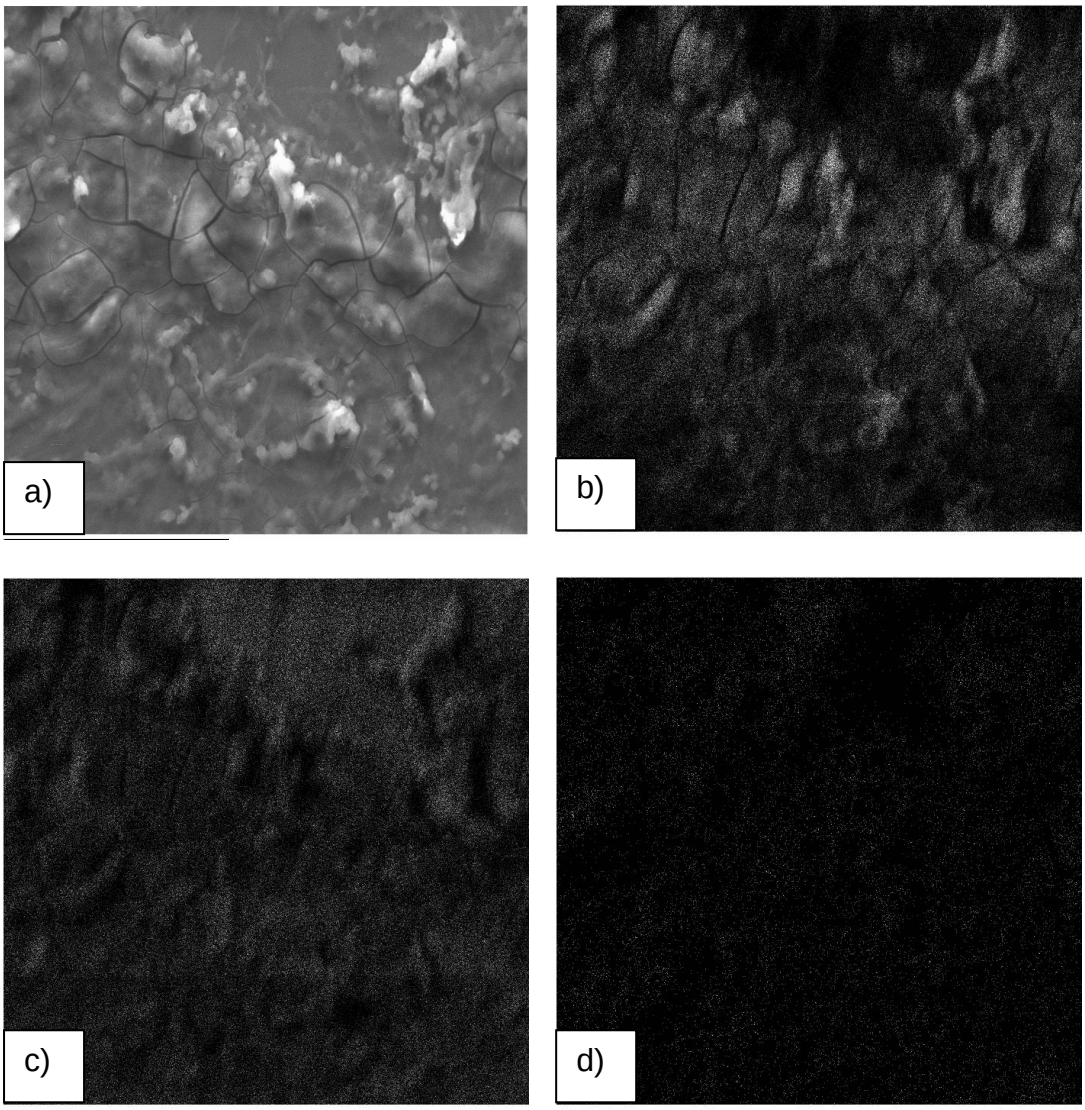

Figure 39: *EDX images of E/C extractives from E. grandis showing a) the topography, b) the distribution of carbon, c) the distribution of oxygen and d) the distribution of nitrogen.*

Table 9: quantities of the elements found in the different extractive films

Spectrum	wt% C	wt% N	wt% Na	wt% Mg	wt% Al	wt% Si	wt% Cl	wt% K	wt% Ca	wt% O
(Am) H_2O extractives	21.4	1.1	1.2	0.3	0.14	6.0	0.5	0.3	0.9	68.2
(Am) E/C extractives	17.8	1.0	3.4	0.8	0.3	10.5	0.0	0.1	1.4	64.7
(Eg) H_2O extractives	19.9	0.7	2.6	0.5	0.2	8.4	0.0	0.1	1.1	66.5
(Eg) E/C extractives	24.6	1.2	0.6	0.2	0.1	1.3	0.1	0.6	0.2	62.9
Glass	2.9	0.8	9.4	2.1	0.7	30.9	0.4	0.2	3.9	49.8

Am: Acacia mearnsii

E.g: Eucalyptus grandis

E/C: Ethanol/cyclohexane

EDX images of wood fibers

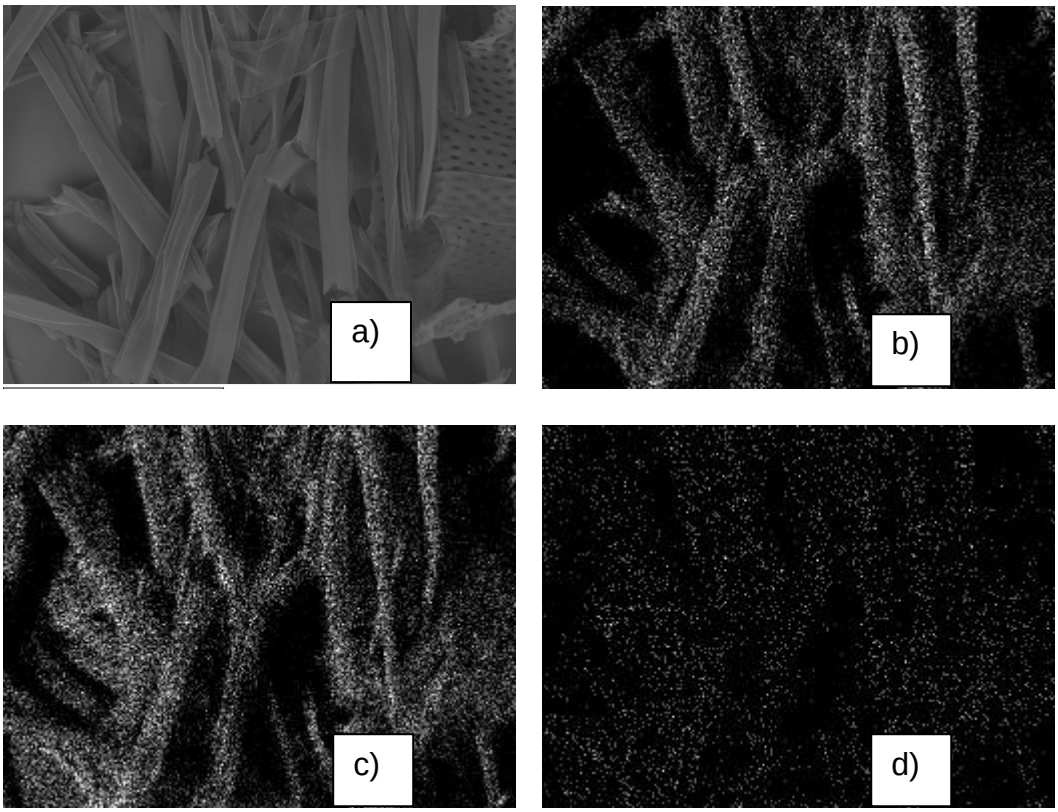

Figure 40: *EDX images of un-pulped A. mearnsii fibres showing a) the topography, b) the distribution of carbon, c) the distribution of oxygen and d) the distribution of nitrogen.*

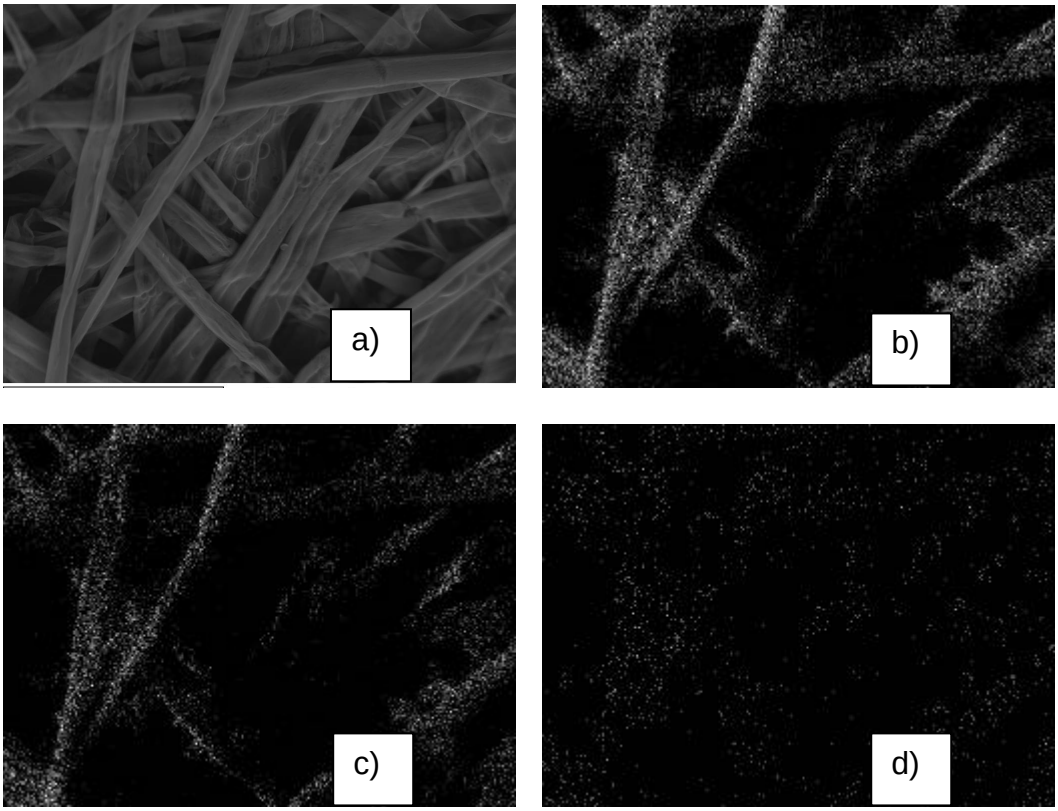

Figure 41: *EDX images of pulped A. mearnsii fibres showing a) the topography, b) the distribution of carbon, c) the distribution of oxygen and d) the distribution of nitrogen.*

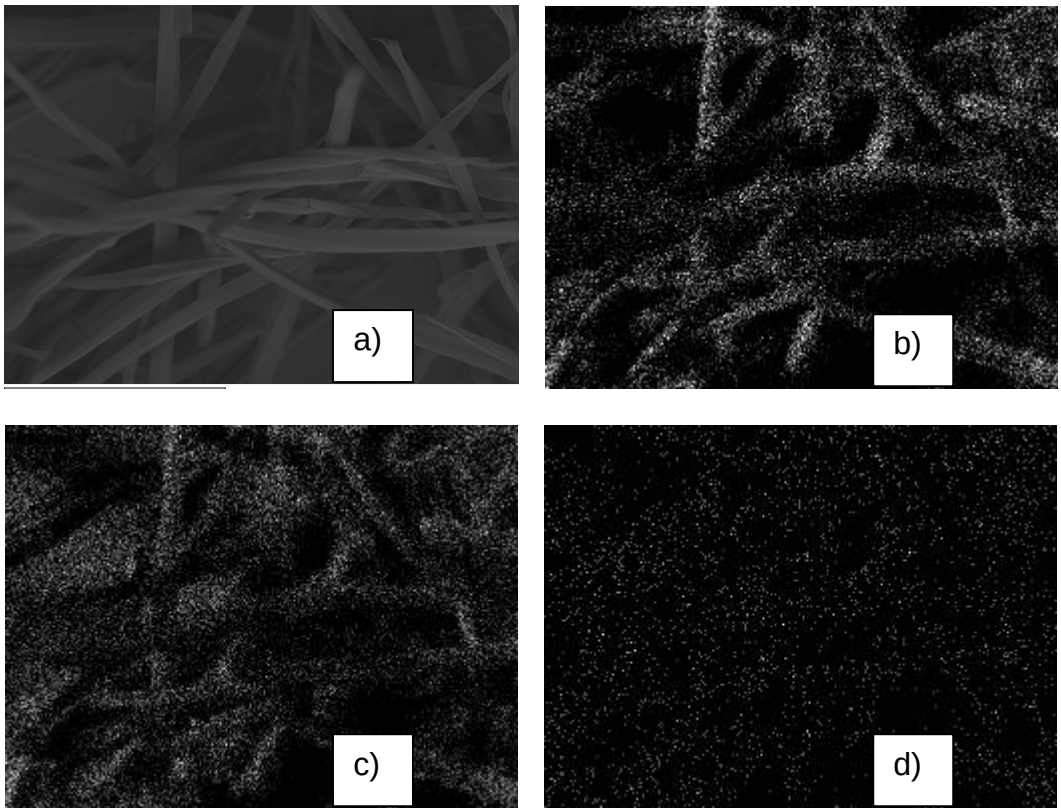

Figure 42: *EDX images of un-pulped E. grandis showing a) the topography, b) the distribution of carbon, c) the distribution of oxygen and d) the distribution of nitrogen.*

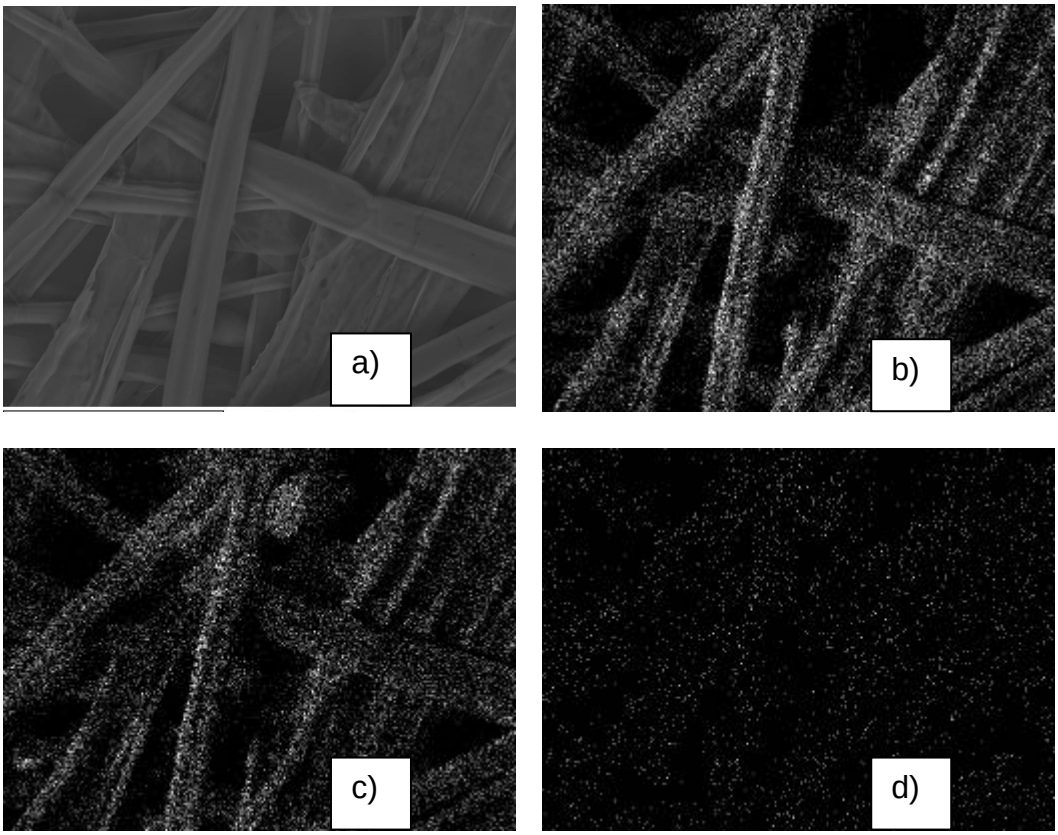

Figure 43: *EDX images of pulped E. grandis fibres showing a) the topography, b) the distribution of carbon, c) the distribution of oxygen and d) the distribution of nitrogen.*

Table 10: Amount of the elements found on untreated and pulped fibres from A. mearnsii and E. grandis

Spectrum	wt% C	wt% N	wt% Na	wt% Mg	wt% Al	wt% Si	wt% Cl	wt% K	wt% Ca	wt% O
(A.m) unpulped	27.3	0.1	2.8	0.2	0.1	3.9	0.1	0.0	0.7	63.4
(A.m) pulped	33.9	0.1	0.0	0.0	0.0	0.1	0.0	0.0	0.1	67.3
(E.g) unpulped	24.0	0.1	4.2	0.3	0.1	5.4	0.0	0.0	1.0	60.6
(E.g) pulped	26.9	0.0	1.4	0.1	0.1	2.2	0.0	0.0	0.0	69.7
Glass	2.9	0.0	9.4	2.2	0.7	30.9	0.4	0.2	3.9	49.8

Appendix B: Presentations and Publications

- Poster at 14th ISWFPC, Durban, 25 - 28 June 2007
- Poster at UNESCO / IUPAC Conference on Macromolecules & Materials, 8 - 11 September 2008, Kruger National Park, South Africa
- Publication: “Localization and Attempted Quantification of Various Functional Groups on Pulp Fibres”, A. Klash, E. Ncube, M. Meincken, Applied Surface Science, 255, 2009, 6318–6324.
- Publication: “Determination of the Cellulose and Lignin Content on Wood Fibre Surfaces of Eucalypts as a Function of Genotype and Site”, A. Klash, E. Ncube, B. du Toit and M. Meincken, European Journal of Forest Research, 129, 2010, 741-748.

Identification and Quantification of Chemical Components of Pulp Fibers

A. Klash[a], M. Meincken[b]

[a] Department for Chemistry and Polymer Science, University of Stellenbosch, Private Bag X1, Matieland 7602, email: klash@sun.ac.za

[b] Department of Forest and Wood Science, University of Stellenbosch, Private Bag X1, Matieland 7602, email: mmein@sun.ac.za

Background

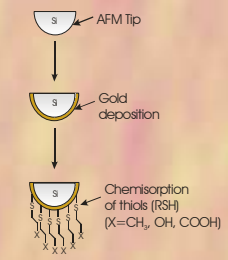

Scheme for chemical modification of AFM tips

Determination of the adhesive force

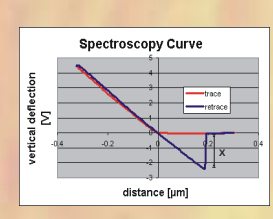

General approach and retract force distance curve

The adhesive force (F) is calculated using Hooke's law

$F=-kX$

X is the pull-off cantilever deflection
k is spring constant of the cantilever.

Samples

Cellulose

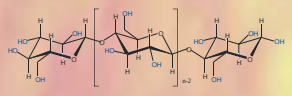

Organic extractives (Fat, Wax, Terpenes and Phenols): mostly -COOH
Ethanol/cyclohexane extractives from *A. cyclops*

Lignins (e.g Lignin Alkali)

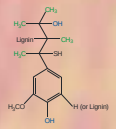

Tip Coatings

COOH coated tip

OH coated tip

CH_3 coated tip

Results

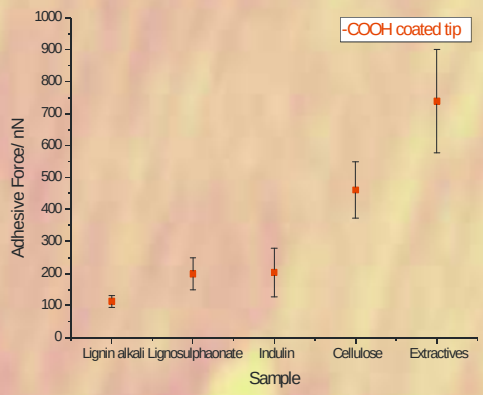

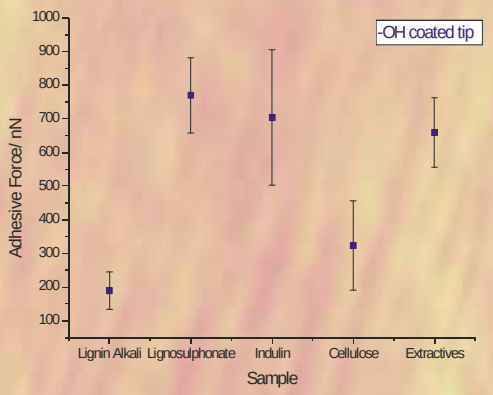

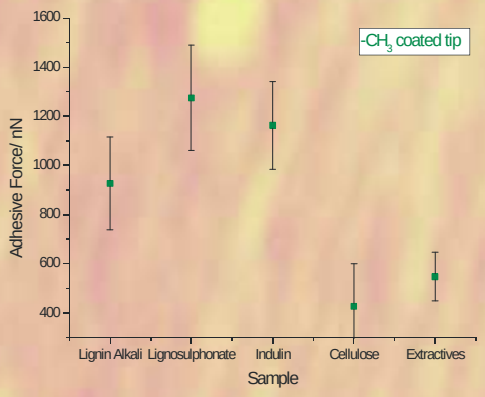

- The adhesive force values determined with the -COOH coated tip shows a higher sensitivity towards the extractives and cellulose than lignin.
- Similar results were obtained with the -OH coated tip with the exception of lignosulphonate and indulin.
- The high adhesive force between the -COOH and -OH coated tips on cellulose and extractives might be due to the high content of OH groups in these samples respectively.
- The -CH_3 coated tip shows a higher sensitivity towards lignin than to cellulose and extractives.

Conclusions and Outlook

The results show that AFM operated with functionalized tips allows the direct quantitative analysis of functional groups on the surface of various samples. A distinction between several functional group and therefore between the major components present in pulp fibres is possible.
This technique will be used to image pulp fibres at various processing stages and determine their chemical surface composition.

Acknowledgments

The authors would like to thank the International Center for Macromolecular Chemistry and Technology in Libya for financial support.

Poster presented at the TAPPSA Durban; 25-28 June 2007

LOCALISATION AND QUANTIFICATION OF FUNCTIONAL GROUPS ON PULP FIBRES

A. Klash[1], R.D. Sanderson[1], M. Meincken[2]*

[1] Department of Chemistry and Polymer Science, [2] Department of Forest and Wood Science, University of Stellenbosch, Private Bag X1, Matieland 7602, South Africa.
Email: mmein@sun.ac.za, Tel.: +27 21 8082618

Introduction

Chemical force microscopy (CFM) is an adaptation of AFM, in which the tip is coated with specific functional groups. The adhesive force determined between the modified tip and the sample surface can be used to gain additional information about the chemical composition of the surface.

The different functional groups proved to have a different sensitivity towards the substrates, which confirms that this method could be used to localise and identify areas of different chemical composition on wood and pulp fibres. This is demonstrated for pulpwood fibres from two different wood species.

Experimental

AFM Tip coating

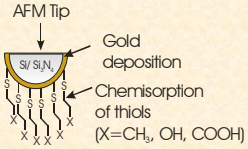

Adhesive force measurements

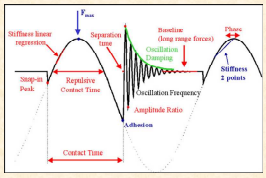

Individual substrate films

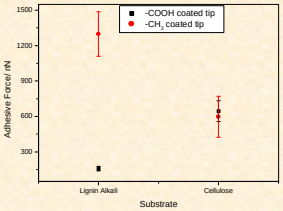

Investigated wood fibers

Untreated and pulped wood Fibres from both *Eucalyptus grandis* and *Acacia mearnsii*

Results & Discussion

ATR-FTIR

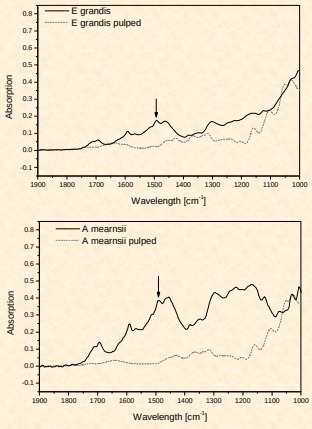

ATR-FTIR spectra of a) untreated and pulped *E. grandis* fibres and b) untreated and pulped *A. mearnsii* fibres.

The absorption band at 1508 is characteristic for lignin and disappears after pulping

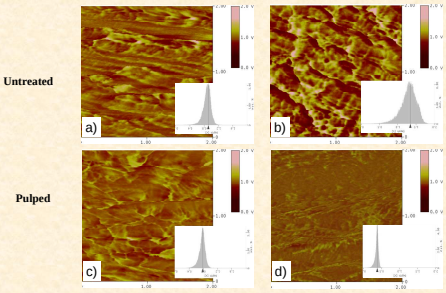

Adhesive force images obtained on the fibre surface of a) -COOH and b) -CH_3 coated tips for untreated *E. grandis*. Adhesive force images obtained on the fibre surface of c) -COOH and d) -CH_3 coated tips pulped for *E. grandis*.

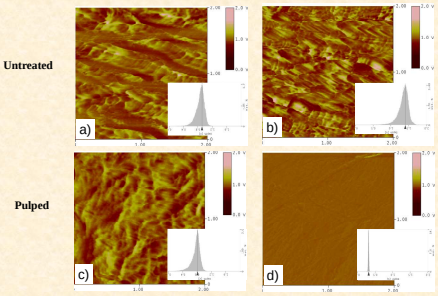

Adhesive force images obtained on the fibre surface of a) -COOH and b) -CH_3 coated tips for untreated *A. mearnsii*. Adhesive force images obtained on the fibre surface of c) -COOH and d) -CH_3 coated tips pulped *A. mearnsii*.

The average adhesive force and standard deviation determined between the functionalised tips and the samples.

Tip coating / Sample	-CH_3 (lignin)		-COOH (cellulose + extr.)	
	Adhesive Force/ nN	STD	Adhesive Force/ nN	STD
E. grandis	1492	166 (121)	1050	144 (87)
Pulped E. grandis	476	83 (32)	942	90 (50)
A. mearnsii	1434	178 (89)	1304	122 (93)
Pulped A. mearnsii	338	155 (12)	1275	153 (89)

Conclusions and Outlook

AFM with functionalised tips could be used to localise, identify and to a degree quantify different chemical components , such as cellulose and lignin on wood fibres.

The adhesive force images obtained with an -COOH coated tip show areas containing cellulose, hemicelluloses and extractives in lighter colours, whereas an adhesive force image obtained with a -CH_3 coated tip will show areas containing lignin in brighter colours.

The average values of the adhesive force determined from the entire image could be used to compare wood fibres that underwent different treatments, such as pulping.

A distinction between cellulose and extractives is, however, not possible with the evaluated functional groups and is subject to ongoing studies.

**10th Annual UNESCO / IUPAC Conference on Macromolecules & Materials,
Berg-en-Dal, Kruger National Park, Mpumalanga, South Africa ; 8-11 September 2008**

Applied Surface Science 255 (2009) 6318–6324

Contents lists available at ScienceDirect

Applied Surface Science

journal homepage: www.elsevier.com/locate/apsusc

Localization and attempted quantification of various functional groups on pulpwood fibres

A. Klash [a], E. Ncube [b], M. Meincken [b,*]

[a] Department of Chemistry and Polymer Science, University of Stellenbosch, Private Bag X1, Matieland 7602, South Africa
[b] Department of Forest and Wood Science, University of Stellenbosch, Private Bag X1, Matieland 7602, South Africa

ARTICLE INFO

Article history:
Received 21 May 2008
Received in revised form 3 February 2009
Accepted 4 February 2009
Available online 14 February 2009

Keywords:
Pulp fibres
Functional groups
Chemical force microscopy
Adhesive force

ABSTRACT

The distribution of different free chemical functional groups on wood and pulp fibres has been determined by means of atomic force microscopy (AFM) with chemically modified tips. Because these functional groups show a higher affinity to similar groups on the substrate surface during scanning, AFM images determined with an additional digital pulsed-force mode (DPFM) controller allow the distribution of the chemical components to be imaged and to a degree also to be quantified. The investigated tip coatings showed a different sensitivity towards the major chemical components present in wood fibres, determined on spin-coated films and on wood fibres. A clear distinction between cellulose and lignin was possible in both cases. This technique could therefore be used to differentiate between cellulose and lignin present on pulp fibre surfaces and confirm the successful removal of lignin by pulping.

1. Introduction

Wood fibres are the main source for pulp and paper [1]. The strength of the final product depends largely on the bonding between individual fibres, which is facilitated by van der Waals forces and hydrogen bonds between hydrophilic groups on the fibre surfaces. A better understanding of the surface chemistry of the wood fibres and the distribution of these polar groups could help to further improve paper quality.

Cellulose is a natural polymer and the most important source of cellulose is wood, which is a natural composite consisting of cellulose, hemicellulose, lignin and extractives. In order to utilize wood fibres effectively, the cellulose needs to be isolated from the other wood components, which inhibit the development of strength properties [2,3]. This isolation process is done by extraction and pulping [4].

Extractives can be removed by hot water, which removes tannins and inorganic salts, or by organic solvents such as hexane, acetone, or diethyl ether, which remove terpenes, fats, wax, and phenols [5]. Despite the fact that the extractive content of wood is typically only a small part of the total wood composition, it has a major effect on wood properties such as odour, colour, decay and density, flammability, hygroscopicity, permeability, and mechanical and chemical processability [6]. Therefore it is vital for further processing to reduce the extractive content as much as possible.

Inter-fibre bonding in paper is negatively affected by the presence of hydrophobic lignin on fibre surfaces, which obstructs the formation of hydrogen bonds between fibres. The removal of the hydrophobic lignin during pulping exposes the cellulose and hemicelluloses and their hydrophilic hydroxyl groups on the fibre surface [6].

Previous studies have tried to find a correlation between the chemical composition and surface properties of wood fibres using X-ray photoelectron spectroscopy (XPS) [7,8], scanning electron microscopy (SEM) [9] and atomic force microscopy (AFM). AFM has been used to investigate the surface morphology of wood, pulp and paper fibres by various groups [10–12]. Koljonen et al. [13] used AFM in tapping mode to reveal the morphological structure of various mechanical pulps and attempted to link this to the chemical composition of the pulp. These experiments were, however, performed with unmodified commercial AFM tips either made from Si_3N_4 or SiO_2. Fardim et al. [14] examined the structure of extractives in wood fibres by AFM and linked this to the chemical composition, determined by XPS and ToF-SIMS.

In this study we investigated the feasibility of digital pulsed-force mode AFM (DPFM-AFM) to identify and localise functional groups on pulpwood fibres. In a previous study [15] we have shown that DPFM-AFM can be used with unmodified silicon tips to detect polar areas on the surface of wood fibres, as the SiO layer forming on the tip is more sensitive towards polar groups on the sample surface. In this study we are investigating the feasibility of different tip coatings in order to determine their sensitivity towards the different chemical components in wood fibres. The objective was to find specific tip coatings for each wood

* Corresponding author. Tel.: +27 21 8082618; fax: +27 21 8083603.
E-mail address: mmein@sun.ac.za (M. Meincken).

0169-4332/$ – see front matter © 2009 Elsevier B.V. All rights reserved.
doi:10.1016/j.apsusc.2009.02.009

component, namely cellulose and lignin, in order to localise, identify and possibly quantify them.

1.1. Chemical force microscopy

Chemical force microscopy (CFM) is an adaptation of AFM, in which the tip is coated with specific functional groups. The adhesive force determined between the modified tip and the sample surface can be used to gain additional information about the chemical composition of the surface [16]. The tip is modified with self-assembling monolayers (SAMs) of alkane thiol compounds, which allow control of the functionality and their chemical and mechanical stabilities [17]. Chemical force microscopy has been established on chemically modified, flat silicon surfaces by Noy et al. [18]. In their study both the silicon substrates and the S_3N_4 tips were coated with gold and then modified with SAMs of alkane thiol compounds terminated with $-CH_3$, –COOH and $-NH_2$ functional groups. They found that the adhesive force was larger if the tip and substrate had the same functionality. Chemical force microscopy also has been used to study cellulose fibres in aqueous media by Bastidas et al. [19]. The focus of their work was on the effect of the pH value on the adhesive force determined with $-CH_3$, –COOH and –OH coated tips. They established that the pH value has a strong effect on the adhesive force values determined with the –COOH tip only.

In this study we determine the adhesive forces between AFM tips coated with –OH, $-CH_3$ and –COOH, respectively and films made from cellulose, lignin and extractives. The different functional groups proved to have a different sensitivity towards the substrates, which indicates that this method could be used to localise and identify areas of different chemical composition on wood and pulp fibres. This is then demonstrated for pulpwood fibres from two different wood species.

2. Materials and methods

2.1. Adhesive force measurements with the DPFM-AFM

All AFM measurements were performed with a Veeco Multimode instrument in conjunction with a Witec DPFM controller. In the pulsed-force mode [20,21] the AFM is operated in contact mode, while a sinusoidal modulation is applied to its *z*-piezo. The modulation frequency is typically between 1 and 10 kHz, which is well below the resonance frequency (f_r) of the cantilever (a force modulation cantilever with a nominal resonance frequency of $f_r \approx 70$ kHz). In this way force–distance curves are measured at every scan point, by continuously bringing the tip into contact with the surface and subsequently retracting it. Thus, topography and physical surface properties, such as stiffness or adhesion, can be measured simultaneously and with the same spatial resolution, and are represented by images displaying either the topography, stiffness or the adhesive force.

In order to quantify the adhesion measured in an adhesion image, the image is displayed as a histogram, as shown in Fig. 1. The histogram shows the distribution of adhesive force values determined across the image and allows the determination of an average adhesive force value and its standard deviation, which serve as error bars in our data presentation. This histogram represents the values determined with a –COOH coated tip on a cellulose surface.

The quantitative value of the adhesive force F_{adh} is given by

$$F_{adh} = V_{adh} kS$$

where V_{adh} is the average voltage value determined from the adhesion image, k is the spring constant of the cantilever and S is the sensitivity of the photodiode. The spring constant k of the force modulation cantilever was 2.8 N/m [22] and the sensitivity S was determined to be 500 nm/V.

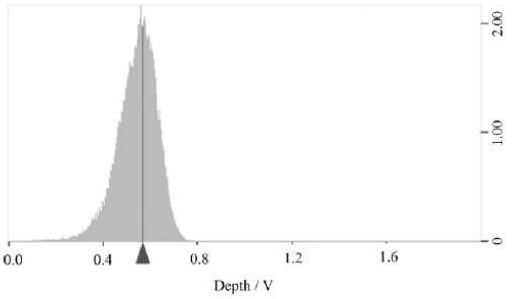

Fig. 1. Typical histogram of the values obtained from an adhesion image.

2.2. Chemical tip modification

Silicon force modulation cantilevers from Nanosensors were used for the tip modifications according to Bastidas et al. [19]. Tips with the following functional groups were prepared:

- Methyl ($-CH_3$) groups, from 1-octadecanethiol $CH_3(CH_2)_{17}SH$ (Acros).
- Hydroxyl (–OH) groups, from 11-mercapto-1-undecanol $HO(CH_2)_{11}SH$ (Aldrich).
- Carboxylic (–COOH) groups, from 11-mercaptoundecanoic acid $HOOC(CH_2)_{10}SH$ (Aldrich).

The silicon tips were first coated with gold and cleaned under a 254 nm UV lamp for 1 h to ensure that all organic material was removed. The gold-coated tips were subsequently immersed in reagent alcohol for 30 min and then in a three mM $CH_3(CH_2)_{17}SH$, $HO(CH_2)_{11}SH$ or $HOOC(CH_2)_{10}SH$ alcoholic solution for 2 h at room temperature. The coated tips were then rinsed with n-heptane (Aldrich) and alcohol, and gently dried in an Argon stream.

2.3. Sample preparation

2.3.1. Substrate films

Films of α-cellulose (Sigma), lignin alkali (Aldrich) and wood extractives (hot water and benzene/ethanol extractives from Acacia) were prepared from solution by spin coating and film casting. For the cellulose film, a mixture of α-cellulose (1.333 g, 8.21 mmol based on glucose units) and *N,N*-dimethylacetamide (DMAc) (50 mL) was heated to 150 °C for 30 min in a round bottomed flask equipped with a condenser. Then, LiCl (1.08 g, 25.5 mmol) was added and the mixture was heated to 166 °C for 8 min. The reaction mixture was then cooled to room temperature and stirred overnight for dissolution [23]. The lignin alkali (2%, w/v) was dissolved in deionised water and for the extractive solution a combination of hot water and ethanol/cyclohexane extractive was used as obtained from the wood extraction. The dissolved materials were spin-coated on freshly cleaved mica surfaces at 1500 rpm for 7 min to accomplish a uniform polymer distribution and film thickness.

2.3.2. Fibre preparation

Fibres from *Eucalyptus grandis* and *Acacia mearnsii* were investigated. If the samples had not already disintegrated into single fibres during pulping they were separated into single fibres by a mild maceration method in Jeffery's solution [24] for 4 h.

Fibres were spread from a water suspension onto a glass slide and left to dry for 12 h. The adhesion due to capillary forces between the cells and the mica substrate was sufficient to keep the fibres in position for AFM analysis. Images with a scan size of 2 μm × 2 μm were acquired with the fast scan axis parallel to the longitudinal fibre axis, in order to minimise shear forces. The fibres spread on mica for AFM analysis were well dispersed and formed a single layer on the substrate, in order to allow imaging of individual fibres. The fibres prepared for FTIR analysis were spread into a thick layer to avoid any absorption peaks originating from the substrate.

2.3.3. Adhesive force

The average polarity of the substrate films was measured from adhesion images obtained at 10 different locations for each sample. The average fibre polarity was determined from adhesion images obtained on 10 different randomly selected fibres. Each adhesion image consists of 65,536 (256 × 256) single measurements in the observed area. The *z*-range was 0–2 V for all images.

In order to compensate for the environmental effect of humidity and temperature, which could lead to a change in adhesive force between the sample and the tip [25–27], the tip was calibrated on a mica surface before each measurement. The adhesive force determined on the mica surface was calculated and normalised to a standard value determined in the first measurement. Any difference in this standard value was the added or subtracted from the adhesive force values determined for the fibre samples.

2.3.4. Sulphite pulping

80 g of ovendry wood chips were pulped in a micro-bomb for 12 h at 140 °C with magnesium bisulphite (bisulphite pulping) at a sulphite concentration of 5%. Before pulping, the chips were impregnated with magnesium bisulphate at 100 °C for 2 h. The filled micro-bombs were then placed in a 15 L digester and covered with water. The temperature of the water was monitored with a thermocouple. After pulping the poorly pulped were separated from the pulp fibres, which were kept for analysis.

2.3.5. Infrared spectroscopy

The removal of lignin due to pulping was confirmed with attenuated total reflectance Fourier transform infrared spectroscopy (ATR-FTIR), consisting of a Smart Golden Gate ATR from Thermo Nicolet attached to a FTIR from Nexus. Each spectrum consisted of 16 spectra, which were recorded with a penetration depth of about 1.2 μm at a resolution of 8 cm^{-1}. The spectra were normalised on the peak originating from the C–O stretching in cellulose at 1029 cm^{-1} and the intensity of the aromatic C=C peak at 1500 cm^{-1} was used to determine the presence of lignin.

3. Results and discussion

The sensitivity of tips coated with free –COOH, $–CH_3$ and –OH groups towards films consisting of the major components found in wood fibres – cellulose, lignin and extractives – was determined in a first experiment on spin-coated films. The results are displayed in Fig. 2a–c.

The –COOH coated tip showed the highest sensitivity towards extractives, followed by cellulose and lignin (Fig. 2a). The –OH coated tip showed similar behaviour but there was a smaller difference between the adhesive force determined on cellulose and extractives. In fact, the OH coated tip provided very similar adhesive forces values to those measured with an uncoated SiO tip [15]. The high affinity of –COOH and –OH towards cellulose and extractives can be explained by the free hydroxyl groups that are abundant in both components.

The $–CH_3$ coated tip showed a higher sensitivity towards lignin than to cellulose and extractives, which can be explained by free methyl groups in the lignin molecules.

These results suggest that a $–CH_3$ coated tip can be used to detect lignin-rich areas on fibre surfaces, while a –COOH and –OH

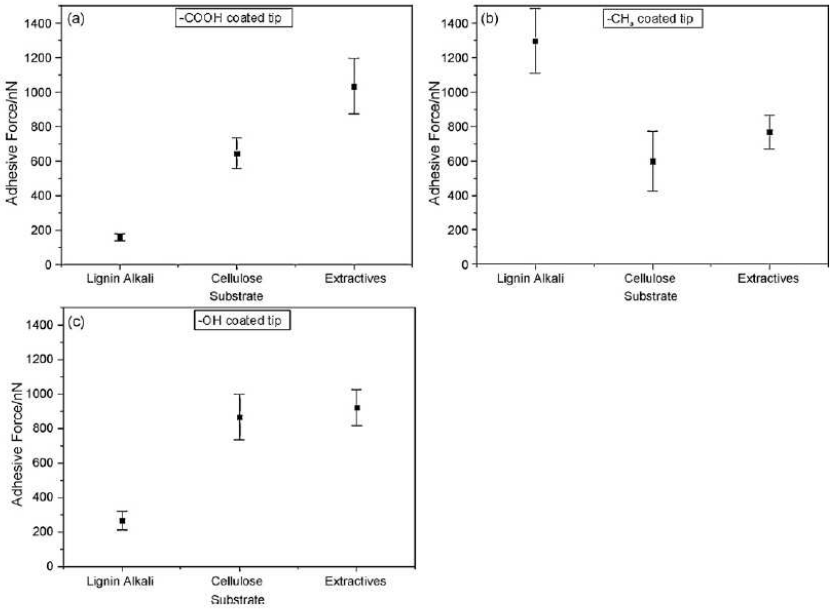

Fig. 2. Adhesive forces determined between the different substrates and (a) –COOH, (b) $–CH_3$ and (c) –OH coated tips.

coated tip will be more sensitive to cellulose and hemicelluloses and possibly extractives. A clear distinction between cellulose and extractives is not possible with any of the three evaluated tip coatings. To develop a coating that contains functional groups that would only be sensitive to some of the more common extractives found in wood is part of an ongoing project.

These films, however, served only as model components for wood fibres, in order to prove that the technique could deliver the necessary material contrast. On wood fibres, cellulose, hemicelluloses, lignin and extractives are blended together in various ratios and no two fibre surfaces show exactly the same composition.

In order to show, that this technique can be used to determine, for example, the lignin removal due to pulping on different wood fibres, –COOH and $–CH_3$ coated tips, which produced large material contrasts, were chosen for a subsequent evaluation of wood fibres and pulped fibres from two different wood species. The surfaces of untreated and pulped fibres from *E. grandis* and *A. mearnsii*, two wood species commonly used for paper manufacturing were investigated.

As pointed out before, the images acquired with the –COOH coated tip (Fig. 3a and c) showed a higher affinity to cellulose, hemicelluloses and extractives, which appear as light areas in adhesion images. The images acquired with the $–CH_3$ coated tip (Fig. 3b and d) show a higher affinity for lignin, which is again represented by the lighter areas in the adhesion images. Fig. 3a and b shows typical adhesion images obtained on the fibre surface of untreated *E. grandis*, while Fig. 3c and d shows the adhesion images obtained on untreated *A. mearnsii*.

The images acquired with –COOH and $–CH_3$ coated tips show a bright colour contrast on both wood species, which suggests the presence of cellulose, hemicelluloses, extractives, as well as lignin on the fibre surfaces. The histograms shows a value distribution around 0.9 V for the –COOH coated tip and around 1.4 V for the $–CH_3$ coated tip on both species.

Fig. 4a–d shows fibres from the same species after sulphite pulping. The images acquired with a $–CH_3$ coated tip (b and d) show a low colour contrast with a narrow colour distribution and an absence of bright areas, which is consistent with the successful removal of most of the lignin by the pulping. No functional groups remained on the fibre surface, to which the CH_3 coated tip was especially sensitive, resulting in a lower average adhesive force value.

The images acquired with a –COOH coated tip (a and c) showed a similarly high colour contrast, as before pulping with many bright areas. Areas without free hydroxyl groups are, however, still displayed as darker areas, resulting in the larger colour deviation within the images. The histograms show a value distribution around 0.9 and 0.8 V for the –COOH coated tip on the two wood species, whereas the values are distributed around 0.35 V in the images acquired with a $–CH_3$ coated tip on both species. This significant shift to lower values – from about 1.4 V in the images of untreated fibres to about 0.35 V in the images of pulped fibres shows clearly that the adhesive force determined between the $–CH_3$ coated tip and the sample surface has been reduced, which can be attributed to a decrease in free methyl groups, which is a measure for the lignin content in the imaged area.

For each image the average adhesive force value was determined with its standard deviation. The average value obtained from 10 images (fibres) and the standard deviation from those values was used to describe the average adhesion determined on fibres of one wood species. The average standard deviation obtained for the 10

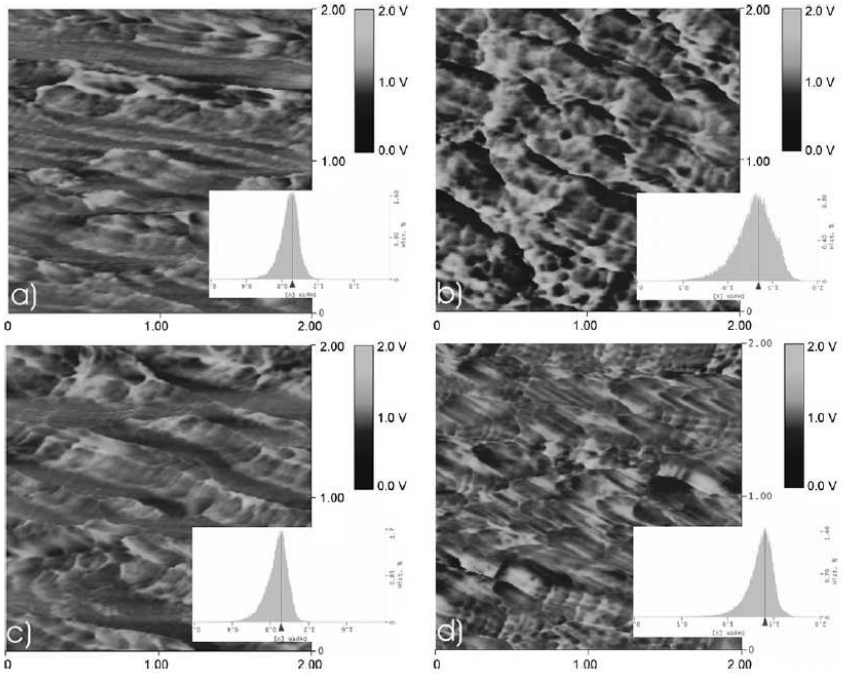

Fig. 3. Adhesive force images and histograms of colour values obtained on the fibre surface of untreated *E. grandis* with (a) –COOH and (b) $–CH_3$ coated tips and on the fibre surface of untreated *A. mearnsii* with (c) –COOH and (d) $–CH_3$ coated tips.

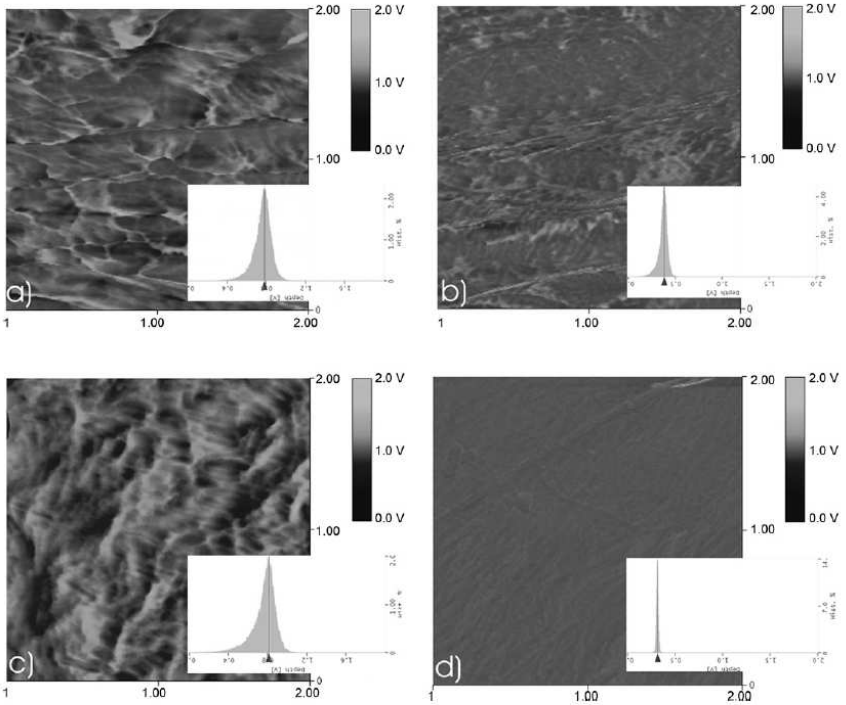

Fig. 4. Adhesive force images and histograms of colour values obtained on the fibre surface of pulped *E. grandis* with (a) –COOH and (b) $–CH_3$ coated tips and on the fibre surface of pulped *A. mearnsii* with (c) –COOH and (d) $–CH_3$ coated tips.

individual images, which is a measure for the distribution of values within one sample, is given in brackets. As Fig. 2 suggested, this average value is proportional to the amount of lignin present on the fibre surface if a $–CH_3$ coated tip was used and to the amount cellulose, hemicelluloses and extractives present on the surface if a –COOH coated tip was used.

It can be observed that the untreated fibre surfaces differ in the adhesive force detected with the –COOH coated tip. This can be explained by the different chemical composition of the two wood species, as the –COOH coated tip is sensitive to cellulose, hemicelluloses and extractives, all of which are known to differ between the two species. Similar results were found in a previous study that characterised the polarity of fibres surfaces with unmodified SiO AFM tips [15].

It can be seen that the effect of sulphite pulping on the surface composition is considerable. The reduction of lignin in the fibres is clearly reflected by the decreased average adhesive force detected with the $–CH_3$ coated tip and this effect is visualized in Fig. 4b and d.

Table 1
The average adhesive force and standard deviation determined between the functionalised tips and the samples.

Tip coating	$–CH_3$ (lignin)		–COOH (cellulose + extr.)	
Sample	Adhesive force (nN)	STD	Adhesive force (nN)	STD
A. mearnsii	1434	178 (89)	1304	122 (93)
Pulped *A. mearnsii*	338	155 (12)	1275	153 (89)
E. grandis	1492	166 (121)	1050	144 (87)
Pulped *E. grandis*	476	83 (32)	942	90 (50)

The average adhesive force determined with the –COOH coated tip remains constant within the range of the standard deviations after pulping. This could be explained by the fact that a de facto increase in the cellulose content does not necessarily lead to an increase in free hydroxyl groups on the fibre surface, as they will also associate with themselves. Furthermore, the extractives content, which added to the adhesive force value, can be expected to be lower after pulping. The adhesive force values determined with the different tip coatings on the two wood species are summarized in Table 1.

The reduction of lignin due to pulping was confirmed by ATR-FTIR. Fig. 5 shows spectra of untreated and pulped fibres from *E. grandis* (Fig. 5a) and *A. mearnsii* (Fig. 5b). The spectra clearly show a decrease in the peak at 1508 cm^{-1}, which is characteristic for the C=C bond in the aromatic rings of lignin. This is consistent with the fact that the amount of lignin amount has been decreased by pulping.

3.1. Limitations of chemical force microscopy

Details of the environment, in which the adhesion measurements are carried out, are an important consideration. In ambient conditions, surfaces may be contaminated with organic compounds, or a layer of condensed water vapour, which varies with humidity. To minimise the effect of this variation, the adhesive force was normalised before each measurement series on a mica surface to the same value.

The condensed water layer can form a contact meniscus between the tip and sample, adding a capillary force to the measured adhesive force. To eliminate this factor, many studies are performed under liquid environments or in ultrahigh vacuum. In

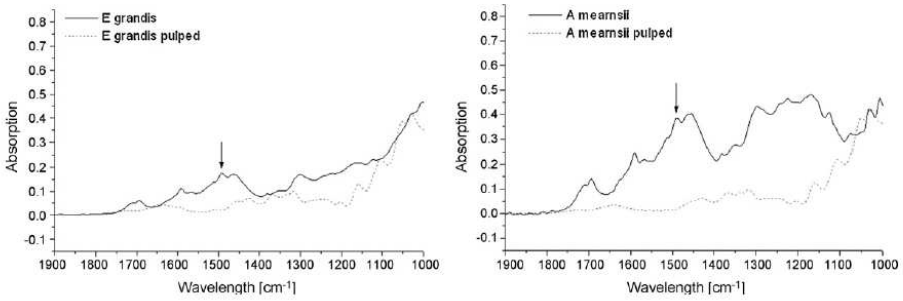

Fig. 5. ATR-FTIR spectra of (a) untreated and pulped *E. grandis* fibres and (b) untreated and pulped *A. mearnsii* fibres.

liquid, however, the solvent will affect the adhesion and affect the pH value and ionic strength of surface charges present. Force measurements conducted in air are more difficult to interpret since the capillary forces may be larger than the chemical interactions and capillary condensation could emphasize the degree of polarity of a surface. The difference between polar and non-polar groups could therefore be exaggerated [16].

The effect of topography on the adhesive force was studied by Sato et al. [28] with PFM-AFM. They found that a variation in the grain size of the sample and multiple contacts between the tip and sample surface resulted in different distribution widths of the observed adhesion forces. Despite those shortcomings, the obvious advantage of AFM as a tool for the surface characterisation of pulp fibres is the simultaneous acquisition of a high-resolution (<10 nm) topography image and spatial chemical information of the observed area.

4. Conclusions

We have successfully demonstrated that AFM with functionalised tips can be used to localise, identify and to a degree quantify different chemical components on wood fibres. Adhesive force images acquired with an additional DPFM controller show areas of different composition with different colour contrast. The adhesive force images obtained with an –OH or –COOH coated tip will show areas containing cellulose, hemicellulose and extractives in lighter colours, whereas an adhesive force image obtained with a $–CH_3$ coated tip will show areas containing lignin in lighter colours. A distinction between polar and non-polar wood components, such as cellulose and lignin could be achieved, although the distinction between cellulose, hemicelluloses and extractives was not possible with the evaluated functional groups and is subject to ongoing studies. The average values of the adhesive force determined from the entire image could be used to compare wood fibres that underwent different treatments, such as pulping and the removal of lignin could be confirmed. Despite some shortcoming this technique proved successful in characterising the surface topography and polarity of pulpwood surfaces. Together with other techniques, such as FTIR, it can be used to describe fibre surfaces and determine the effects of various surface treatments.

Acknowledgements

The authors wish to thank R. Sanderson from the Department of Chemistry and Polymer Science for his contribution and the use of the Veeco Multimode SPM, which he has on loan from the Centre for Macromolecular Chemistry and Technology in Tripoli, Libya. Financial support was obtained from the National Research Foundation (NRF) of South Africa under the grant ICD2006060600004.

References

[1] G. Koch, in: H. Sixta (Ed.), Handbook of Pulp, Wiley-VCH, Weinheim, 2006 pp. 21–68.
[2] T. Lindstroem, C. Soeremark, L. Westman, The colloidal behaviour of kraft lignin, Colloids Polym. Sci. 258 (1977) 168–173.
[3] X. Zhang, R.P. Beatson, Y.J. Cai, J.N. Saddler, Accumulation of specific dissolved colloidal substances during white water recycling affecting paper properties, J. Pulp Pap. Sci. 25 (1999) 206–210.
[4] J. Schurz, A bright future for cellulose, Prog. Polym. Sci. 24 (1999) 481–483.
[5] R. Alen, in: P. Stenius (Ed.), Forest Products Chemistry,, Fapet Oy, Helsinki, Finland, 2000, pp. 12–54.
[6] H.H. Nimz, U. Schmitt, E. Schwab, O. Wittmann, F. Wolf, Wood, Ullmann's Encyclopedia of Industrial Chemistry, Wiley-VCH Verlag GmbH & Co., KGaA Weinheim, 2002, pp. 1–54.
[7] W.T.Y. Tze, G. Bernhardt, D.J. Gardner, A.W. Christiansen, X-ray photoelectron spectroscopy of wood treated with hydroxymethylated resorcinol, Int. J. Adhes. Adhes. 26 (2006) 550–554.
[8] F.P. Liu, T.G. Rials, Relationship of wood surface energy to surface composition, Langmuir 14 (1998) 536–541.
[9] P. Fardim, N. Durán, Modification of fibre surfaces during pulping and refining as analysed by SEM, XPS and ToF-SIMS, Colloids Surf. A 223 (2003) 263–276.
[10] G. Piantanida, M. Bicchieri, C. Coluzza, Atomic force microscopy characterization of the ageing of pure cellulose paper, Polymer 46 (2005) 12313–12321.
[11] T.C. Pesacreta, L.C. Carlson, B.A. Triplett, Atomic force microscopy of cotton fiber cell wall surfaces in air and water: quantitative and qualitative aspects, Planta 202 (1997) 435–442.
[12] K. Koljonen, M. Osterberg, M. Kleen, A. Fuhrmann, P. Stenius, Precipitation of lignin and extractives on kraft pulp: effect on surface chemistry, surface morphology and paper strength, Cellulose 11 (2004) 209–224.
[13] K. Koljonen, M. Österberg, L.-S. Johansson, P. Stenius, Surface chemistry and morphology of different mechanical pulps determined by ESCA and AFM, Colloids Surf. A 228 (2003) 143–158.
[14] P. Fardim, J. Gustafsson, J. Sebastian von Schoultz, Peltonen B. Holmbom, Extractives on fiber surfaces investigated by XPS, ToF-SIMS and AFM, Colloids Surf. A 255 (2005) 91–103.
[15] M. Meincken, Atomic force microscopy used to determine the surface roughness and surface polarity of different cell types of hardwoods commonly used for pulping, S. Afr. J. Sci. 103 (2007) 4–6.
[16] A. Noy, D.V. Vezenov, C.M. Lieber, Chemical force microscopy, Annu. Rev. Mater. Sci. 27 (1997) 381–421.
[17] G.G. Baralia, A.-S. Duwez, B. Nysten, A.M. Jonas, Kinetics of exchange of alkanethiol monolayers self-assembled on polycrystalline gold, Langmuir 21 (2005) 6825–6829.
[18] A. Noy, C.D. Frisbie, L.F. Rozsnyai, M.S. Wrighton, C.M. Lieber, Chemical force microscopy: exploiting chemically-modified tips to quantify adhesion, friction, and functional group distributions in molecular assemblies, J. Am. Chem. Soc. 117 (1995) 7943–7951.
[19] J.C. Bastidas, R. Venditti, J. Pawlak, R. Gilbert, S. Zauscher, J.F. Kadla, Chemical force microscopy of cellulosic fibers, Carbohydr. Polym. 62 (2005) 369–378.
[20] O. Marti, T. Stifter, H. Waschipky, M. Quintus, S. Hild, Scanning probe microscopy of heterogeneous polymers, Colloids Surf. A. 154 (1999) 65–73.
[21] H. Krotil, T. Stifter, H. Waschipky, K. Weishaupt, S. Hild, O. Marti, Pulsed force mode: a new method for the investigation of surface properties, Surf. Interf. Anal. 27 (1999) 336–340.
[22] Nanoworld, Product Guide, 2006.
[23] B. Tosh, C.N. Saikia, N.N. Dass, Homogeneous esterification of cellulose in the lithium chloride–N,N-dimethylacetamide solvent system: effect of temperature and catalyst, Carbohydr. Res. 327 (2000) 345–352.
[24] J.S. Han, T. Mianowski, Y. Lin, Validity of plant fiber length measurement Forest Products Laboratory, Agric. Biol. Eng. (1999) 149–167.

[25] M. Fuji, K. Machida, T. Takei, T. Watanabe, M. Chikazawa, Effect of wettability on adhesion force between silica particles evaluated by atomic force microscopy measurement as a function of relative humidity, Langmuir 15 (1999) 4584–4589.
[26] D.L. Sedin, K.L. Rowlen, Adhesion forces measured by atomic force microscopy in humid air, Anal. Chem. 72 (2000) 2183–2189.
[27] T. Thundat, X.-Y. Zheng, G.Y. Chen, S.L. Sharp, R.J. Warmack, L.J. Schowalter, Characterization of atomic force microscope tips by adhesion force measurements, Appl. Phys. Lett. 63 (1993) 2150–2152.
[28] F. Sato, H. Okui, U. Akiba, K. Suga, M. Fujihira, A study of topographic effects on chemical force microscopy using adhesive force mapping, Ultramicroscopy 97 (2003) 303–314.

Eur J Forest Res (2010) 129:741–748
DOI 10.1007/s10342-010-0380-5

ORIGINAL PAPER

Determination of the cellulose and lignin content on wood fibre surfaces of eucalypts as a function of genotype and site

A. Klash · E. Ncube · B. du Toit · M. Meincken

Received: 24 April 2009 / Revised: 8 February 2010 / Accepted: 15 March 2010 / Published online: 1 April 2010

Abstract We compared the chemical composition of wood fibres and fibre surfaces of several eucalypt species and hybrids originating from various growth sites in South Africa. The objective was to test for differences in chemical surface composition due to genetics or site with the ultimate aim to facilitate a tailor-made supply of wood for pulping that results in an optimal blend of fibres that can be pulped together with similar yields. This, however, requires a sound knowledge of the fibre properties. The surface functionality on the single fibre level is a key property, because it determines how good inter-fibre bonding will be when paper is formed, which depends amongst other fibre properties on the amount of free hydroxyl groups that are available and therefore on the cellulose content on the fibre surface. The cellulose and lignin content on the fibre surface were determined with chemical force microscopy, a variation of atomic force microscopy. Since the general bulk composition of the fibre and the surface composition might differ, both parameters were determined. We found significant differences in the cellulose and lignin content on fibre surfaces, with regard to genotype and site, respectively. In some, but not all, cases, the surface composition of wood fibres followed the bulk composition, and differences were generally more pronounced. Differences due to genotype were significant, especially with regard to the surface lignin content—but variation due to site was also distinctly recognisable. This variation in surface functionality could be the reason why some pulpwood blends result in a lower pulp yield and different quality.

Keywords Genetic effects · Site effects · Wood properties · Pulp fibres · Surface composition · Functional groups · Free hydroxyl groups · Chemical force microscopy

Communicated by T. Seifert.

A. Klash
Department of Chemistry and Polymer Science, University of Stellenbosch, Matieland, South Africa

E. Ncube · B. du Toit · M. Meincken (✉)
Department of Forest and Wood Science, University of Stellenbosch, Private Bag X1, Matieland 7602, South Africa
e-mail: mmein@sun.ac.za

Introduction

South Africa is the largest African producer of pulp and paper and produces approximately 1.9 million tons of wood pulp, 1.2 million tons of newsprint, printing and writing paper and more than 1 million tons of other paper products per year. South Africa has a relatively rich source of raw materials from its plantation forests in the KwaZulu-Natal and Mpumalanga regions. The warm climate of these areas leads to a faster tree growth than in most paper- and pulp-producing countries north of the equator (Mbendi Information Services 2009).

South Africa's major pulpwood source is *Eucalyptus*, and several eucalypt genotypes are commercially grown depending on the site characteristics. The growth regions for pulpwood production encompass different climate zones, ranging from warm, subtropical areas near the east coast to cooler sites on the escarpment with elevations above 1,000 m.

Species choice is usually based on climatic risk factors (e.g. snow, frost or drought risk), mean annual temperature (MAT), mean annual precipitation (MAP), soil characteristics as well as wood and pulping characteristics.

On subtropical sites near the coast (MAT > 19°C), *E. grandis* × *urophylla* and *E. grandis* × *camaldulensis* are the most widely planted genotypes. These hybrids have a superior disease resistance compared to pure species, such as *E. grandis*, which can also be grown in this zone. In addition, *E. grandis* × *urophylla* has excellent pulping properties and is thus the preferred genotype in the subtropical area.

In the warm, temperate climates (KwaZulu-Natal Midlands and Mpumalanga escarpment with MAT 16–19°C), *E. grandis*, *E. dunnii*, *E. saligna* and *E. smithii* are commonly planted. *E. grandis* has a fast growth rate but may be prone to drought risk on sites with low levels of available soil water, and it is sensitive to snow damage and to frost when young. *E. smithii* has highly desirable pulp properties but is relatively more susceptible to *Phytophthora* root rot on soils with poor drainage.

On cold temperate sites with a MAT of 15–16°C, *E. dunnii*, *E. grandis* × *nitens*, *E. saligna* and *E. smithii* can still be grown since they are moderately hardy to frost. However, on sites with a MAT below 15°C, species tolerant of snow—such as *E. nitens*—or frost and drought—such as *E. macarthurii*—are often preferred, despite having slightly less desirable pulping properties, especially in the latter case. Other species with desirable wood properties that show promise for cold temperate sites are *E. benthamii* and *E. badjensis* (Smith et al. 2005).

The pulp and paper quality of these species depends strongly on fibre properties, such as fibre length, diameter and chemical composition. The fibre dimensions determine how well the inter-fibre contact will be when paper is formed, and the chemical composition, i.e. the availability of free hydroxyl groups to form hydrogen bonds, determines how well these fibres will bind together, which in turn affects the paper quality. The importance of fibre properties—in addition to other tree improvement efforts—for any further use such as pulping has been highlighted by Lundqvist (2002).

That wood quality and more specifically fibre properties depend strongly on the environment has been demonstrated by many studies. Gindl et al. (2000), for example, showed that the lignin content in the secondary cell wall correlated positively with temperature in terminal latewood tracheids. Leal et al. (2007) reported tree growth variability within five different conifer species in the Austrian Alps depending on species and altitude. Kaakinen et al. (2007) studied the effects of growth differences due to geographical location and nitrogen fertilisation on the chemical composition of Norway spruce (*Picea abies* (L.) Karst.) at two sites in Finland. They found that nitrogen fertilisation caused only small changes in the chemical composition, while the differences due to different sites were significantly larger.

Various studies have discussed wood and fibre quality of *Eucalyptus*. Clarke et al. (1997) studied a variety of wood characteristics including the average density, fibre length and chemical composition of nine eucalypt species in three provenances from established trial sites in South Africa. These authors revealed significant differences in density, fibre length and chemical composition between the species and between sites. Naidoo et al. (2006) found a negative correlation between moisture availability and wood density and vessel amount in *Eucalyptus grandis* in the warm temperate region of South Africa. Miranda and Pereira (2002) studied the differences in wood density, fibre morphology, chemical composition and pulp yield in four provenances of *Eucalyptus globulus* at three different sites in Portugal. Their findings suggest no significant effect of provenance and site on the wood density. However, provenance and site caused significant variation in fibre length, cell wall thickness and lumen diameter. With regard to the chemical composition, only the extractive content showed any significant provenance and site effects.

Based on the effects of site quality and fibre properties, this study explores further ways of scrutinising the fibres quality. This is done by the use of chemical force microscopy to characterise the chemical surface composition of pulpwood fibres and compare this to the chemical bulk composition, which might differ considerably (Koljonen et al. 2004; Hannuksela et al. 2003; Fardim and Holbom 2005a; Fardim et al. 2005b). Nevertheless, typically the bulk chemical composition is determined to describe pulpwood fibres. To our knowledge, information on the surface composition of wood fibres has so far not been investigated or published.

The surface properties of fibres are, however, especially important for further processing, such as paper making, as they determine, for example, the degree of inter-fibre bonding. The formation of hydrogen bonds between pulp fibres depends on available hydrophilic hydroxyl (–OH) groups and small inter-fibre distances. The removal of the hydrophobic lignin from the fibre surface during pulping exposes cellulose and hemicelluloses containing –OH groups, while precipitation of hydrophobic lignin hinders the formation of hydrogen bonds (Laine et al. 1994). Furthermore, any lignin still present in pulp fibres results in an increased fibre stiffness, which inhibits good inter-fibre bonding. The fibres become more flexible when lignin is removed, and simultaneously, the amount of free hydroxyl groups on the fibre surface is increased, which promotes the formation of hydrogen bonds between the fibres. These bonds are responsible for the mechanical strength of the

final paper product (Maximova et al. 2001), and e.g. the tensile strength a paper sheet depends mostly on the number of hydrogen bonds per unit volume available between the fibre surfaces.

The objective of this study was to reveal possible differences in chemical composition of the fibre surfaces with regard to site and genotype. The investigated species consisted of different *Eucalyptus* species grown at various sites in South Africa. These sites varied in the availability of water, or mean annual precipitation (MAP) and mean annual temperature (MAT). Both factors can be expected to have an influence on the chemical composition of wood fibres.

A difference in surface functionality could be expected to affect the pulp quality and explain a variation therein.

An important part of that objective was to determine whether the traditionally used bulk composition is comparable with the surface composition that we assessed with chemical force microscopy (CFM), a technique that allowed us to scrutinise whether the fibre surface differs in its cellulose and lignin content from the fibre bulk.

Chemical force microscopy (CFM) is an adaptation of atomic force microscopy (AFM), in which the tip is coated with specific functional groups. The adhesive force determined between the modified tip and the sample surface can be used to gain additional information about the chemical composition of the surface (Noy et al. 1997). The tip is modified with self-assembling monolayers (SAMs) of alkane thiol compounds, which allow control of the functionality and their chemical and mechanical stabilities (Baralia et al. 2005). Chemical force microscopy has been established on chemically modified, flat silicon surfaces by Noy et al. (1995). In their study, both the silicon substrates and the S_3N_4 tips were coated with gold and then modified with SAMs of alkane thiol compounds terminated with $–CH_3$, –COOH and $–NH_2$ functional groups. They found that the adhesive force was larger if the tip and substrate had the same functionality. Chemical force microscopy has also been used to study cellulose fibres in aqueous media by Bastidas et al. (2005), who determined the effect of the pH value on the adhesive force determined with $–CH_3$,- –COOH- and –OH-coated tips.

In this study, we determined the adhesive forces between AFM tips coated with $–CH_3$ and –COOH, respectively. In a previous study (Klash et al. 2009), we could show successfully that $–CH_3$ groups are more sensitive to lignin, while –COOH groups are more sensitive to cellulose and hemicelluloses. The thus functionalised tips can therefore be used to quantify the cellulose and lignin content on the surface of pulpwood fibres. Figure 1 shows a sketch of the experimental setup and an example of an AFM image that is used to quantify functional groups on the surface.

Materials and methods

Sample preparation

Samples of different eucalypt genotypes, namely *E. dunnii*, *E. grandis* (grown from genetically variable seedlings), *E. grandis* (clonal material) as well as *E. grandis* × *nitens* and *E. grandis* × *camaldulensis* hybrid clones, were collected from different growth sites with either cool temperate, warm temperate or subtropical (hot) MAT and on sites with a MAP that was either dry, moist or wet according to the classification by Smith et al. (2005). Not all species were available from all growth sites.

The MAT, MAP, average age, diameter at breast height (DBH), site index at 5 years (SI_5), basal area (BA) and mean annual increment (MAI) of the investigated species are given in Table 1.

The trees were between six (fast growing species) and eight (slower growing species) years old when harvested. Only straight trees without any reaction wood that would result in a different cellulose and lignin content were cut on each sample site, and discs were cut at DBH directly after harvesting. These discs were chipped, and fibres were prepared from the chips by a mild maceration in Jeffrey's solution for 4 h (Han et al. 1999). The maceration removed only the middle lamellae and left the mostly amorphous primary cell wall exposed. This has been shown by AFM images of the fibre surfaces in a previous publication by Meincken (2007).

The separated fibres were subsequently kept in distilled water. For AFM analysis, they were spread onto a glass slide and left to dry for 12 h. The adhesion due to capillary forces between the cells and the glass substrate was sufficient to keep the fibres in position for AFM analysis. The low concentration of fibres in the water ensured that the fibres did not overlap and only formed a single layer on the substrate. Images were acquired with the fast scan axis parallel to the longitudinal fibre axis, in order to minimise shear forces.

In order to verify the reproducibility of results, two sample sets were prepared for AFM measurements from randomly chosen wood chips, where enough material was available. This was, however, not possible for all samples.

Tip modification for CFM

Silicon force modulation cantilevers from nanosensors were modified according to Bastidas et al. (2005). Tips with the following functional groups were prepared:

- methyl ($–CH_3$) groups, from 1-octadecanethiol $CH_3(CH_2)_{17}SH$ (Acros).

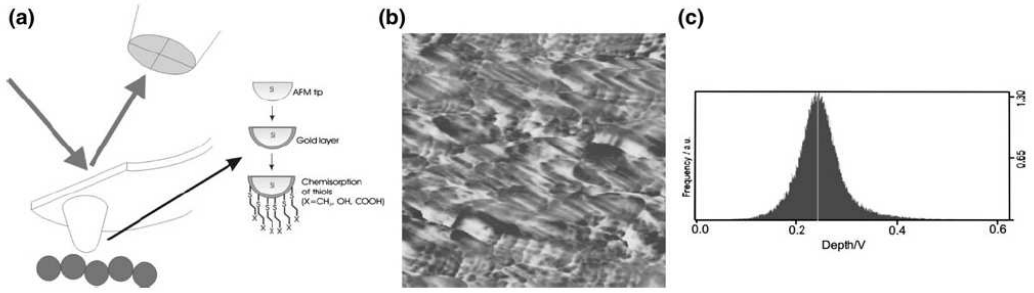

Fig. 1 **a** Schematic drawing of an AFM with a chemically modified tip, **b** adhesive force image obtained with a COOH-coated tip that shows the distribution of cellulose as brighter areas and **c** representation of the image as histogram to determine the average grey value

Table 1 Medium annual temperature (MAT), medium annual precipitation (MAP), age, diameter at breast height (DBH), site index at 5 years (SI_5), basal area (BA) and mean annual increment (MAI) of the sampled *Eucalyptus* genotypes

Species	MAT	MAP	Age [years]	DBH [cm]	SI_5 [m]	BA [m^2/ha]	MAI [m^3/ha/year]
E. grandis	Warm	Moist	6	14.5	18.1	17.8	23.5
E. grandis clone	Cool	Moist	8	19.9	19.9	12.4	14.9
E. dunnii	Warm	Moist	8	14.0	13.8	17.8	15.2
E. dunnii	Warm	Wet	7	18.0	17.4	16.8	21
E. grandis × *camaldulensis*	Cool	Moist	8	13.2	15.3	18.7	17.5
E. grandis × *nitens*	Cool	Moist	7	20.6	21.0	21.4	41.4
E. grandis × *nitens*	Warm	Moist	7	15.6	16.2	10.7	24.1
E. grandis × *nitens*	Hot	Dry	7	17.7	17.0	11.8	12.9

- carboxylic (–COOH) groups, from 11-mercaptoundecanoic acid $HOOC(CH_2)_{10}SH$ (Aldrich).

The silicon tips were first coated with gold with a sputter coater and cleaned under a 254-nm UV lamp for 1 h to ensure that all organic material was removed. The gold-coated tips were subsequently immersed in reagent alcohol for 30 min and then in a 3 mM $CH_3(CH_2)_{17}SH$ or $HOOC(CH_2)_{10}SH$ alcoholic solution for 2 h at room temperature. The coated tips were then rinsed with *n*-heptane (Aldrich) and alcohol and gently dried in an Argon stream.

AFM imaging

AFM images were acquired with a Multimode AFM from Veeco combined with a digital pulsed force mode (DPFM) controller from Witec. This leads to the simultaneous acquisition of a topography and an adhesive force image, which displays the adhesive force between the substrate and the tip on each image pixel. Images were acquired with a scan range of 2 × 2 µm and a scan speed of 0.7 lines/s.

In order to compensate for the environmental effect of humidity and temperature, which could lead to a change in surface polarity, the tip was calibrated on a mica surface before each measurement.

The average polarity of a single fibre was determined from one adhesion image, which consists of 65,536 (256 × 256) single measurements in the observed area. This was done for ten different fibres, resulting in one average adhesive force value to describe the sample.

Bulk chemical composition

Typically, hardwoods contain about 40-50% cellulose, 20-30% hemicelluloses, 18–25% lignin and less than 10% extractives (Walker 2006).

To determine the chemical bulk composition, the wood chips were ground into flour in a Retsch Ultra centrifugal mill and screened for size. The fraction retained in the 80 mesh sieve was extracted in triplicate for 4 h in a Soxhlet apparatus with 1:2 v/v 95% ethanol/cyclohexane (E/C) mixture and then with distilled hot water (ASTM 2001a; Fengel and Przyklenk 1983; TAPPI 1988a).

The solvent was evaporated at 40°C under vacuum, after which the residue was oven-dried at 102 ± 3°C for 20 min to determine the dry mass extractives content.

Three replicates of 0.5 mg extractive-free wood were then hydrolysed with 7.5 ml, 72% (w/w) sulphuric acid at 20°C for 2 h. The acid was diluted to a concentration of 3%

by adding 280 ml of distilled water. The residue was cooled and washed in a porosity 2 filtering crucible with 250 ml of boiling water. The solid residue was dried at 102 ± 3°C to a constant weight to determine the percentage of acid-insoluble, i.e. Klason lignin (ASTM 2001b; TAPPI 1988b).

The cellulose content was determined according to the Seifert method (Browning 1967) using acetylacetone from Sigma–Aldrich and dioxane, hydrochloric acid, methanol and diethyl ether from Merck Chemicals.

Statistical analysis

The resulting data were not evaluated with ANOVA, because the sample set was not complete, i.e. not all genotypes were available from all growth sites. For the average adhesive force values determined from ten AFM images per sample, an average value and a 95% confidence interval were calculated with a *t*-test.

Results and discussion

The bulk chemical composition of eucalypt genotypes from sites with cool or medium MAT and medium MAP values is given in Table 2.

The amount of cellulose did not differ significantly between the investigated genotypes and ranged from 44 to 48%. The *E. grandis* clone had with 48% the highest cellulose content, followed by *E. grandis* and the two hybrids, *E. grandis* × *nitens* and *E. grandis* × *camaldulensis* with about 46%. The lowest cellulose content was found in *E. dunnii* with 44%. The lignin content followed the same trend–the *E. grandis* clone showed with 21% the largest amount of lignin and *E. dunnii* with 13% the lowest. The maximum variation in the bulk lignin content between the species was 8%.

The chemical surface composition of the fibres determined with CFM revealed considerably larger differences between the species than the bulk composition. Figure 2 displays the adhesive forces and 95% confidence intervals determined with –COOH (cellulose sensitive) or $–CH_3$ (lignin sensitive) functionalised tips on the fibre surfaces of wood originating from similar growth sites but from different species. The determined adhesive force values are directly proportional to the amount of cellulose or lignin present on the surface, although they do not yield a percentage value for the cellulose or lignin amount.

The adhesive forces of different *Eucalyptus* genotypes from comparable sites with a cool/moist MAT/MAP are shown in Fig. 2a. It shows that similar adhesive force values were obtained with the CH_3-coated tip on fibres from *E. grandis* clone and *E. grandis* × *camaldulensis*, and they were significantly higher than the values observed on fibres from *E. grandis* × *nitens*. This indicates that fibres of *E. grandis* × *nitens* have a lower lignin content on the surface than that of *E. grandis* clone and *E. grandis* × *camaldulensis*, and this result was confirmed in a second set of measurements on *E. grandis* × *nitens* fibres.

The adhesive forces determined with a COOH-coated tip showed similar values for all four species within the 95% confidence interval. Although the adhesive forces determined for *E. grandis* × *nitens* in the two measurement sets differ, the COOH-coated tip showed a higher sensitivity towards the fibre surface than the CH_3-coated tip for both measurements. This suggests a higher cellulose content on the fibre surfaces compared to the lignin content. Fibres from *E. grandis* clone and *E. grandis* × *camaldulensis* on the other hand showed a comparable cellulose and lignin content on the surface.

Comparison between the chemical surface composition of the fibres determined with CFM and the bulk composition showed that the amount of cellulose did not differ significantly between the examined genotypes for both methods. The amount of lignin on the surface, however, showed considerable differences between the species with a higher (and similar) lignin content determined on fibres from *E. grandis* clone and *E. grandis* × *camaldulensis* than for *E. grandis* × *nitens*.

Figure 2b shows the surface functionality of different *Eucalyptus* genotypes from comparable sites with a warm/moist MAT/MAP. It can be seen that the adhesive force values were well reproducible where two measurement sets were performed.

As for the cool/moist climate, *E. grandis* and *E. grandis* × *nitens* displayed a slightly higher sensitivity towards

Table 2 Chemical bulk composition of various *Eucalyptus* genotypes from cool (c) or warm (w) MAT sites with standard deviation in brackets

Species	Lignin (%)	Cellulose (%)	E/C extractives (%)	H_2O extractives (%)
E. grandis (w)	14.8 (4.5)	45.6 (2.2)	2.2 (0.7)	1.9 (0.9)
E. grandis clone (c)	20.9 (1.3)	47.6 (2.5)	3.3 (1.7)	2.0 (2.0)
E. dunnii (w)	12.7 (3.1)	44.1 (2.2)	5.4 (0.1)	2.7 (1.4)
E. grandis × *nitens* (w)	16.5 (1.2)	45.2 (2.8)	4.3 (2.3)	1.8 (1.5)
E. grandis × *camaldulensis* (c)	15.5 (0.7)	45.9 (3.0)	4.7 (1.7)	3.6 (1.7)

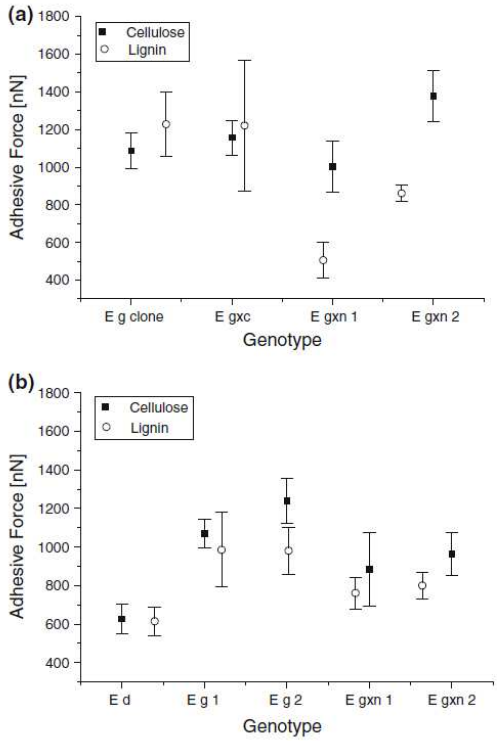

Fig. 2 **a** Different *Eucalyptus* genotypes from comparable sites with a cool/moist MAT/MAP, **b** different *Eucalyptus* species from comparable sites with warm/moist MAT/MAP

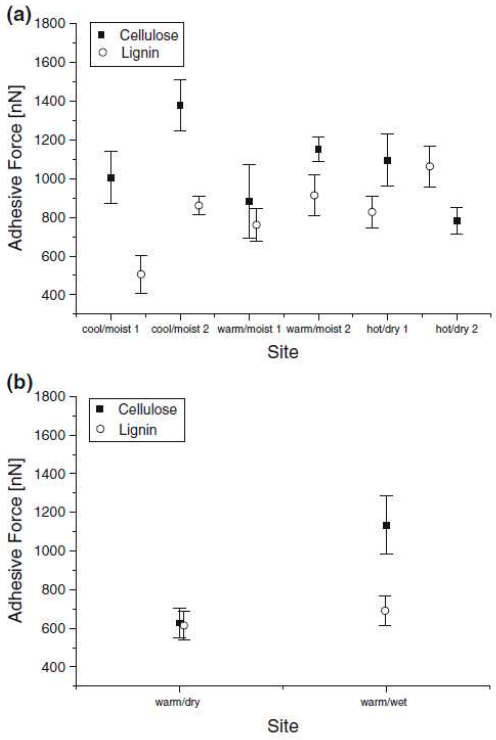

Fig. 3 Same *Eucalyptus* genotypes from sites with differing climate. **a** *E. grandis* × *nitens* hybrids, **b** *E. dunnii*

the COOH-coated tip than towards the CH_3-coated tip, although this was only significant in the second measurement set. This can be attributed to a higher cellulose content on the fibre surface. Both the cellulose and lignin content were significantly lower in *E. dunnii* than in *E. grandis* and *E. grandis* × *nitens*. This distribution was confirmed, although not quite as pronounced, by the bulk chemical composition. The lignin content on the surfaces of *E. grandis* fibres was significantly higher than on fibres from *E. dunnii* or *E. grandis* × *nitens*, which agrees well with the results displayed in Fig. 3a, which showed a higher surface lignin content for *E. grandis* clone than for *E. grandis* × *camaldulensis*.

The adhesive forces determined on fibres from the same species, but from different growth sites, are presented in Fig. 3.

The adhesive forces determined on fibres from *E. grandis* × *nitens* hybrids across a MAT/MAP gradient are displayed in Fig. 3a. Most fibres showed a higher sensitivity towards the COOH-coated tip than towards the CH_3-coated tip, which means that the cellulose content on the surface was higher than the lignin content in these samples. The only exception was the second set of fibres originating from a hot and dry site, where the results were contradictory. The highest cellulose content was found for cool and moist growth conditions, and it decreased with increasing MAT and decreasing MAP. At the same time, the lignin content at the fibre surface increased slightly with increasing MAT and decreasing MAP.

The adhesive forces determined on fibres from *E. dunnii* across an MAP gradient are displayed in Fig. 3b. Fibres originating from the warm/dry site showed comparable sensitivity to the CH_3- and COOH-coated tips, whereas the fibres from the warm/wet site had a considerably higher affinity to the COOH-coated tip. This means that the cellulose content on the surface of fibres originating from moist sites is significantly higher than that from dry sites, whereas the surface content of lignin remains the same.

The results show that the chemical composition on the fibre surface differs in some cases from the bulk and that differences in composition between genotypes and growth

site can be more pronounced on the fibre surface than in the bulk. This affects further processing of the fibres such as pulping and paper formation. Statistically significant differences with regard to genotype were found in *E. grandis* × *nitens*, which showed a lower lignin content on the fibre surface and *E. dunnii*, which had a considerably lower lignin and cellulose content on the fibre surface compared to *E. grandis* and *grandis* × *camaldulensis*.

The differences due to growth site were less significant, but the trend showed that the cellulose content on the fibre surface decreased with increasing temperature and decreasing moisture, whereas the lignin content on the fibre surface increased.

If a blend of fibres is pulped together, a comparable fibre composition is desirable so that the amount of pulping chemicals can be adjusted accordingly and evenly distributed. Large differences in the fibre stock could result in uneven pulping and consequently in a yield with variable end-product quality.

Conclusion

In conclusion, we could show that the surface composition of the fibres followed the trend of the bulk composition in some, but not all, cases. The cellulose content of fibres from different species but various growth sites was comparable within the standard deviations in the fibre bulk, as well as on the fibre surface. The lignin content, on the other hand, showed considerably more variation on the fibre surface than in the fibre bulk. While *E. grandis*, *E. grandis* clone and *E. grandis* × *camaldulensis* showed comparable values, *E. grandis* × *nitens* and *E. dunnii* had a significantly lower surface lignin content than that suggested by the bulk composition.

The effect of MAT and MAP on the surface composition on pulpwood fibres was recognisable. The surface cellulose content of *E. grandis* × *nitens* hybrids decreased with increasing MAT and decreasing MAP, while in turn the surface lignin content increased with increasing MAT and decreasing MAP. This could be confirmed by increasing surface cellulose content on fibres from *E. dunnii* with increasing MAP.

These results could prove useful for the pulp and paper industry as they indicate why some species produce pulp of lower quality and also why some species cannot be pulped well together.

Acknowledgments The authors wish to thank M. du Plessis from Mondi, Forestry Operations for the supply of fibre samples and R. Sanderson from the Department of Chemistry and Polymer Science for his contributions and the use of the Veeco Multimode SPM, which he has on loan from the Centre for Macromolecular Chemistry and Technology in Tripoli, Libya. Financial support was obtained from the National Research Foundation (NRF) of South Africa under the grant ICD2006060600004.

References

ASTM (2001a) D1105-96, standard test method for preparation of extractive free wood

ASTM (2001b) D1106-96, standard test method for acid insoluble lignin in wood

Baralia GG, Duwez AS, Nysten B, Jonas AM (2005) Kinetics of exchange of alkanethiol monolayers self-assembled on polycrystalline gold. Langmuir 21:6825–6829

Bastidas JC, Venditti R, Pawlak J, Gilbert R, Zauscher S, Kadla JF (2005) Chemical force microscopy of cellulosic fibers. Carbohydr Polym 62:369–378

Browning BL (1967) The chemistry of wood, 1st edn. Interscience, USA, p 407

Clarke CRE, Garbutt DCF, Pearce J (1997) Growth and wood properties of provenances and trees of nine eucalypt species. Appita J 50:121–130

Fardim P, Holbom B (2005) Origin and surface distribution of anionic groups in different papermaking fibres. Colloids Surf A 252:237–242

Fardim P et al (2005) Extractives on fiber surfaces investigated by XPS, ToF-SIMS and AFM. Colloids Surf A 255:91–103

Fengel D, Przyklenk M (1983) Comparative extract determination for replacing benzene with cyclohexane. Holz als Roh- und Werkstoff 5:193–194

Gindl W, Grabner M, Wimmer R (2000) The influence of temperature on latewood lignin content in treeline norway spruce compared with maximum density and ring width. Trees 14:409–414

Han JS, Mianowski T, Lin Y (1999) Validity of plant fiber length measurement, Chap. 14. In: Kenaf properties, processing and products. Mississippi State University, Ag & Bio Engineering, pp 149–167

Hannuksela T, Fardim P, Holbom B (2003) Sorption of spruce *O*-acetylated galactoglucomannans onto different pulp fibres. Cellulose 10:317–324

Kaakinen S, Saranpää P, Vapaavuori E (2007) Effects of growth differences due to geographic location and N-fertilisation on wood chemistry of Norway spruce. Trees 21:131–139

Klash A, Ncube E, Meincken M (2009) Localization and attempted quantification of various functional groups on pulpwood fibres. Appl Surf Sci 255:6318–6324

Koljonen K et al (2004) Precipitation of lignin and extractives on kraft pulp: effect on surface chemistry, surface morphology and paper strength. Cellulose 11:209–224

Laine J et al (1994) Surface characterization of unbleached kraft pulps by means of ESCA. Cellulose 1:145–160

Leal S et al (2007) Tree-ring growth variability in the Austrian alps: the influence of site, altitude, tree species and climate. Boreas 36:427–440

Lundqvist SO (2002) Efficient wood and fiber characterization—a key factor in research and operation. Ann For Sci 59:491–501

Maximova N, Österberg M, Koljonen K, Stenius P (2001) Lignin adsorption on cellulose fibre surfaces: effect on surface chemistry, surface morphology and paper strength. Cellulose 8:113–125

Mbendi Information Services (2009) http://www.mbendi.com, Accessed 8. April 2009

Meincken M (2007) Atomic force microscopy to determine the surface roughness and surface polarity of cell types of hardwoods commonly used for pulping. S Afr J Sci 103:4–6

Miranda I, Pereira H (2002) Variation of pulpwood quality with provenances and site in *Eucalyptus globulus*. Ann For Sci 59:283–291

Naidoo S, Zboňák A, Ahmed F (2006) The effect of moisture availability on wood density and vessel characteristics of Eucalyptus grandis in the warm temperate region of South Africa. IUFRO symposium "Wood structure and Properties"

Noy A, Frisbie CD, Rozsnyai LF, Wrighton MS, Lieber CM (1995) Chemical force microscopy: exploiting chemically-modified tips to quantify adhesion, friction, and functional group distributions in molecular assemblies. J Am Chem Soc 117:7943–7951

Noy A, Vezenov DV, Lieber CM (1997) Chemical force microscopy. Annu Rev Mat Sci 27:381–421

Smith CW, Pallett RN, Kunz RP, Gardner RAW, du Plessis M (2005) A strategic forestry site classification for the summer rainfall region of southern Africa based on climate, geology and soils. ICFR Bulletin, Series 03/05, Pietermaritzburg, South Africa

TAPPI (1988a) T222om-88, Acid-insoluble lignin in wood and pulp

TAPPI (1988b) T264om-88, preparation of wood for chemical analysis

Walker JCF (ed) (2006) Basic wood chemistry and cell wall ultrastructure, Chap. 2. In: Primary wood processing: principles and practice. Springer, Dordrecht, pp 23–67